BIOSYNTHESIS OF THE O-METHYL PHOSPHORAMIDATE MODIFICATION IN THE CAPSULAR POLYSACCHARIDES OF *CAMPYLOBACTER JEJUNI*

A Dissertation

by

ZANE W. TAYLOR

Submitted to the Office of Graduate and Professional Studies of
Texas A&M University
in partial fulfillment of the requirements for the degree of

DOCTOR OF PHILOSOPHY

Chair of Committee,	Frank M. Raushel
Committee Members,	David P. Barondeau
	Thomas D. Meek
	Jennifer K. Herman
Head of Department,	Josh Wand

May 2020

Major Subject: Biochemistry

ABSTRACT

Campylobacter jejuni is a Gram-negative pathogenic bacterium that is the leading cause of gastroenteritis worldwide. Like many other Gram-negative bacteria, *C. jejuni* produces a capsular polysaccharide (CPS) that helps improve the overall fitness of the organism and contributes to its pathogenicity. Previously, the structure of the CPS from the NCTC 11168 strain was determined, and has revealed the presence of a unique *O*-methyl phosphoramidate (MeOPN), that can be found on C-4 of a heptose and C-3 of an N-acetyl galactofuranose residue. Investigations into the role of MeOPN on the CPS suggest that it is involved in the evasion of immune responses, and serum resistance. Previously, the biosynthesis of the MeOPN modifications found on the CPS were unknown.

We have characterized the first four enzymes involved in the biosynthesis of the phosphoramidate moiety of the MeOPN modification. The first enzyme, Cj1418, is a novel glutamine kinase that catalyzes the ATP dependent phosphorylation of the amide nitrogen of L-glutamine, resulting in L-glutamine phosphate. Next, the nucleotidyl transferase, Cj1416 uses L-glutamine phosphate to displace pyrophosphate from CTP, forming CDP-L-glutamine. CDP-L-glutamine is then hydrolyzed by Cj1417, releasing glutamate and cytidine diphosphoramidate. Cj1415 catalyzes the phosphorylation of the 3'-hydroxyl group of cytidine diphosphoramidate. The resulting cofactor is very similar to the 3'-phosphoadenylyl sulfate (PAPS) that is used by many biological systems for the transfer of sulfate. Presumably 3'-phosphocytidine diphosphoramidate is used to

transfer the phosphoramidate moiety to the capsule, and then methylated resulting in the final MeOPN modification.

DEDICATION

I dedicate this dissertation to all the teachers and professors who have made learning fun, and who have pushed me to follow my dreams. And to my family for all their love and support throughout my journey.

ACKNOWLEDGEMENTS

I would like to thank my advisor Professor Frank Raushel, for mentoring and supporting me throughout my Ph.D. This would not have been possible without you. You have pushed me and molded me into the researcher that I am today, and for that I will be forever grateful. I would also like to thank my committee, Professor David Barondeau, Professor Thomas Meek, and Professor Jennifer Herman for their guidance and support throughout my Ph.D. I would like to thank my co-authors Dr. Hazel Holden and Dr. Haley Brown for their efforts in structure determination and Dr. Tamari Narindoshvili for her assistance in chemical synthesis. I would like to acknowledge Dr. Jamison Huddleston, Dr. Dao Feng Xiang, and Dr. Andrew Bigley for their patience, suggestions, and assistance they have provided over the years. I would like to acknowledge Alexandra Chamberlain, Chesley Johnson, and Erin Prause, undergraduate researchers who have provided support on various projects. I would like to recognize Ed Janousek and Andrea Scott for always being friendly faces to work with, and helping the lab run smoothly. A special acknowledgement for my best friend at Texas A&M University Dr. Tessily Hogancamp for your help in lab, and all the shenanigans that have made graduate school enjoyable. Drake Mellott, thank you for all of the discussions about experiments, and your friendship. I would like to recognize the Chemistry and Biochemistry Department of Mercyhurst University, and especially Drs. Chris Taylor, Amy Danowitz and Clinton Jones for their support both as an undergraduate and as a graduate student. I would like to give special attention to my parents, grandparents,

brother, and extended family for your love and support. I would not be here today if it was not for all of you.

CONTRIBUTORS AND FUNDING SOURCES

Contributors

This work was supervised by a dissertation committee consisting of Professor Frank M. Raushel, Professor Thomas D. Meek, and Professor Jennifer K. Herman of the Department of Biochemistry and Biophysics and Professor David P. Barondeau of the Department of Chemistry.

The plasmids for the expression of Cj1418 (Sections 2 and 5), Cj1416 (Sections 3 and 6), Cj1417 (Section 3), and Cj1415 (Section 4) were obtained from Professor Christine Szymanski from the University of Georgia. The chemical synthesis and characterization of L-glutamine phosphate was performed by Dr. Tamari Narindoshvili. Mass spectrometry was performed by the Mass Spectrometry Laboratories in the Chemistry Department and the Interdisciplinary Life Sciences Building. Alexandra Chamberlain assisted in determining the kinetic constants, characterizing the reaction products, and in the generation of the histidine 737 mutant in Section 5.

All other work conducted for the dissertation was completed by the student independently.

Funding Sources

Graduate student was supported by a teaching assistantship from Texas A&M University for 2015-2016 and a research assistantship from Texas A&M University and the Robert A. Welch Foundation under Grant Number A-840 for 2016-2020 and the

National Institute of Health under grant number GM 122825 for 2018-2020. Its contents are solely the responsibility of the authors and do not necessarily represent the official views of the Robert A. Welch Foundation, National Institute of Health, and Texas A&M University.

NOMENCLATURE

ADP	Adenosine 5’-diphosphate
ADP-NH_2	Adenosine 5’-diphosphoramidate
AMP	Adenosine 5’-monophosphate
AMP-NH_2	Adenosine 5’-phosphoramidate
APS	Adenylyl sulfate
Arg	Arginine
Asn	Asparagine
ATP	Adenosine 5’-triphosphate
C3	Carbon 3
CDP	Cytidine 5’-diphosphate
CDP-Me	CDP-methyl phosphonate
CDP-NH_2	Cytidine 5’-diphosphoramidate
CDP-OMe	CDP-methyl phsophate
CMP	Cytidine 5’-monophosphate
CPS	Capsular polysaccharide
COG	Cluster of orthologous groups
CTP	Cytidine 5’-triphosphate
dCTP	2’-deoxycytidine-5’-triphosphate
C. jejuni	*Campylobacter jejuni*
Da	Dalton

D_2O	Deuterium oxide
DNA	Deoxyribonucleic acid
E. coli	Escherichia coli
ESI	Electrospray ionization
g	Gram
h	Hour
His	Histidine
HS	Hot start
Hz	Hertz
Ile	Isoleucine
IPTG	Isopropyl-β-thiogalactoside
J	Coupling Constant
k_{cat}	Turnover number
K_m	Michaelis Constant
kDa	Kilodalton
KOH	Potassium Hydroxide
L	Liter
Lys	Lysine
MeOPN	O-Methyl phosphoramidate
min	Minute
MIX	Molecular isotope exchange
mg	Milligram

$MgCl_2$	Magnesium chloride
mL	Milliliter
MgATP	Magnesium Adenosine 5’-triphosphate
mM	millimolar
$MnCl_2$	Manganese chloride
NAD^+/NADH	Nicotinamide adenine dinucleotide
nm	Nanometer
NMR	Nuclear magnetic resonance
OD_{600}	Optical Density at 600 nanometers
PAPS	3’-Phosphoadenosine-5’-phosphosulfate
PDB	Protein Data Bank
PEP	Phosphoenolpyruvate
Phe	Phenylalanine
Pi	Phosphate
PIX	Positional isotope exchange
PPi	Pyrophosphate
ppm	Part per million
RNA	Ribonucleic acid
Ser	Serine
SSN	Sequence similarity network
tRNA	Transfer ribonucleic acid
µg	Microgram

μM	Micromolar
UDP	Uridine 5’-diphosphate
UDP-NH_2	Uridine 5’-diphosphoramidate
UV	Ultraviolet

TABLE OF CONTENTS

Page

LIST OF FIGURES

Page

LIST OF TABLES

Page

LIST OF SCHEMES

Page

1. INTRODUCTION

1.1. Phosphoramidate Natural Products

Phosphorus containing functional groups are essential to the life of all biological organisms. The most common phosphorus containing functional group is phosphate. Phosphate esters are important to DNA and RNA but also play important roles in metabolism, from high energy intermediates such as ATP, to regulation, such as post translational modifications (1,2). While phosphate receives most of the attention, other phosphorus containing functional groups appear in natural products such as phosphoramidates (phosphorus-nitrogen bonds), phosphorothioates (phosphorus-sulfur bonds), and phosphonates (phosphorus-carbon bonds).

Phosphoramidates are compounds that contain a high energy phosphorus nitrogen bond. Currently, there are approximately 55 phosphoramidate containing natural products known to exist (3). Phosphoramidates are believed to be rare in nature; however, due to their instability the prevalence of phosphoramidates may be overlooked due to biased isolation methods. A defining characteristic of phosphoramidate bonds is acid lability, so any method utilizing acid is biased against detecting phosphoramidates (4). Formic acid is often added to samples analyzed by mass spectrometry to assist in the ionization of the molecule. While the amount of formic acid is small, usually 0.1%, this may be enough to hydrolyze the phosphoramidate bond before analysis (5). In the initial determination of the capsular polysaccharide structure in *Campylobacter jejuni* NCTC11168 no phosphoramidate was detected (6). A study later showed that the initial

characterization was incomplete, and the capsule contained two O-methyl phosphoramidate modifications, and upon further analysis it is now believed that 70% of all *C. jejuni* strains contain this phosphoramidate (7,8).

Approximately 55 different phosphoramidate natural products are known to exist and are discussed in a recent review (2). Surprisingly very little is known about the biosynthesis of phosphoramidate bonds. Currently four strategies for the formation of phosphoramidate bonds have been elucidated. The first strategy utilizes a kinase that catalyzes the ATP dependent phosphorylation of a substrate generating ADP and the phosphorylated product. A second strategy employs the use of a different family of kinases that are related to phosphoenolpyruvate synthase and pyruvate phosphate dikinase. Members of this family of kinases generate AMP and phosphate in addition to their phosphorylated product. The third strategy for the synthesis of a phosphoramidate involves the use of an enzyme related to tRNA synthetase where the phosphoramidate bond is formed by adenylation and not phosphorylation. The fourth and final strategy utilizes an ammonia adenylyltransferase enzyme. Where ammonia acts as a nucleophile to attack an activated phosphoryl center. These four strategies will be discussed here.

1.2. Strategy 1: Direct Phosphorylation (Phosphagen Kinases)

The first strategy for the formation of a phosphoramidate bond uses kinases that catalyze the direct phosphorylation of their substrate using ATP, resulting in the formation of ADP and the phosphoramidate product. Currently there are nine natural products known that are formed in this manner, phosphoarginine, phosphocreatine,

phosphotaurocyamine, phosphohypotaurocyamine, phosphoguanidinoacetate phosphoagmatine, phospholombricine, phosphoopheline, and phosphothalassemine (Scheme 1) (2,9). Each of these natural products has a specific kinase associated with its formation (creatine kinase, arginine kinase, etc.) (10-18).

Scheme 1 Phosphagen Natural Products

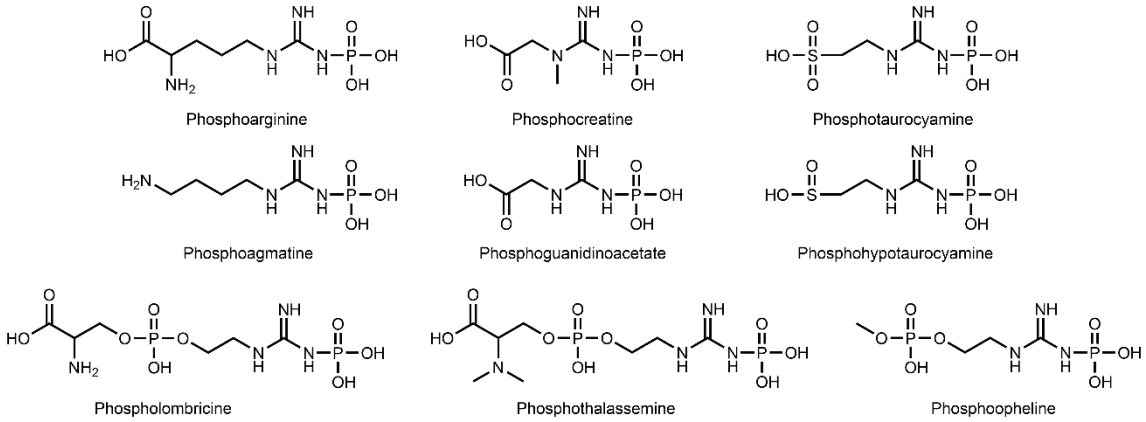

All nine of the characterized natural products share a structural similarity in that each product has been phosphorylated on a guanidino nitrogen. These natural products are all classified as phosphagens. Phosphagens and their respective kinases are used as a biological buffer for intracellular ATP and ADP concentrations. Higher levels of phosphagens and phosphagen kinases are found in cells that have variable energy requirements, for example skeletal muscles (2). This buffer system allows for rapid conversion of phosphagen and ADP to ATP and the phosphagen precursor (2).

1.3. Strategy 2: AMP Forming Kinases

Another strategy for the formation of a phosphoramidate bond is through the use of an AMP forming kinase. These kinases are related to phosphoenolpyruvate (PEP) synthase and pyruvate phosphate dikinase. This family of kinases differs from those previously discussed in that the product of these kinases is AMP and not ADP. Pyruvate phosphate dikinases and PEP synthase both consist of three separate domains, an ATP-grasp domain, a pyruvate/PEP binding domain and a phosphohistidine domain (19,20). Characterization of these enzymes shows that the phosphohistidine domain has a nucleophilic histidine residue that attacks the β-phosphoryl group of ATP, generating AMP and a pyrophosphorylated enzyme intermediate, this pyrophosphorylated enzyme intermediate is then hydrolyzed, and the phosphorylated histidine is used to transfer phosphate to pyruvate forming PEP (20,21). Currently there are two characterized enzymes that use a similar mechanism to form a phosphoramidate bond (25,27). Systems that use this strategy to form a phosphoramidate bond may contain a gene annotated as a phosphoenolpyruvate synthase.

O-methyl phosphoramidate is an unusual modification that is found on the capsular polysaccharide of *Campylobacter jejuni* that helps the organism evade host immune responses (Scheme 2) (22,23). A gene cluster has previously been identified as likely being responsible for the biosynthesis of this phosphoramidate (6,24). Within this gene cluster the gene *cj1418* was initially annotated as a PEP synthetase/ pyruvate phosphate dikinase. Initial predictions thought Cj1418 would catalyze the phosphorylation of ammonia, however ammonia showed no activity with the enzyme

(25). The enzyme has been shown to catalyze the phosphorylation of L-glutamine to form L-glutamine phosphate (Scheme 2) (25). The formation of L-glutamine phosphate has been characterized by NMR and mass spectrometry. This is the first example of an enzyme catalyzing the phosphorylation of an amide, and is the first instance in which L-glutamine has ever been shown to be phosphorylated. More information about glutamine kinase can be found in chapters 2 and 5.

Scheme 2 Structure of the *Campylobacter jejuni* O-Methyl Phosphoramidate Modification and the Reaction Catalyzed by Glutamine Kinase (Cj1418).

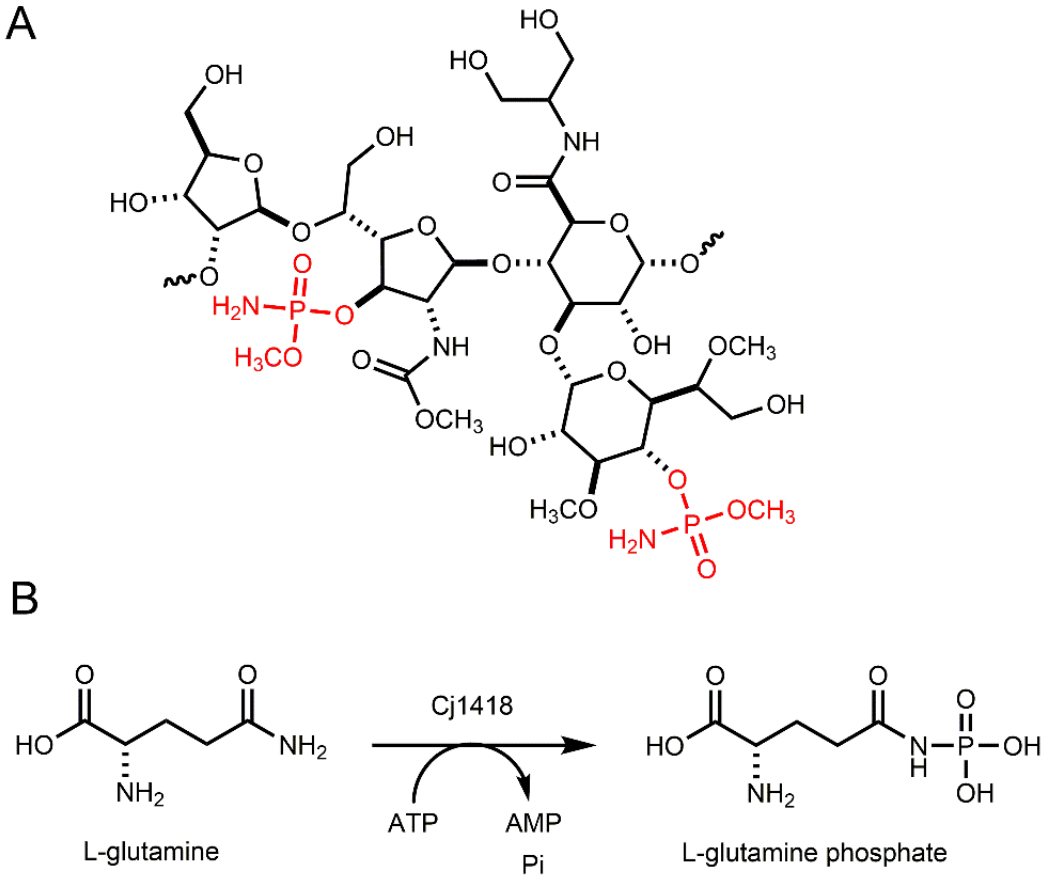

Phosphoramidon (Scheme 23) has previously been isolated from *Streptomyces* cultures and has been shown to have activity as a metalloendopeptidase inhibitor (26). Recently the genome of *Streptomyces mozunenis* MK-23, was sequenced and a gene cluster for the biosynthesis of phosphoramidon was identified and characterized (27). One gene with the locus tag *talE* was annotated as a potential PEP synthase/ pyruvate phosphate dikinase. Due to the structure of phosphoramidon it was predicted that TalE would catalyze the phosphorylation of the α-amino group of the leucine-tryptophan dipeptide precursor (27). The activity of the enzyme was confirmed by NMR, and it was demonstrated that TalE catalyzed the phosphorylation of the α-amino group as predicted (27). TalE is recognized as being the first enzyme in natural product biosynthesis to catalyze the phosphorylation of a primary amine.

Scheme 3 Structure of Phosphoramidon

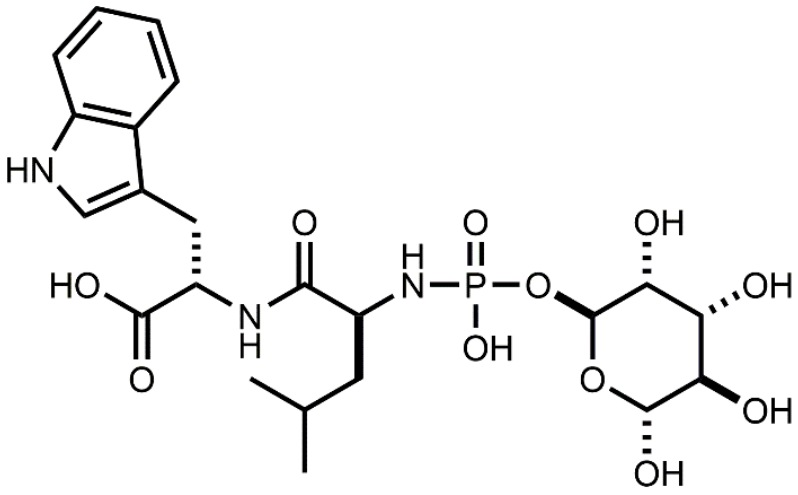

Phosphagen kinases and AMP forming kinases differ in two significant ways. Phosphagen kinases are similar to a majority of known kinases and catalyze the direct phosphorylation of their respective substrate. In this reaction only one phosphoanhydride bond has been cleaved and ADP is the product. These phosphagen kinases must be reversible, as their physiological role is to act as an ATP buffer system (9). AMP forming kinases cleave both the phosphoanhydride bonds of ATP, releasing more energy than the phosphagen kinase. This dual hydrolysis may be out of necessity in that phosphorylating a primary amine or an amide may require more energy than a guanidino group. However the reaction these kinases catalyze are irreversible, and this dual hydrolysis may be a commitment step to their respective metabolic pathways. It is unclear as to why L-glutamine and a leucine-tryptophan dipeptide would require a special kinase.

1.4. Strategy 3: Adenylation (tRNA Synthetases)

The third strategy for the formation of a phosphoramidate is through the use of a class of enzymes that are related to tRNA synthetases. Currently, Microcin C7 is the only known phosphoramidate containing natural product to use an enzyme related to tRNA synthetases (Scheme 4) (28). Microcin C7 is an *E. coli* produced peptide that is adenylylated through a phosphoramidate bond on the C-terminus (29). Hydrolysis of this peptide between residues six and seven results in the release of an adenylylated aspartic acid analogue that inhibits aspartyl-tRNA synthetase, preventing protein synthesis (Scheme 4) (28,30). The enzyme responsible for the formation of the

phosphoramidate bond is MccB. The mechanism for the formation of the phosphoramidate bond is proposed (28).

Scheme 4 Structure of Microcin C7 and the Toxic Adenylated Aspartic Acid Analogue

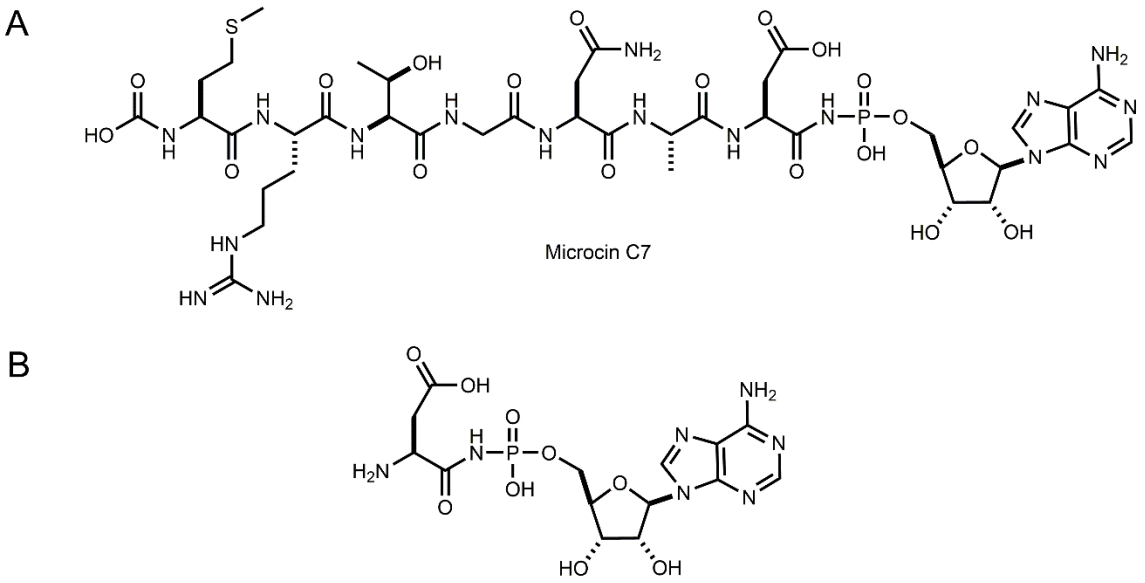

In the proposed mechanism the carboxylate group of the C-terminal asparagine residue attacks the α-phosphate of ATP forming pyrophosphate and an adenylylated peptide (28). The side chain amide group from asparagine attacks the acyl-AMP anhydride which generates AMP and a succinimide. A synthetic version of the succinimide was tested as a substrate for MccB, and activity was observed confirming this as an intermediate in the MccB reaction (28). Then it is proposed that the nitrogen

of the succinimide group attacks the α-phosphate group of the second equivalent of ATP, resulting in the final phosphoramidate product (28).

This strategy is unique from both AMP forming kinases and phosphagen kinases, in that the mode of generating the phosphoramidate is by adenylylation and not through phosphorylation. There is however a similarity between AMP forming kinases and MccB, in that the formation requires two phosphoanhydride bonds to be cleaved for the formation of the phosphoramidate. One is cleaved to activate aspartate, forming a succinimide ring, and the second is the formation of the final product. Annotated enzymes that may use this strategy for phosphoramidate biosynthesis are potentially annotated as tRNA synthetases.

1.5. Strategy 4: Ammonia Adenylyltransferase

The final known strategy for the formation of a phosphoramidate bond is through the use of an ammonia adenylyltransferase. This enzyme was first discovered in the green algae *Auxenochlorella pyrenoidosa* but homologs have been identified in many other organisms including *E. coli* (31,32). Ammonia adenylyltransferase catalyzes the nucleophilic attack of ammonia to the α-phosphate group of adenylyl sulfate, resulting in the formation of adenosine 5'-phosphoramidate (AMP-NH_2) and sulfate (Scheme 5). Despite being found in many different organisms, including mammals, the biological role of AMP-NH_2 is unknown.

Scheme 5 Reaction Catalyzed by Ammonia Adenylyltransferase

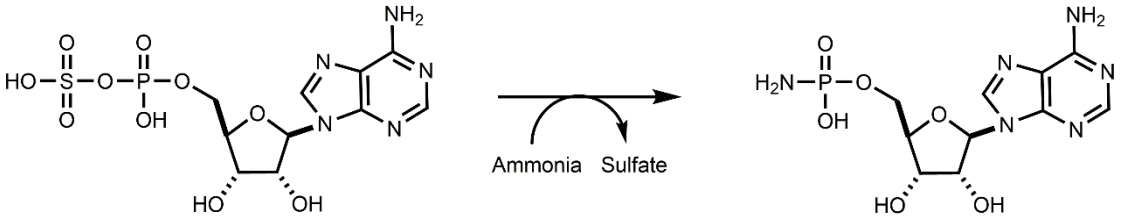

While the biological role of AMP-NH_2 is unknown, several enzymes have been identified that are capable of degrading this natural product (33). Enzymes that degrade AMP-NH_2 either hydrolyze the phosphoramidate bond and produce AMP or displace ammonia with phosphate and form ADP (33). The enzymes that catalyze these reactions belong to the histidine triad superfamily (34).

1.6. Uncharacterized Biosynthetic Pathways

Currently the biosynthesis of phosphoramidate containing natural products is poorly understood. In many cases the genes responsible for the biosynthesis of the phosphoramidate natural product have not been identified, or the genome is not available, making the biosynthetic characterization of these phosphoramidates difficult or impossible. Currently the biosynthetic gene cluster has been identified for two phosphoramidate containing natural products, but the formation of the phosphoramidate is still not characterized.

1.6.1. Agrocin 84

Agrocin 84 contains two phosphoramidate moieties and has been isolated from *Agrobacterium radiobacter* K84 (Scheme 6) (35). This compound has been found to have antimicrobial activity against *Agrobacterium tumefaciens* which is responsible for crown gall disease in plants (36). *A. radiobacter* K84 has been used successfully to protect plants from crown gall disease; however, strains unable to make Agrocin 84 are unable to prevent disease (36). While the structure of Agrocin 84 has been determined, the biosynthesis of this compound is unknown.

Scheme 6 Structure of Agrocin 84

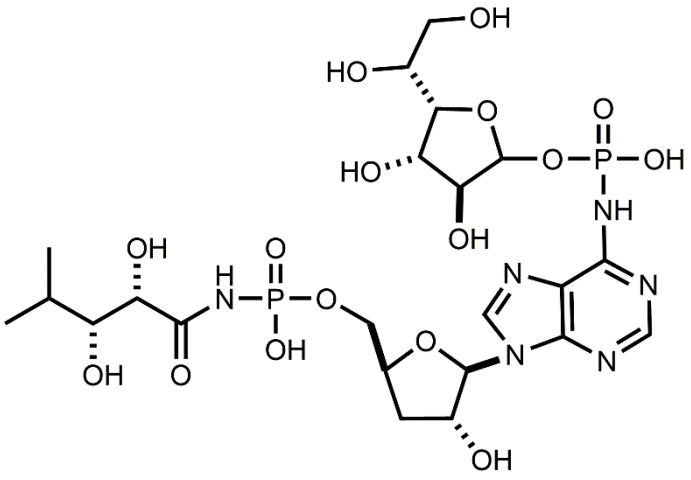

The genes for the biosynthesis, and immunity to Agrocin 84 were identified on a 45 kb plasmid pAgK84 (35). This plasmid has been shown to contain 36 possible open reading frames and of these possible reading frames, one is an annotated asparaginyl-tRNA synthetase, and two and annotated phosphoenolpyruvate synthases (35). Agrocin 84, like microcin C7 contains a phosphoramidate bond on the α-phosphoryl group of AMP. It is predicted that the annotated asparaginyl-tRNA synthase may catalyze the formation of the phosphoramidate bond in a similar manner as MccB (28). The formation of the second phosphoramidate bond on the amino group of adenine could be formed by the annotated phosphoenolpyruvate synthases. However both of these synthases (467 and 301 amino acids) are small in comparison to glutamine kinase (779 amino acids) and TalE (712 amino acids). Since members of the phosphoenolpyruvate synthetase family contain three separate domains, it could be that these two enzymes form a complex and together form the second phosphoramidate bond.

While the biosynthesis of the phosphoramidate bonds in Agrocin 84 are unknown, the biosynthetic gene cluster contains both enzymes similar to aspartyl-tRNA synthetase, and phosphoenolpyruvate synthetase. It is not clear if this is how the two phosphoramidate linkages are formed, it however multiple strategies for forming phosphoramidate bonds may be employed to form a single natural product.

1.6.2. Phaseolotoxin

Phaseolotoxin is a phosphoramidate natural product isolated from *Pseudomonas syringae phaseolicola*, and causes halo blight disease in beans (37). Phaseolotoxin is a

tripeptide natural product, which upon cleavage by a protease releases octicidin which is a reversible inhibitor of ornithine carbamoyltransferase (Scheme 7). Octicidin is a unique natural product, as it contains the only know tri-phosphoramidate moiety and it is sulfated (Scheme 7) (38). The gene cluster for the biosynthesis of phaseolotoxin has previously been identified and consists of four operons and 23 genes (38). Within this cluster six genes have been characterized. ArgK encodes for an octicidin resistant homolog of ornithine carbamoyltransferase (39). PhtQ and PhtU which are both peptide ligases responsible for the formation of the phaseolotoxin tripeptide, and AmtA an amidino transferase that converts lysine and arginine to ornithine and homoarginine (40,41). PhtS and PhtA are an adenylyl sulfate kinase and a sulfotransferase which catalyzes the transfer of sulfate to the final phaseolotoxin product (42).

Scheme 7 Structures of Phaseolotoxin and Octicidin

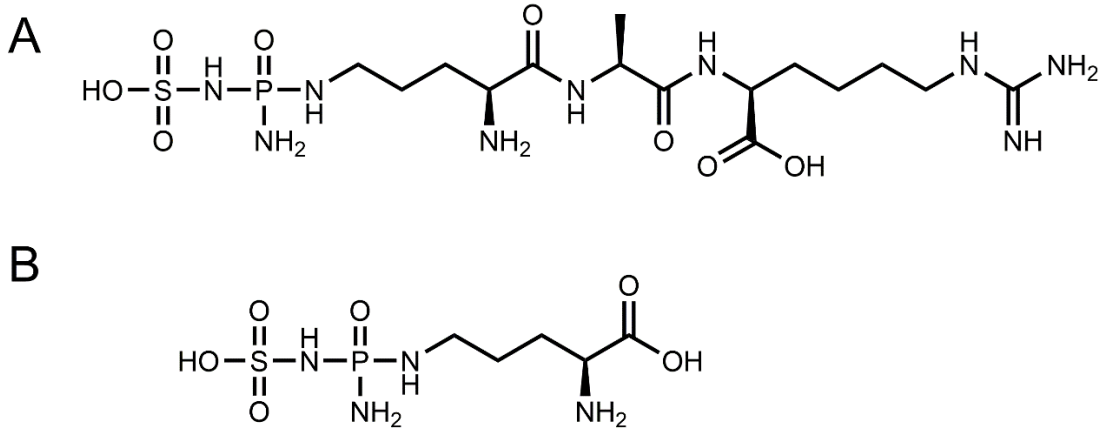

Within the phaseolotoxin biosynthesis gene cluster phtL is annotated as a phosphoenolpyruvate synthase (43,44). Investigations into the role of this protein in the biosynthesis have shown that PhtL is essential for the formation of phaseolotoxin and it appears to act as a regulator for the pathway (43). It is predicted that PhtL will catalyze the phosphorylation of ornithine, generating the first of three phosphoramidate bonds found in phaseolotoxin. Previously Chris Walsh's group from Harvard attempted to characterize the biosynthetic pathway for the formation of phaseolotoxin, however issues with solubility and protein expression hampered any progress (42). While it seems likely that PhtL will catalyze the formation of the first phosphoramidate bond, it is unclear how the second two phosphoramidates are formed, perhaps PhtJ and PhtK, two annotated dCTP deaminases or PhtF an annotated ornithine aminotransferase may play a role in the phosphoramidate formation.

1.7. O-Methyl Phosphoramidate

In this dissertation the discovery of L-glutamine kinase (Cj1418) from *Campylobacter jejuni* is discussed. L-glutamine kinase represents the first AMP forming kinase characterized that results in the formation of a phosphoramidate bond. In addition to L-glutamine kinase the activities of three other enzymes involved in the biosynthesis of O-methyl phosphoramidate are examined, Cj1416 a CTP:phosphoglutamine cytididylyltransferase, Cj1417 a γ-glutamyl-CDP-amidate hydrolase, and Cj1415 a cytidine diphosphoramidate kinase (25,45-48). The substrate specificity and chemical mechanism of L-glutamine kinase is also discussed, as is the

manganese induced promiscuity of Cj1416 (47,28). Together these four enzymes, Cj1418, Cj1417, Cj1416, and Cj1415, represent the first four enzymatic steps in the biosynthesis of the O-methyl phosphoramidate modification and produce a novel cofactor that can be used in the transfer of the phosphoramidate moiety.

1.8. References

1. Westheimer, F. (1987) Why Nature Chose Phosphates, *Science 235*, 1173-1178.
2. Hunter, T. (2012) Why Nature Chose Phosphate to Modify Proteins, *Philosophical transactions of the Royal Society of London. Series B, Biological sciences 367*, 2513-2516.
3. Petkowski, J. J., Bains, W., and Seager, S. (2019) Natural Products Containing 'Rare' Organophosphorus Functional Groups, *Molecules 24*, 866.
4. Garrison, A. W., and Boozer, C. E. (1968) The Acid-Catalyzed Hydrolysis of a Series of Phosphoramidates, *J. Am. Chem. Soc. 90*, 3486-3494.
5. Petrović, M., Hernando, M. D., Díaz-Cruz, M. S., and Barceló, D. (2005) Liquid Chromatography–Tandem Mass Spectrometry for the Analysis of Pharmaceutical Residues in Environmental Samples: a Review, *J. Chromatogr. 1067*, 1-14.
6. St., M. F., M., S. C., Jianjun, L., H., C. K., Huan, K. N., Suzon, L., W., W. W., Jean-Robert, B., and A., M. M. (2002) The Structures of the Lipooligosaccharide and Capsule Polysaccharide of *Campylobacter jejuni* Genome Sequenced Strain NCTC 11168, *Eur. J. Biochem. 269*, 5119-5136.
7. McNally, D. J., Lamoureux, M. P., Karlyshev, A. V., Fiori, L. M., Li, J., Thacker, G., Coleman, R. A., Khieu, N. H., Wren, B. W., Brisson, J.-R., Jarrell, H. C., and Szymanski, C. M. (2007) Commonality and Biosynthesis of the O-Methyl Phosphoramidate Capsule Modification in *Campylobacter jejuni*, *J. Biol. Chem. 282*, 28566-28576.

8. Szymanski, C. M., Michael, F. S., Jarrell, H. C., Li, J., Gilbert, M., Larocque, S., Vinogradov, E., and Brisson, J.-R. (2003) Detection of Conserved N-Linked Glycans and Phase-variable Lipooligosaccharides and Capsules from Campylobacter Cells by Mass Spectrometry and High Resolution Magic Angle Spinning NMR Spectroscopy, *J. Biol. Chem. 278*, 24509-24520.
9. Ellington, W. R. (2001) Evolution and Physiological Roles of Phosphagen Systems, *Annu. Rev. Physiol. 63*, 289-325.
10 Morrison, J. F., Griffiths, D. E., and Ennor, A. H. (1957) The Purification and Properties of Arginine Phosphokinase, *Biochem. J. 65*, 143-153.
11. Ennor, A. H., Rosenberg, H., and Armstrong, M. D. (1955) Specificity of Creatine Phosphokinase, *Nature 175*, 120.
12. Bush, D. J., Kirillova, O., Clark, S. A., Davulcu, O., Fabiola, F., Xie, Q., Somasundaram, T., Ellington, W. R., and Chapman, M. S. (2011) The Structure of Lombricine Kinase: Implications for Phosphagen Kinase Conformational Changes, *J. Biol. Chem. 286*, 9338-9350.
13. Piccinni, E., and Coppellotti, O. (1979) Phosphagens in protozoa—II. Presence of phosphagen kinase in Ochromonas danica, *Comparative Biochemistry and Physiology Part B: Comparative Biochemistry 62*, 287-289.
14. Van Thoai, N., Di Jeso, F., Robin, Y., and Der Terrossian, E. (1966) Sur la nouvelle acide adenosine 5′-triphosphorique: guanidine phosphotransferase, l'opheline kinase, *Biochimica et Biophysica Acta (BBA) - Enzymology and Biological Oxidation 113*, 542-550.

15. Nguyen Van, T., Robin, Y., and Guillou, Y. (1972) New phosphagen, N'-phosphorylguanidinoethylphospho-O-(α-N,N-dimethyl)serine (phosphothalassemine), *Biochemistry 11*, 3890-3895.
16. Virden, R., and Watts, D. C. (1964) The Distribution of Guanidine-Adenosine Triphosphate Phosphotransferases and Adenosine Triphosphatase in Animals from Several Phyla, *Comp. Biochem. Physiol. 13*, 161-177.
17. Van Thoai, N., Robin, Y., and Pradel, L.-A. (1963) Hypotaurocyamine Phosphokinase Comparaison Avec la Taurocyamine Phosphokinase, *Biochimica et Biophysica Acta (BBA) - Specialized Section on Enzymological Subjects 73*, 437-444.
18. Uda, K., Tanaka, K., Bailly, X., Zal, F., and Suzuki, T. (2005) Phosphagen Kinase of the Giant Tubeworm Riftia pachyptila: Cloning and expression of Cytoplasmic and Mitochondrial Isoforms of Taurocyamine Kinase, *Int. J. Biol. Macromol. 37*, 54-60.
19. Cooper, R. A., and Kornberg, H. L. (1967) The Mechanism of the Phosphoenolpyruvate Synthase Reaction, *Biochimica et Biophysica Acta (BBA) - General Subjects 141*, 211-213.
20. Lim, K., Read, R. J., Chen, C. C. H., Tempczyk, A., Wei, M., Ye, D., Wu, C., Dunaway-Mariano, D., and Herzberg, O. (2007) Swiveling Domain Mechanism in Pyruvate Phosphate Dikinase, *Biochemistry 46*, 14845-14853.

21. Evans, H. J., and Wood, H. G. (1968) The Mechanism of the Pyruvate, Phosphate Dikinase Reaction, *Proceedings of the National Academy of Sciences 61*, 1448-1453.
22. van Alphen, L. B., Wenzel, C. Q., Richards, M. R., Fodor, C., Ashmus, R. A., Stahl, M., Karlyshev, A. V., Wren, B. W., Stintzi, A., Miller, W. G., Lowary, T. L., and Szymanski, C. M. (2014) Biological Roles of the O-Methyl Phosphoramidate Capsule Modification in *Campylobacter jejuni*, *PLoS One 9*, e87051.
23. Young, K. T., Davis, L. M., and Dirita, V. J. (2007) *Campylobacter jejuni*: Molecular Biology and Pathogenesis, *Nat. Rev. Microbiol. 5*, 665-679.
24. Karlyshev, A. V., Champion, O. L., Churcher, C., Brisson, J.-R., Jarrell, H. C., Gilbert, M., Brochu, D., St Michael, F., Li, J., Wakarchuk, W. W., Goodhead, I., Sanders, M., Stevens, K., White, B., Parkhill, J., Wren, B. W., and Szymanski, C. M. (2005) Analysis of *Campylobacter jejuni* Capsular Loci Reveals Multiple Mechanisms for the Generation of Structural Diversity and the Ability to form Complex Heptoses, *Mol. Microbiol. 55*, 90-103.
25. Taylor, Z. W., Brown, H. A., Narindoshvili, T., Wenzel, C. Q., Szymanski, C. M., Holden, H. M., and Raushel, F. M. (2017) Discovery of a Glutamine Kinase Required for the Biosynthesis of the O-Methyl Phosphoramidate Modifications Found in the Capsular Polysaccharides of *Campylobacter jejuni*, *J. Am. Chem. Soc. 139*, 9463-9466.

26. Umezawa, S., Tatsuta, K., Izawa, O., Tsuchiya, T., and Umezawa, H. (1972) A New Microbial Metabolite Phosphoramidon (Isolation and Structure), *Tetrahedron Lett. 13*, 97-100.
27. Baulig, A., Helmle, I., Bader, M., Wolf, F., Kulik, A., Al-Dilaimi, A., Wibberg, D., Kalinowski, J., Gross, H., and Kaysser, L. (2019) Biosynthetic Reconstitution of Deoxysugar Phosphoramidate Metalloprotease Inhibitors using an N–P-Bond-Forming Kinase, *Chemical Science 10*, 4486-4490.
28. Roush, R. F., Nolan, E. M., Löhr, F., and Walsh, C. T. (2008) Maturation of an *Escherichia coli* Ribosomal Peptide Antibiotic by ATP-Consuming N−P Bond Formation in Microcin C7, *J. Am. Chem. Soc. 130*, 3603-3609.
29. Novoa, M. A., Díaz-Guerra, L., San Millán, J. L., and Moreno, F. (1986) Cloning and Mapping of the Genetic Determinants for Microcin C7 Production and Immunity, *J. Bacteriol. 168*, 1384-1391.
30. Metlitskaya, A., Kazakov, T., Kommer, A., Pavlova, O., Praetorius-Ibba, M., Ibba, M., Krasheninnikov, I., Kolb, V., Khmel, I., and Severinov, K. (2006) Aspartyl-tRNA Synthetase Is the Target of Peptide Nucleotide Antibiotic Microcin C, *J. Biol. Chem. 281*, 18033-18042.
31. Fankhauser, H., Berkowitz, G. A., and Schiff, J. A. (1981) A Nucleotide with the Properties of Adenosine 5′ Phosphoramidate from *Chlorella* Cells, *Biochem. Biophys. Res. Commun. 101*, 524-532.
32. Fankhauser, H., Schiff, J. A., and Garber, L. J. (1981) Purification and Properties of Adenylyl Sulphate:Ammonia Adenylyltransferase from *Chlorella* Catalysing the

Formation of Adenosine 5' -Phosphoramidate from Adenosine 5' -Phosphosulphate and Ammonia, *The Biochemical Journal 195*, 545-560.

33. Wojdyła-Mamoń, Anna M., and Guranowski, A. (2015) Adenylylsulfate–Ammonia Adenylyltransferase Activity is Another Inherent Property of Fhit Proteins, *Biosci. Rep. 35*. 1-8
34. Chou, T.-F., Baraniak, J., Kaczmarek, R., Zhou, X., Cheng, J., Ghosh, B., and Wagner, C. R. (2007) Phosphoramidate Pronucleotides: A Comparison of the Phosphoramidase Substrate Specificity of Human and Escherichia coli Histidine Triad Nucleotide Binding Proteins, *Mol. Pharm. 4*, 208-217.
35. Kim, J.-G., Park, B. K., Kim, S.-U., Choi, D., Nahm, B. H., Moon, J. S., Reader, J. S., Farrand, S. K., and Hwang, I. (2006) Bases of Biocontrol: Sequence Predicts Synthesis and mode of Action of Agrocin 84, the Trojan Horse Antibiotic that Controls Crown Gall, *Proceedings of the National Academy of Sciences 103*, 8846-8851.
36. Otten, L., Burr, T., and Szegedi, E. (2008) Agrobacterium: A Disease-Causing Bacterium, In *Agrobacterium: From Biology to Biotechnology* (Tzfira, T., and Citovsky, V., Eds.), pp 1-46, Springer New York, New York, NY.
37. Mitchell, R. E., and Bieleski, R. L. (1977) Involvement of Phaseolotoxin in Halo Blight of Beans, *Transport and Conversion to Functional Toxin 60*, 723-729.
38. Aguilera, S., López-López, K., Nieto, Y., Garcidueñas-Piña, R., Hernández-Guzmán, G., Hernández-Flores, J. L., Murillo, J., and Alvarez-Morales, A. (2007) Functional characterization of the gene cluster from Pseudomonas syringae pv.

phaseolicola NPS3121 involved in synthesis of phaseolotoxin, *J. Bacteriol. 189*, 2834-2843.

39. Chen, L., Li, P., Deng, Z., and Zhao, C. (2015) Ornithine Transcarbamylase ArgK Plays a Dual role for the Self-defense of Phaseolotoxin Producing Pseudomonas syringae pv. phaseolicola, *Sci. Rep. 5*, 12892.
40. Hernández-Guzmán, G., and Alvarez-Morales, A. (2001) Isolation and Characterization of the Gene Coding for the Amidinotransferase Involved in the Biosynthesis of Phaseolotoxin in Pseudomonas syringae pv. phaseolicola, *Mol. Plant-Microbe Interact. 14*, 545-554.
41. Arai, T., and Kino, K. (2008) A Novel <small>L</small>-Amino Acid Ligase Is Encoded by a Gene in the Phaseolotoxin Biosynthetic Gene Cluster from Pseudomonas syringae pv. phaseolicola 1448A, *Biosci., Biotechnol., Biochem. 72*, 3048-3050.
42. Roush, R. F. (2011) Biosynthesis of Nitrogen-Phosphorus Bond Containing Peptide Natural Products, *ProQuest Dissertations and Theses*, 1-163.
43. González-Villanueva, L., Arvizu-Gómez, J. L., Hernández-Morales, A., Aguilera-Aguirre, S., and Álvarez-Morales, A. (2014) The PhtL Protein of *Pseudomonas syringae pv. phaseolicola* NPS3121 Affects the Expression of both Phaseolotoxin Cluster (Pht) and Non-Pht Encoded Genes, *Microbiol. Res. 169*, 221-231.
44. Aguilera, S., Alvarez-Morales, A., Murillo, J., Hernández-Flores, J. L., Bravo, J., and De la Torre-Zavala, S. (2017) Temperature-Mediated Biosynthesis of the

Phytotoxin Phaseolotoxin by *Pseudomonas syringae pv. phaseolicola* Depends on the Autoregulated Expression of the phtABC Genes, *PLoS One 12*, e0178441.

45. Taylor, Z. W., Brown, H. A., Holden, H. M., and Raushel, F. M. (2017) Biosynthesis of Nucleoside Diphosphoramidates in *Campylobacter jejuni*, *Biochemistry 56*, 6079-6082.
46. Taylor, Z. W., and Raushel, F. M. (2018) Cytidine Diphosphoramidate Kinase: An Enzyme Required for the Biosynthesis of the O-Methyl Phosphoramidate Modification in the Capsular Polysaccharides of *Campylobacter jejuni*, *Biochemistry 57*, 2238-2244.
47. Taylor, Z. W., and Raushel, F. M. (2019) Manganese-Induced Substrate Promiscuity in the Reaction Catalyzed by Phosphoglutamine Cytidylyltransferase from *Campylobacter jejuni*, *Biochemistry 58*, 2144-2151.
48. Taylor, Z. W., Chamberlain, A. R., and Raushel, F. M. (2018) Substrate Specificity and Chemical Mechanism for the Reaction Catalyzed by Glutamine Kinase, *Biochemistry 57*, 5447-5455.

2. DISCOVERY OF A GLUTAMINE KINASE REQUIRED FOR THE BIOSYNTHESIS OF THE O-METHYL PHOSPHORAMIDATE MODIFICATIONS FOUND IN THE CAPSULAR POLYSACCHARIDES OF *CAMPYLOBACTER JEJUNI*[*]

2.1. Introduction

Campylobacter jejuni is a Gram-negative bacterium that causes foodborne gastroenteritis in humans worldwide (1). It is commonly found in chickens, and as a consequence contaminated poultry are a significant reservoir for human disease. Whereas infection with *C. jejuni* is typically self-limiting, in rare cases it can lead to the subsequent development of Guillain-Barré syndrome, a devastating acute polyneuropathy (2). Like many Gram-positive and Gram-negative organisms, *C. jejuni* produces capsular polysaccharides, which are composed of chains of sugars that form extensive layers surrounding the outer surface of the bacterium. In some cases, these chains can be composed of more than 200 sugars (3). The capsular polysaccharides, hereafter referred to as CPS, protect the organism from the environment and from complement-mediated phagocytosis and killing (4). It is now well documented that, in *C. jejuni*, the CPS is important for colonization and invasion of the host organism (5). More than 40 serological strains of *C. jejuni* have been identified, and each strain is

[*] Reprinted with permission from " Discovery of a Glutamine Kinase Required for the Biosynthesis of the O-Methyl Phosphoramidate Modifications Found in the Capsular Polysaccharides of *Campylobacter jejuni*" by Zane W. Taylor, Haley A. Brown, Tamari Narindoshvili, Cory Q. Wenzel, Christine M. Szymanski, Hazel M. Holden, and Frank M. Raushel, *Journal of the American Chemical Society*, (2017) *139* (28), pp 9463-9466, Copyright 2017 American Chemical Society

likely to produce structural variations to the CPS (6,7). These modifications are involved in a complex strategy for evasion of both bacteriophage predation and host defense systems (4,8). In *C. jejuni* strain NCTC11168, a cluster of 35 genes has been identified as being responsible for the synthesis and export of the CPS (9).

By far the most unusual modification to the CPS of *C. jejuni* is the addition of O-methyl phosphoramidate groups (MeOPN) attached to the polysaccharide backbone. For example, in *C. jejuni* strain NCTC11168, C3 of a 2-acetamido-2-deoxy-β-D-galactofuranose (**I**) moiety is decorated with an O-methyl phosphoramidate group, and the CPS of the hypermotile variant of this strain (11168H) has an additional MeOPN modification at C4 of a derivative of D-glycero-α-L-gluco-heptopyranose (**II**) as illustrated in Scheme 8 (6,7). The occurrence of P−N bonds in biological systems is relatively rare (creatine phosphate and arginine phosphate are notable exceptions), and the presence of the O-methyl phosphoramidate groups in the capsular polysaccharides of *C. jejuni* plays a significant role in its pathogenicity (5). In *C. jejuni* 11168H, genes with the locus tags cj1418c, cj1417c, cj1416c, and cj1415c have been implicated in the biosynthesis of the phosphoramidate moiety (**III**) of the CPS but the pathway leading to the formation of the P−N bond in this organism has not been elucidated (10).

Scheme 8 Phosphoramidate Intermediates and Products

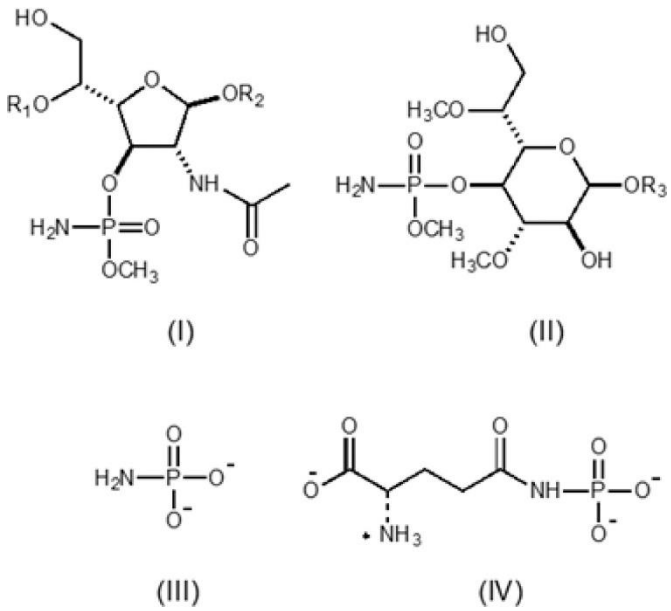

The focus of this investigation is on the catalytic functions of Cj1418 and Cj1417. Cj1418 is a member of cog0574, and this enzyme is currently annotated as a putative PEP synthase or a pyruvate phosphate dikinase (11,12). Structurally characterized enzymes in this family are composed of three distinct protein segments, including an ATP-grasp domain, a PEP/pyruvate binding region, and a phosphohistidine domain (9). The amino acid sequence of Cj1418 suggests that it has an N-terminal ATP-grasp domain (residues 1−219) and a C-terminal phosphohistidine domain (residues 694−767). However, its central domain (residues 220−693) does not appear to be homologous to any of the known PEP/pyruvate binding regions. The closest structurally characterized homologue to Cj1418 with a known catalytic activity is rifampin phosphotransferase (23% sequence identity) from *Listeria monocytogenes* (PDB id: 5FBS, 5FBT, and 5FBU) (13). This enzyme catalyzes the ATP-dependent phosphorylation of the antibiotic rifampin via a mechanism that involves the pyrophosphorylation of His-825, hydrolysis of this intermediate to generate a phosphorylated histidine intermediate, and subsequent phosphoryl transfer to rifampin (13,14).

Cj1417 is a member of cog2071 and is annotated as a type I glutamine amidotransferase (11,15). This class of enzymes catalyzes the hydrolysis of glutamine (or structurally similar glutamine analogs) via the formation of a thioester intermediate with an active site cysteine residue (15). In many cases, such as in carbamoyl phosphate synthetase, the hydrolysis of glutamine is coupled to an ATP-dependent phosphorylation of a second substrate by an associated synthetase domain/subunit (16). We thus initially

proposed that the combined activities of Cj1418 and Cj1417 would likely be required for the *in vivo* formation of the putative phosphoramidate intermediate (III) during the biosynthesis of the O-methylphosphoramidate groups. In our proposed mechanism, the first reaction is initiated by the Cj1417 dependent hydrolysis of glutamine to form glutamate and ammonia. This step is subsequently followed by the phosphorylation of ammonia via the catalytic activity of Cj1418 Scheme 9.

Scheme 9 Predicted Functions of Cj1417 and Cj1417

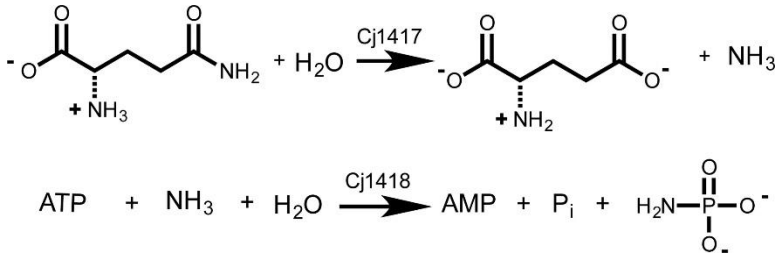

2.2. Expression and Purification of Cj1418

The gene for the expression of Cj1418 with an N-terminal hexa-histidine purification tag was cloned from the genomic DNA of *C. jejuni* 11168H into a modified form of the pET-28b expression vector (17). This vector was subsequently used to transform Rosetta (DE3) *Escherichia coli*, and the cells were subsequently grown in a medium of lysogeny broth at 30 °C. Following induction with 1.0 mM IPTG, the cells were allowed to grow at 16 °C for 16 h. After cell lysis and centrifugation,

Cj1418 was purified using Ni-affinity chromatography and the excess imidazole was removed by dialysis. The purified protein was concentrated and stored at −80 °C. Approximately 4 mg of Cj1418 were purified from 1.0 L of the original cell culture.

2.3. Results and Discussion

To test our initial prediction that Cj1418 was required for the ATP-dependent phosphorylation of ammonia, we first incubated the enzyme (5.0 μM) in the presence of 2.0 mM $MgCl_2$ and 1.0 mM ATP in 100 mM HEPES buffer (pH 8.0) at 30 °C. This control experiment was monitored using anion exchange chromatography by measuring the changes in the concentration of ATP at 255 nm. After an incubation period of ~60 min, the concentration of ATP (retention time of 8.2 min) did not change significantly but relatively small amounts of AMP (retention time of 5.3 min) and ADP (retention time of 7.1 min) could be detected (Figure 1A). The addition of 100 mM NH_4Cl did not change the amounts of AMP or ADP that were produced (Figure 1B).

Since catalytic activity was not observed with ammonia, Cj1418 was next assayed in the presence of 5.0 mM L-glutamine. After an incubation period of ~60 min, all of the ATP was converted to AMP (Figure 1C). The reaction mixture was subsequently examined by ^{31}P NMR spectroscopy, and resonances were observed for AMP at 4.36 ppm and at 3.03 ppm for inorganic phosphate (Figure 2A). Two additional resonances were observed at −3.57 and −4.06 ppm. Integration of the signal intensities for the sum of these two resonances equaled those observed for either AMP or Pi. The observed chemical shifts (−3.57 and −4.06 ppm) for the new phosphate containing product(s) did not match the ^{31}P NMR spectrum for authentic phosphoramidate (**III**) at 1.3 ppm (18).

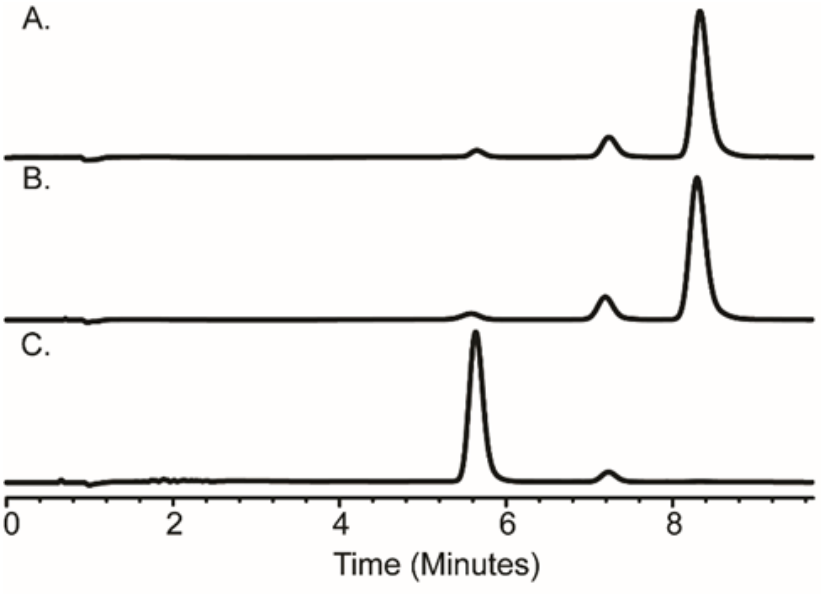

Figure 1. Anion exchange chromatograms of the reaction products when Cj1418 (5.0 μM) and 100 mM HEPES buffer (pH 8.0) were incubated for 60 minutes at room temperature with: (A) 1.0 mM ATP and 2.0 mM $MgCl_2$. (B) 1.0 mM ATP, 2.0 mM $MgCl_2$ and 100 mM NH_4Cl. (C) 1.0 mM ATP, 2.0 mM $MgCl_2$, and 5.0 mM L-glutamine. Peak retention times correspond to the following: AMP (5.3 minutes), ADP (7.1 minutes) and ATP (8.2 minutes).

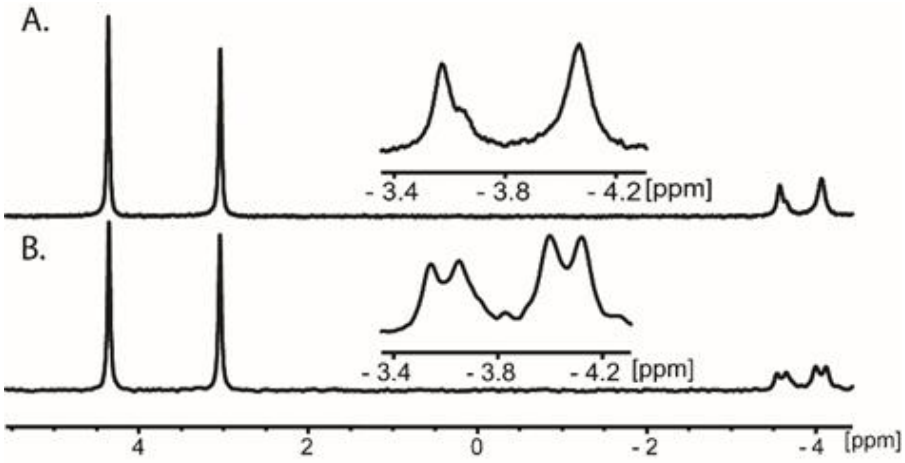

Figure 2 (A) ^{31}P NMR spectrum of the reaction products when Cj1418 was mixed with MgATP and L-glutamine. The resonance at 4.36 ppm is from AMP, and the resonance at 3.03 ppm is from inorganic phosphate. The resonances at -3.57 and -4.06 ppm correspond to L-glutamine phosphate (**IV**). (B) ^{31}P NMR spectrum of the reaction products when Cj1418 was mixed with MgATP and L-glutamine-(amide-^{15}N). The phosphorus resonances at -3.57 and -4.06 are now doublets due to the apparent spin coupling with the adjacent ^{15}N-nucleus.

The most likely (but initially unexpected) product to form from the reaction catalyzed by Cj1418 is L-glutamine-phosphate (**IV**) where the amide nitrogen is phosphorylated. To test this conjecture, the reaction was repeated using L-glutamine with an ^{15}N-label exclusively at the amide nitrogen. The two ^{31}P resonances of the reaction product now appear as doublets, due to the apparent spin coupling with the ^{15}N-labeled amide nitrogen (Figure 2B). The observed coupling constants $J(^{15}N–^{31}P)$ are 18 Hz for the phosphorus resonance at −3.57 ppm and 21 Hz for the resonance at −4.06 ppm. The magnitude of this coupling constant is consistent with that previously observed for phosphocreatine, which exhibits a $J(^{15}N–^{31}P)$ coupling constant of 18−20 Hz (19). The most likely explanation for the observation of two distinct ^{31}P NMR signals for this compound is the restricted rotation of the amide functional group thereby giving rise to separate resonances for the *syn*- and *anti*- conformations of the L-glutamine-phosphate product. This conclusion is further supported by the direct chemical synthesis of L-glutamine phosphate (20). Two phosphorus resonances for the sodium salt of this compound are observed in D_2O at−3.5 and −3.7 ppm. A single resonance is observed at −5.10 ppm for the free acid where the rate of rotation about the amide bond is expected to increase.

The formation of L-glutamine-phosphate after incubation of Cj1418, ATP, and L-glutamine is further supported by the mass spectrum (ESI negative mode) of the unfractionated reaction mixture. A peak that corresponds to the mass of the expected L-glutamine phosphate is observed with an m/z of 225.03 for the $(M - H)^-$ species and at an m/z of 247.01 $(M - 2H + Na)^-$ for the sodium adduct (Figure 3). Several other major peaks are observed that correspond to the known compounds in the unfractionated reaction mixture including phosphate (m/z = 96.96), HEPES (m/z = 237.09), and AMP (m/z = 346.05).

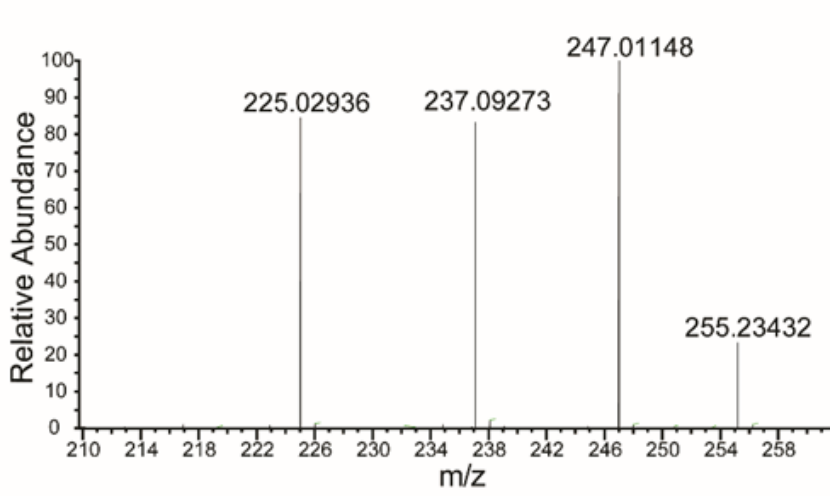

Figure 3 Negative ESI mass spectrum of the reaction mixture when Cj1418 was mixed with 2.0 mM ATP and 5.0 mM L-glutamine at pH 8.0 in 100 mM sodium bicarbonate buffer (pH 8.0). The identified ions correspond to L-glutamine phosphate (m/z = 225.03 for M-H and m/z = 247.01 for M-2H+Na), and HEPES (from enzyme purification) (m/z = 237.09 for M-H).

The kinetic parameters for the phosphorylation of L-glutamine by ATP as catalyzed by Cj1418 at pH 8.0 and 30 °C were determined spectrophotometrically at 340 nm using a coupled enzyme assay that measures the formation of AMP. The assay contained adenylate kinase (8 units/mL), pyruvate kinase (8 units/mL), and lactate dehydrogenase (8 units/mL) in the presence of 11 mM $MgCl_2$, 0.40 mM NADH, and 2.0 mM PEP (21). Under these conditions the apparent kinetic constants for Cj1418 are k_{cat} = 2.5 ± 0.3 s^{-1}, K_{ATP} = 340 ± 70 μM, k_{cat}/K_{ATP} = 7400 ± 1700 M^{-1} s^{-1}, K_{Gln} = 640 ± 60 μM, and k_{cat}/K_{Gln}= 3900 ± 800 M^{-1} s^{-1}. No catalytic activity was observed (<1% of the rate with L-glutamine) in the presence of either L-glutamate (10 mM) or L-asparagine (10 mM).

Quite unexpectedly, we have shown that Cj1418, an enzyme involved in the biosynthesis of the O-methyl phosphoramidate groups in *C. jejuni*, catalyzes the phosphorylation of the amide nitrogen of L-glutamine, rather than ammonia. However, it has been shown previously that utilization of $^{15}NH_4Cl$ in the medium for growth of *C. jejuni* results in ^{15}N-labeling of the MeOPN groups in whole cells (22). Our current results suggest that the ammonia must first be transformed to L-glutamine, presumably by the action of L-glutamine synthetase. To the best of our knowledge our results represent the first documented case of an enzyme-catalyzed phosphorylation of a simple amide nitrogen. However, similar compounds have been chemically synthesized as potential inhibitors of D-alanine:D-alanine ligase (20,23) and aspartate semi-aldehyde dehydrogenase (24). Glutamine synthetase has also been demonstrated to catalyze the phosphorylation of L-methionine-S-sulfoximine on nitrogen (25). The identity of L-

glutamine phosphate was confirmed by ^{31}P NMR experiments, ^{15}N-labeling, and mass spectrometry. These results have further demonstrated that the initial series of steps as proposed in Scheme 9 for the biosynthesis of the O-methyl phosphoramidate capsule modification in *C. jejuni* is incorrect. A more likely scenario for phosphoramidate biosynthesis is illustrated in Scheme 10. In this modified pathway, L-glutamine phosphate is hydrolyzed by Cj1417 to generate phosphoramidate (**III**). The closest functionally characterized homologue of Cj1417 is γ-L-glutamyl-γ-aminobutyrate hydrolase (PuuD) from *E. coli*. This protein has a 23% sequence identity with Cj1417, and thus homologous amidotransferase enzymes can catalyze the hydrolysis of substrates other than L-glutamine (26). In the next step we postulate that Cj1416 catalyzes the displacement of pyrophosphate by phosphoramidate (**III**) from a nucleotide triphosphate (NTP) to form the phosphoramidate of NDP (**V**). Cj1416 is a member of cog1213, and homologous enzymes have been shown to catalyze similar reactions. For example, CTP:phosphocholine cytidylyltransferase from Streptococcus pneumonia (LicC) catalyzes the formation of CDP-choline from CTP and choline phosphate (27). Alternatively, Cj1416 may catalyze the formation of NDP-glutamine (**VI**) through the displacement of pyrophosphate from NTP by L-glutamine-phosphate (IV). The NDP phosphoramidate (**V**) would then be formed by the catalytic activity of Cj1417. Experiments are currently under way to firmly establish the catalytic activities of Cj1417, Cj1416, and the remaining transformations that lead to the biosynthesis of this fascinating modification to the capsular polysaccharides of *C. jejuni*.

Scheme 10 Proposed Pathway for MeOPN Biosynthesis

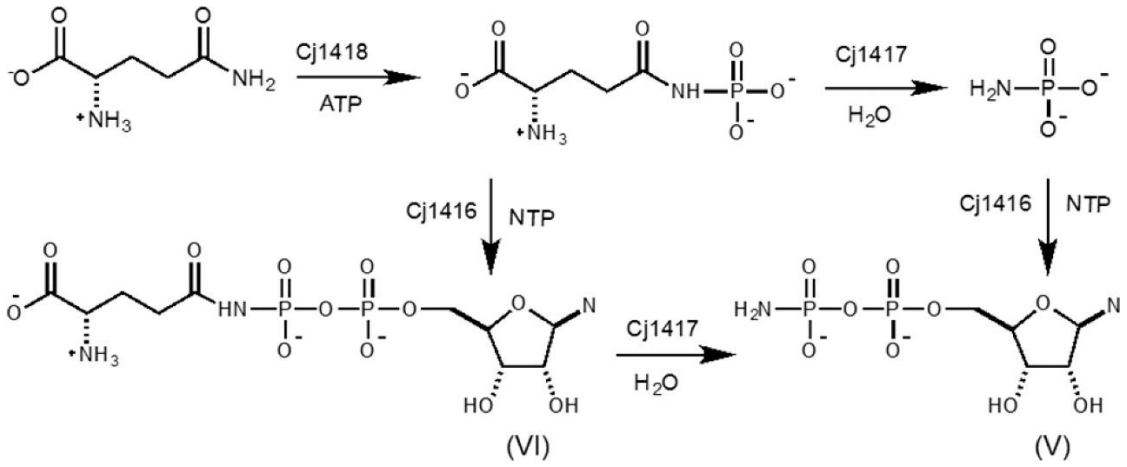

2.4. References

1. Young, K. T., Davis, L. M., and Dirita, V. J. (2007) *Campylobacter jejuni*: Molecular Biology and Pathogenesis, *Nat. Rev. Microbiol. 5*, 665-679.
2. Nyati, K. K., and Nyati, R. (2013) Role of *Campylobacter jejuni* Infection in the Pathogenesis of Guillain-Barré; Syndrome: An Update, *BioMed Res. Int. 2013*, 13.
3. Pelkonen, S.; Hayrinen, J.; and Finne, J., *J.* (1988) Polyacrylamide Gel Electrophoresis of the Capsular Polysaccharides of *Escherichia coli* K1 and other Bacteria. *Bacteriol., 170*, 2646-2653.
4. Guerry, P., Poly, F., Riddle, M., Maue, A. C., Chen, Y.-H., and Monteiro, M. A. (2012) Campylobacter Polysaccharide Capsules: Virulence and Vaccines, *Front. Cell. Infect. Microbiol. 2*, 7.
5. van Alphen, L. B., Wenzel, C. Q., Richards, M. R., Fodor, C., Ashmus, R. A., Stahl, M., Karlyshev, A. V., Wren, B. W., Stintzi, A., Miller, W. G., Lowary, T. L., and Szymanski, C. M. (2014) Biological Roles of the O-Methyl Phosphoramidate Capsule Modification in *Campylobacter jejuni*, *PLoS One 9*, e87051
6. Karlyshev, A. V.; Champion, O. L., Churcher, C., Brisson J. R., Jarrell, H. C., Gilbert, M., Brochu, D., St. Michael, F.; Li, J.; Wakarchuk, W. W.; Goodhead, I.; Sanders, M.; Stevens, K.; White, B.; Parkhill, J.; Wren, B. W.; Szymanski, C. M., (2005) Analysis of *Campylobacter jejuni* Capsular Loci Reveals Multiple Mechanisms for the Generation of Structural Diversity and the ability to form Complex Heptoses. *Mol. Microbiol. 55*, 90-103.

7. St. Michael, F.; Szymanski, C. M.; Li, J.;, Chan, K. H.; Khieu, N. H.; Larocque, S.; Wakarchuk, W. W.; Brisson, J. R.; Monteiro, M. A., (2002). The Structures of the Lipooligosaccharide and the Capsule Polysaccharide of *Campylobacter jejuni* Genome Sequenced Strain NCTC 11168. *Eur. J. Biochem. 269*, 5119-5136.
8. Sørensen, M. C.; van Alphen, L. B.; Harboe, A.; Li, J.; Christensen, B. B.; Szymanski, C. M.; Brøndsted, L., (2011). Bacteriophage F336 Recognizes the Capsular Phosphoramidate Modification of *Campylobacter jejuni* NCTC 11168. *J. Bacteriol*. *193*, 6742-6749.
9. Karlyshev, A. V., Linton, D., Gregson, N. A., Lastovica, A. J., and Wren, B. W. (2000) Genetic and Biochemical Evidence of a *Campylobacter jejuni* Capsular Polysaccharide that Accounts for Penner Serotype Specificity, *Mol. Microbiol. 35*, 529-541.
10. McNally, D. J., Lamoureux, M. P., Karlyshev, A. V., Fiori, L. M., Li, J., Thacker, G., Coleman, R. A., Khieu, N. H., Wren, B. W., Brisson, J.-R., Jarrell, H. C., and Szymanski, C. M. (2007) Commonality and Biosynthesis of the O-Methyl Phosphoramidate Capsule Modification in *Campylobacter jejuni*, *J. Biol. Chem. 282*, 28566-28576.
11. Finn, R. D., Attwood, T. K., Babbitt, P. C., Bateman, A., Bork, P., Bridge, A. J., Chang, H.-Y., Dosztányi, Z., El-Gebali, S., Fraser, M., Gough, J., Haft, D., Holliday, G. L., Huang, H., Huang, X., Letunic, I., Lopez, R., Lu, S., Marchler-Bauer, A., Mi, H., Mistry, J., Natale, D. A., Necci, M., Nuka, G., Orengo, C. A., Park, Y., Pesseat, S., Piovesan, D., Potter, S. C., Rawlings, N. D., Redaschi, N.,

Richardson, L., Rivoire, C., Sangrador-Vegas, A., Sigrist, C., Sillitoe, I., Smithers, B., Squizzato, S., Sutton, G., Thanki, N., Thomas, P. D., Tosatto, Silvio C. E., Wu, C. H., Xenarios, I., Yeh, L.-S., Young, S.-Y., and Mitchell, A. L. (2017) InterPro in 2017—Beyond Protein Family and Domain Annotations, *Nucleic Acids Res. 45*, D190-D199.

12. Herzberg, O., Chen, C. C., Kapadia, G., McGuire, M., Carroll, L. J., Noh, S. J., and Dunaway-Mariano, D. (1996) Swiveling-Domain Mechanism for Enzymatic Phosphotransfer Between Remote Reaction Sites, *Proc. Natl. Acad. Sci. U. S. A. 93*, 2652-2657.
13. Stogios, P. J., Cox, G., Spanogiannopoulos, P., Pillon, M. C., Waglechner, N., Skarina, T., Koteva, K., Guarné, A., Savchenko, A., and Wright, G. D. (2016) Rifampin Phosphotransferase is an Unusual Antibiotic Resistance Kinase, *Nat. Commun. 7*, 11343.
14. Qi, X., Lin, W., Ma, M., Wang, C., He, Y., He, N., Gao, J., Zhou, H., Xiao, Y., Wang, Y., and Zhang, P. (2016) Structural Basis of Rifampin Inactivation by Rifampin Phosphotransferase, *Proceedings of the National Academy of Sciences 113*, 3803-3808.
15. Massière, F., and Badet-Denisot, M.-A. (1998) The mechanism of glutamine-dependent amidotransferases, *Cell. Mol. Life Sci. 54*, 205-222.
16. Thoden, J. B., Holden, H. M., Wesenberg, G., Raushel, F. M., and Rayment, I. (1997) Structure of Carbamoyl Phosphate Synthetase: a Journey of 96 Å from Substrate to Product, *Biochemistry 36*, 6305-6316.

17. Thoden, J. B.; Holden, H. M., (2005). The Molecular Architecture of Galactose Mutarotase/UDP-Galactose 4-Epimerase from *Saccharomyces cerevisiae*. *J. Biol. Chem*. **2005**, *280*, 32784-32791.

18. Makoto, W., Shoji, S., and Khosaku, W. (1990) The Hydrolytic Property of Imidodiphosphate in Solid and in an Aqueous Medium, *Bull. Chem. Soc. Jpn. 63*, 1243-1245.

19. Reddick, R. E., and Kenyon, G. L. (1987) Syntheses and NMR Studies of Specifically Labeled [2-^{15}N]-Phosphocreatine, [2-^{15}N]-Creatinine, and Related ^{15}N-Labeled Compounds, *J. Am. Chem. Soc. 109*, 4380-4387.

20. Chakravarty, P. K., Greenlee, W. J., Parsons, W. H., Patchett, A. A., Combs, P., Roth, A., Busch, R. D., and Mellin, T. N. (1989) (3-Amino-2-oxoalkyl)Phosphonic Acids and their Analogs as Novel Inhibitors of D-alanine:D-alanine Ligase, *J. Med. Chem. 32*, 1886-1890.

21. Blondin, C., Serina, L., Wiesmuller, L., Gilles, A. M., and Barzu, O. (1994) Improved Spectrophotometric Assay of Nucleoside Monophosphate Kinase Activity Using the Pyruvate Kinase/Lactate Dehydrogenase Coupling System, *Anal. Biochem. 220*, 219-221.

22. McNally, D. J.; Lamoureux, M.; Li, J.; Kelly, J.; Brisson, J.-B.; Szymanski, C. M.; Jarrell, H. C., (2006) HR-MAS NMR Studies of ^{15}N-labled Cells Confirm the Structure of the O-Methyl Phosphoramidate CPS Modification in *Campylobacter jejuni* and provide Insight into its Biosynthesis. *Can. J. Chem*. *84*, 676-684.

23. Parsons, W. H., Patchett, A. A., Bull, H. G., Schoen, W. R., Taub, D., Davidson, J., Combs, P. L., Springer, J. P., and Gadebusch, H. (1988) Phosphinic Acid Inhibitors of D-alanyl-D-alanine Ligase, *J. Med. Chem. 31*, 1772-1778.

24. Cox, R. J.; Gibson, J. S.; Mayo Martín, M. B., (2002). Aspartyl Phosphonates and Phosphoramidates: The First Synthetic Inhibitors of Bacterial Aspatrate-Semialdehyde Dehydrogenase. *ChemBioChem 3*, 874-886.

25. Ronzio, R. A., and Meister, A. (1968) Phosphorylation of Methionine Sulfoximine by Glutamine Synthetase, *Proc. Natl. Acad. Sci. U. S. A. 59*, 164-170.

26. Kurihara, S., Oda, S., Kato, K., Kim, H. G., Koyanagi, T., Kumagai, H., and Suzuki, H. (2005) A Novel Putrescine Utilization Pathway Involves γ-Glutamylated Intermediates of *Escherichia coli* K-12, *J. Biol. Chem. 280*, 4602-4608.

27. Kwak, B.-Y., Zhang, Y.-M., Yun, M., Heath, R. J., Rock, C. O., Jackowski, S., and Park, H.-W. (2002) Structure and Mechanism of CTP:Phosphocholine Cytidylyltransferase (LicC) from *Streptococcus pneumoniae*, *J. Biol. Chem. 277*, 4343-4350.

3. BIOSYNTHESIS OF NUCLEOSIDE DIPHOSPHORAMIDATES IN *CAMPYLOBACTER JEJUNI*[*]

3.1. Introduction

The pathogenic Gram-negative bacterium *Campylobacter jejuni* is a leading cause of food-borne gastroenteritis (1). While pathogenic to humans, *C. jejuni* is a commensal organism in chickens, and as a result, contaminated poultry serves as a common route of human infection. While most *C. jejuni* infections cause a case of gastroenteritis, approximately 1 in 1000 infections results in the autoimmune disease Guillain-Barré syndrome (2,3). Like many other organisms, *C. jejuni* uses a capsular polysaccharide (CPS) to improve fitness. The capsular polysaccharide of *C. jejuni* protects the organism from bacteriophages and shields it from the host immune response (4,5). More than 40 different strains of *C. jejuni* have been identified to date, and each strain is believed to produce a unique CPS variant (6,7). In *C. jejuni* strain NCTC 11168, a cluster of approximately 35 genes is responsible for the synthesis and export of the CPS (8). Moreover, *C. jejuni* has evolved the ability to synthesize a unique O-methyl phosphoramidate (MeOPN) modification found on the CPS that improves the pathogenicity of the bacterium and promotes evasion of the host immune response (9). The structures of the MeOPN modification to the CPS in *C. jejuni* strain NCTC 11168 and hypermotile strain 11168H are illustrated in Scheme 11.

[*] Reprinted with permission from "Biosynthesis of Nucleoside Diphosphoramidates in *Campylobacter jejuni*" by Zane W. Taylor, Haley A. Brown, Hazel M. Holden, and Frank M. Raushel, *Biochemistry*, (2017), *56* (46), pp 6079-6082, Copyright 2017 American Chemical Society

Scheme 11 Structures of the O-Methyl Phosphoramidate Modifications to the CPS in *C. jejuni*

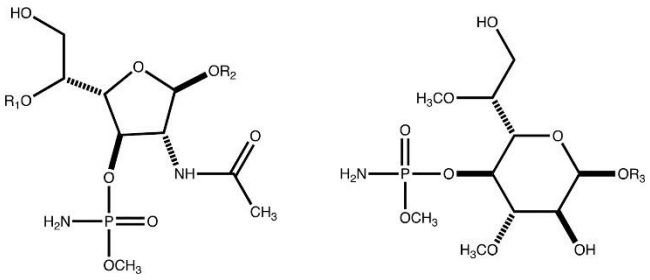

We have recently shown that the enzyme denoted with the locus tag Cj1418 from *C. jejuni* strain 11168H catalyzes the first committed step in the biosynthesis of the MeOPN (10). This enzyme, L-glutamine kinase, catalyzes the unprecedented ATP-dependent phosphorylation of the amide nitrogen of L-glutamine (**1**) to form L-glutamine phosphate (**2**) as shown in Scheme 12A. However, the subsequent metabolic fate of this novel enzyme intermediate has not been addressed. The primary focus of this investigation is to identify those enzymes that can harness the phosphoramidate moiety contained within L-glutamine phosphate for the ultimate construction of the O-methyl phosphoramidate modification of the CPS.

Scheme 12 Reaction Catalyzed by Cj1418 and the Predicted Functions of Cj1417 and Cj1416

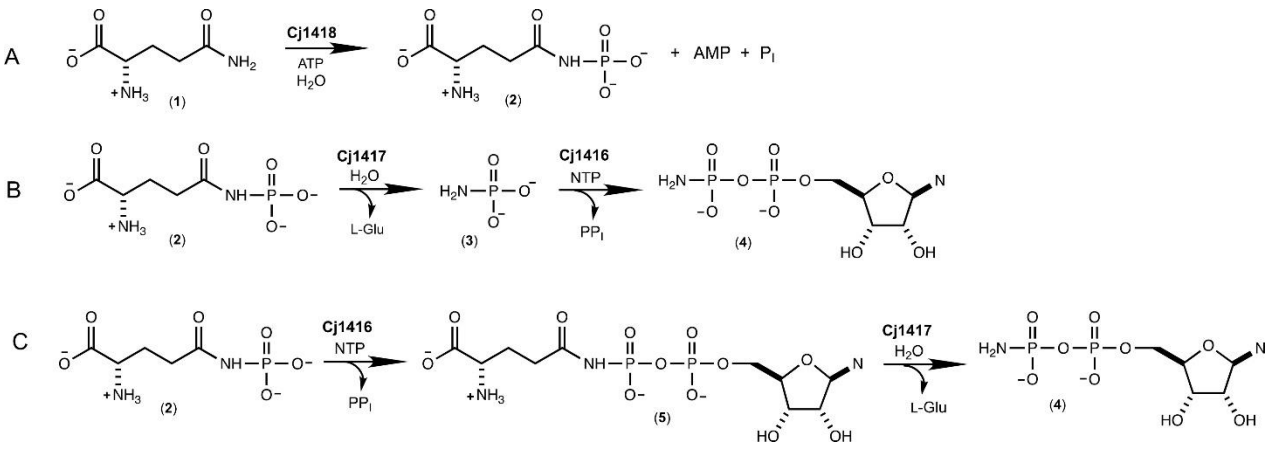

3.2. Methods

3.2.1. Gene Expression and Enzyme Purification

The genes used for the expression of Cj1416 and Cj1417 were cloned from the genomic DNA of *C. jejuni* NCTC11168 into a pet30b vector with a C-terminal hexahistidine tag. The expression plasmids for Cj1416 and Cj1417 were used to transform Rosetta (DE3) *E. coli* cells. Cells containing Cj1416 were grown in LB at 30 °C and were then induced with 1.0 mM IPTG and grown at 16 °C for 16 hours. Cells containing Cj1417 were grown in TB in a 5.0 mL starter culture for 8 hours at 37 °C, and then the 5.0 mL cultures were used to inoculate 1.0 L cultures. The 1.0 L cultures of Cj1417 were allowed to grow for 16 hours at 25 °C. The enzymes Cj1416 and Cj1417 were purified using Ni-affinity chromatography, and excess imidazole was removed by dialysis. The purified proteins were concentrated and stored at -80 °C.

Cj1416 yielded 25 mg of purified protein per liter of cell culture, and Cj1417 yielded 4 mg of protein per liter of cell culture.

3.2.2. Enzyme Assays and Determination of Kinetic Constants

The kinetic constants for Cj1416 were determined at pH 8.0 in 100 mM HEPES/KOH and 100 mM KCl using anion exchange chromatography to monitor the change in concentration of the substrates and products as a function of time. The samples were first loaded onto the ion exchange column and then washed with 10 mM triethanolamine (pH 8.0). The products were eluted with a linear gradient of 10 mM triethanolamine (pH 8.0), and 2.0 M KCl. Each reaction was carried out at 25 °C, with a minimum of five time points collected for each concentration. The kinetic constants for Cj1417 were determined using a glutamate dehydrogenase (8 units/mL) coupled enzyme assay that monitors the reduction of NAD^+ (0.5 mM) at 340 nm. These reactions were done using 100 mM HEPES/KOH (pH 8.0), 100 mM KCl, at 25 °C. The CDP-L-glutamine (**5**) for these assays was synthesized using a mixture of Cj1416, 10 mM CTP, 10 mM L-glutamine phosphate, 12 mM MgCl2 and 10 units/ml of inorganic pyrophosphatase. The reaction was allowed to go to completion, the enzymes were removed, and the CDP-L-glutamine was quantified by HPLC and NMR.

3.3. Results and Discussion

The two most likely enzymes of unknown function from *C. jejuni* to utilize L-glutamine phosphate as a substrate during the biosynthesis of the O-methyl phosphoramidate modification of the CPS are Cj1417 and Cj1416. Cj1417 is functionally annotated as a Type I amidotransferase from cog2071. Members of the Type I amidotransferase family of enzymes typically catalyze the hydrolysis of L-glutamine or amide substituted derivatives of this amino acid (11,12). Currently, the closest functionally characterized homologue to Cj1417 is the enzyme PuuD (23% identical sequence) from *Escherichia coli*, an enzyme that catalyzes the hydrolysis of 4-(γ-L-glutamylamino)butanoate to 4-aminobutanoate and L-glutamate (12). Cj1416 is currently annotated as a nucleotidyltransferase from cog1213. The closest functionally characterized homologue of Cj1416 is CTP:phosphocholine cytidylyltransferase from *Streptococcus pneumoniae* with a sequence identity of 28% (13). This enzyme catalyzes the formation of CDP-choline and pyrophosphate from CTP and choline phosphate. We therefore predict that the combination of Cj1417 and Cj1416 will catalyze the synthesis of a nucleoside diphosphoramidate (**4**) using L-glutamine phosphate (**2**) and a nucleoside triphosphate as substrates.

The biosynthesis of a nucleoside diphosphoramidate (**4**) by the consecutive reactions catalyzed by Cj1417 and Cj1416 can be envisioned to occur via one of two possible reaction schemes. In the first scenario, Cj1417 catalyzes the hydrolysis of L-glutamine phosphate (**2**) to L-glutamate and phosphoramidate (**3**). This reaction is followed by the displacement of pyrophosphate from a nucleoside triphosphate by phosphoramidate (**3**) to generate the nucleoside diphosphoramidate (**4**) in a reaction

catalyzed by Cj1416 as illustrated in Scheme 12B. Alternatively, Cj1416 catalyzes the displacement of pyrophosphate from a nucleoside triphosphate by L-glutamine phosphate to form NDP-L-glutamine (**5**). This reaction is subsequently followed by the hydrolysis of this intermediate by Cj1417 to form L-glutamate and the nucleoside diphosphoramidate (**4**) as presented in Scheme 12C.

To test our initial prediction that the combination of Cj1416 and Cj1417 catalyzes the formation of a nucleoside diphosphoramidate, these two enzymes were incubated together in the presence of MgCTP and an excess of L-glutamine phosphate (**2**) at pH 8.0. After 45 min, all of the CTP [retention time of 8.7 min (Figure 4A)] was converted to a new product with a retention time of 5.9 min (Figure 4B). The retention time of the new reaction product formed in the presence of Cj1417 and Cj1416 is identical to that of authentic cytidine diphosphoramidate (Figure 4E) (14).

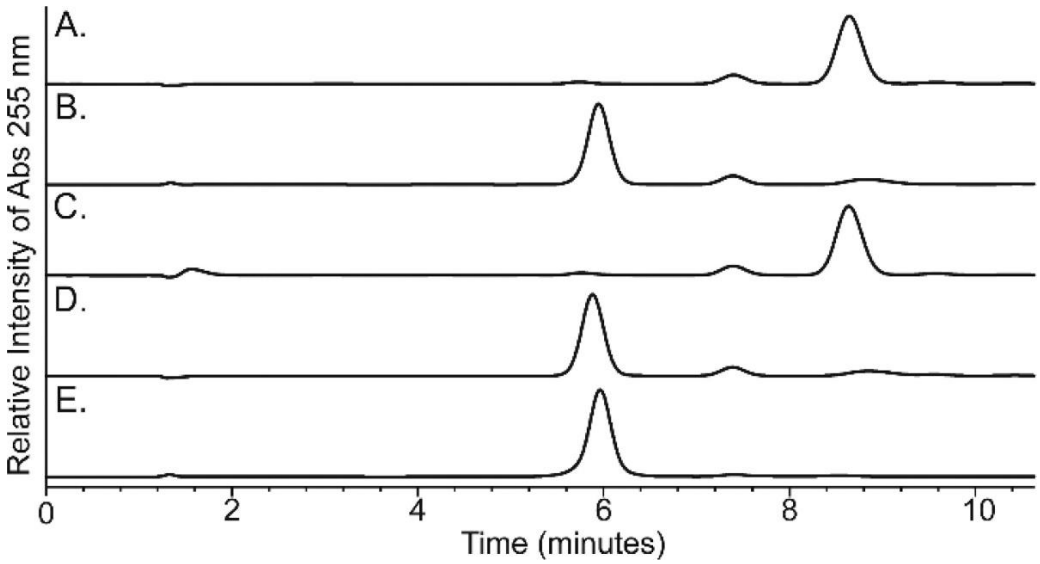

Figure 4 Anion exchange chromatograms of nucleotide standards and enzyme-catalyzed reaction products formed in 100 mM HEPES (pH 8.0) at 25 °C with an incubation time of 45 min. The elution profiles were monitored at 255 nm. The nucleotides were separated using a 0 to 17% gradient of 10 mM triethanolamine (pH 8) and 2 M KCl over 17 column volumes on a 1 mL Resource Q column. (A) Control sample of 1.0 mM CTP and 2.0 mM $MgCl_2$ in the absence of any added enzyme. (B) Sample containing 1.0 mM CTP, 2.0 mM $MgCl_2$, 5.0 mM l-glutamine phosphate, Cj1416 (5 μM), and Cj1417 (5 μM). (C) Sample containing 1.0 mM CTP, 2.0 mM $MgCl_2$, 5.0 mM phosphoramidate (3), 5 μM Cj1416, and 5 units/mL pyrophosphatase. (D) Sample containing 1.0 mM CTP, 2.0 mM $MgCl_2$, 5.0 mM l-glutamine phosphate, 5 μM Cj1416, and 5 units/mL pyrophosphatase. (E) Control sample of chemically synthesized CDP phosphoramidate.

The identity of the new reaction product as cytidine diphosphoramidate [**4** (Scheme 12C)] was confirmed by ^{31}P nuclear magnetic resonance (NMR) spectroscopy. A reaction mixture containing CTP, $MgCl_2$, and an excess of L-glutamine phosphate (**2**) was incubated at pH 8.0 for 90 min in the presence of Cj1416 and Cj1417 until the reaction was quenched by the addition of 10 mM EDTA. The ^{31}P NMR spectrum of the control reaction (Figure 5A), obtained in the absence of Cj1416 and Cj1417, showed the expected resonances for CTP [−20.99 ppm (β-P), −10.33 ppm (α-P), and −5.51 ppm (γ-P)] and L-glutamine phosphate (−3.57 and −3.83 ppm). In the presence of Cj1416 and Cj1417, the resonances for CTP and L-glutamine phosphate (**2**) essentially disappear and are replaced by new resonances for pyrophosphate (−6.63 ppm) and a pair of doublets at −0.42 ppm (β-P) and −10.23 ppm (α-P) for cytidine diphosphoramidate (Figure 5B). The ^{31}P NMR spectrum for authentic cytidine diphosphoramidate is presented in Figure 5C. The formation of cytidine diphosphoramidate was further supported by the acquisition of the negative ion electrospray ionization (ESI) mass spectrum of the unfractionated reaction mixture upon incubation of MgCTP, L-glutamine phosphate, Cj1417, and Cj1416 at pH 8.0 in ammonium bicarbonate buffer. A peak at m/z 401.03 was observed that is consistent with that expected for cytidine diphosphoramidate (Figure 6). These experiments demonstrate that Cj1417 and Cj1416 use MgCTP and L-glutamine phosphate (**2**) to catalyze the formation of CDP-phosphoramidate, pyrophosphate, and L-glutamate.

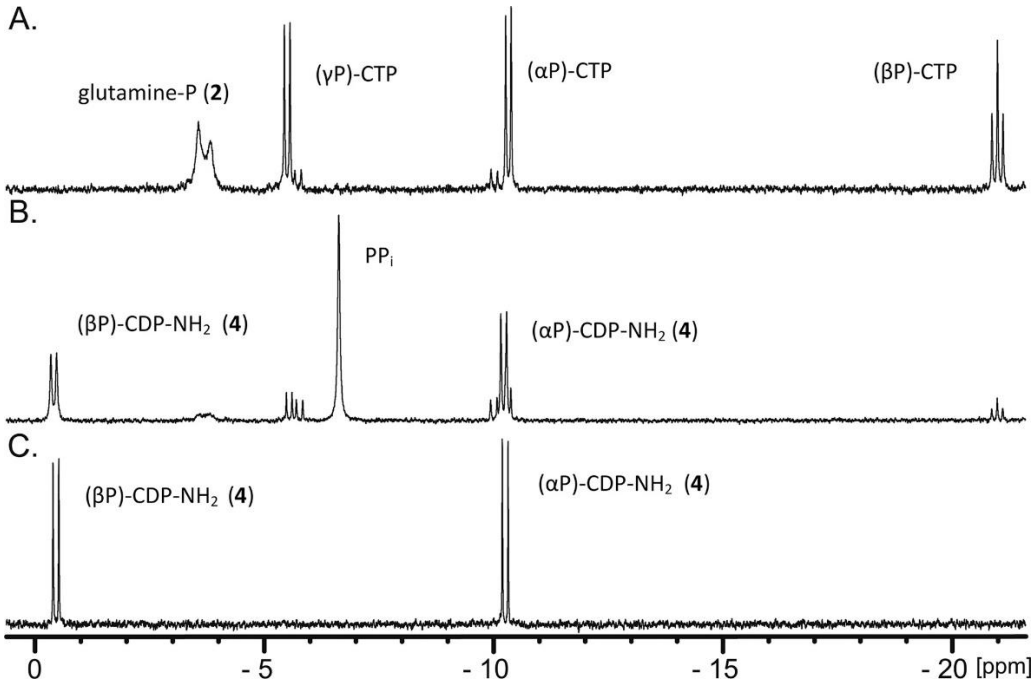

Figure 5 ^{31}P NMR spectra of nucleotide standards and enzyme-catalyzed reaction products formed in 100 mM HEPES (pH 8.0) at 25 °C with an incubation time of 90 min before the reaction was quenched with 10 mM EDTA. (A) Control sample containing 5.0 mM CTP, 5.0 mM $MgCl_2$, and 6.0 mM l-glutamine phosphate. (B) Sample containing 5.0 mM CTP, 5.0 mM $MgCl_2$, 6.0 mM l-glutamine phosphate, 20 μM Cj1416, and 20 μM Cj1417. (C) Control sample of 5.0 mM CDP phosphoramidate.

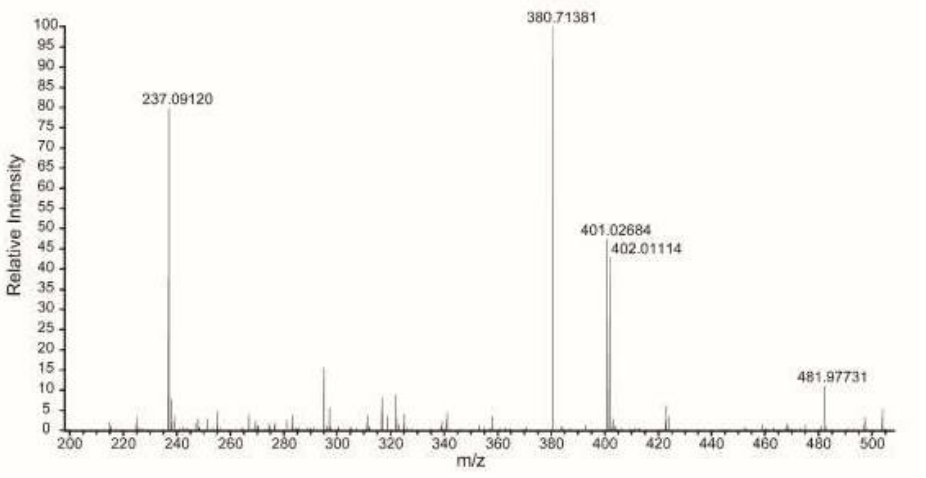

Figure 6 ESI negative ion mass spectrum of the unfractionated reaction mixture formed after incubation of Cj1416, Cj1417, MgCTP, and L-glutamine phosphate. The peak that corresponds to the mass of CDP-diphosphoramidate can be observed with an m/z of 401.02 for the (M-H)- species ($C_9H_{15}O_{10}N_4P_2$). Several other peaks are observed that correspond to known compounds in the unfractionated reaction mixture including CDP (m/z = 402.01), HEPES (m/z = 237.09) and CTP (m/z = 481.97). The peak at an m/z of 380.71 is a contaminant from the chemical synthesis of L-glutamine phosphate that corresponds to triiodide anion (I_3^-).

In parts B and C of Scheme 12, we have proposed that either phosphoramidate (**3**) or L-glutamine phosphate (**2**) is used to displace pyrophosphate from a nucleoside triphosphate to form either a nucleoside diphosphoramidate (**4**) or NDP-L-glutamine (**5**) as an intermediate. The reactivity of Cj1416 with each of these potential substrates was tested with MgCTP as the acceptor nucleotide, and the reaction was monitored by ion exchange chromatography at 255 nm. In separate experiments, either phosphoramidate (**3**) or L-glutamine phosphate (**2**) was incubated with CTP, $MgCl_2$, and Cj1416 at pH 8.0 for 45 min. Utilizing the chemically synthesized phosphoramidate (**3**) as a potential substrate, there was no change in the high performance liquid chromatography chromatogram when compared to that of CTP alone (Figure 4C) (15). However, when Cj1416 was incubated with L-glutamine phosphate (**2**) and MgCTP, all of the CTP was converted to a new product that corresponds to a molecule with a net charge of approximately −2(Figure 4D) (10). This result demonstrates that Cj1416 is fully capable of using L-glutamine phosphate (**2**) to displace pyrophosphate from CTP.

To provide further spectroscopic support for the Cj1416 catalyzed formation of CDP-L-glutamine, the reaction products were analyzed by ^{31}P NMR spectroscopy. In this experiment, Cj1416 was incubated with CTP, $MgCl_2$, L-glutamine phosphate (**2**), and inorganic pyrophosphatase until the reaction was quenched with EDTA. After an incubation period of 90 min, essentially all of the CTP and L-glutamine phosphate (**2**) were converted to products (Figure 7A). A new resonance is observed at 3.02 ppm for phosphate (from the hydrolysis of pyrophosphate), and two new doublets are observed at −10.98 ppm (α-P) and −16.13 ppm (β-P) for CDP-L-glutamine. The formation of CDP-L-glutamine was further supported by the acquisition of the negative ion ESI mass spectrum of the unfractionated reaction mixture upon incubation of MgCTP, L-glutamine phosphate, and Cj1416 at pH 8.0 in ammonium bicarbonate buffer. A peak at m/z 530.07 was observed that is consistent with that expected of CDP-L-glutamine (Figure 8).

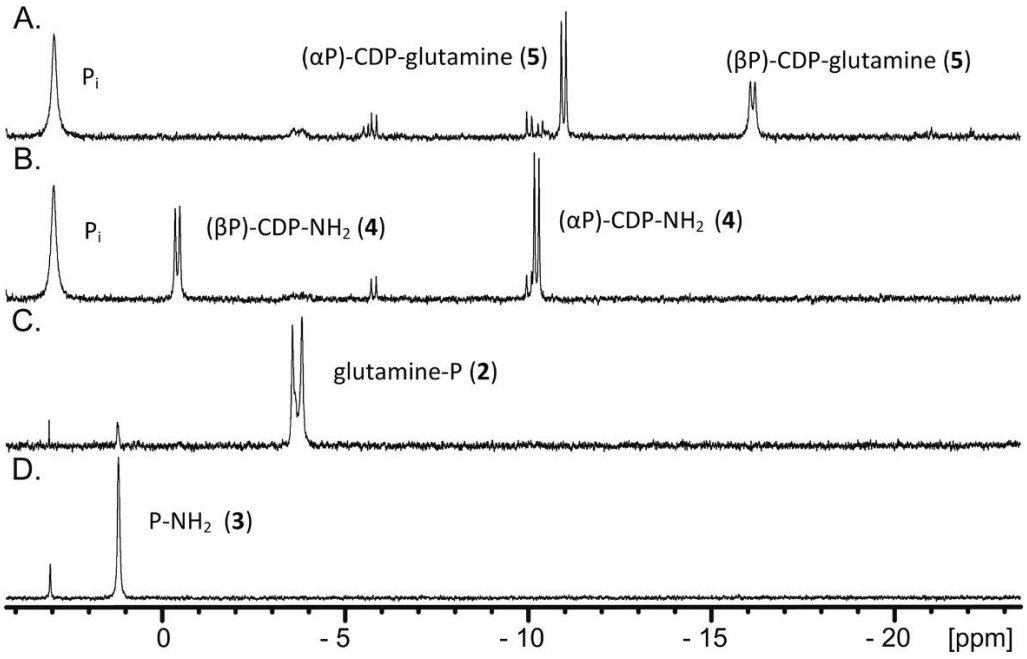

Figure 7. ^{31}P NMR spectra of nucleotide standards and enzyme-catalyzed reaction products formed in 100 mM HEPES (pH 8.0) at 25 °C with an incubation time of 90 min before the reaction was quenched with 10 mM EDTA. (A) Sample containing 5.0 mM CTP, 5.0 mM $MgCl_2$, 5 units/mL pyrophosphatase, and 20 μM Cj1416. (B) Cj1417 (20 μM) was added to the reaction mixture shown in panel A and the mixture allowed to react for an additional 90 min. (C) Sample containing 20 μM Cj1417 and 5.0 mM glutamine phosphate. (D) Control sample of 5.0 mM phosphoramidate.

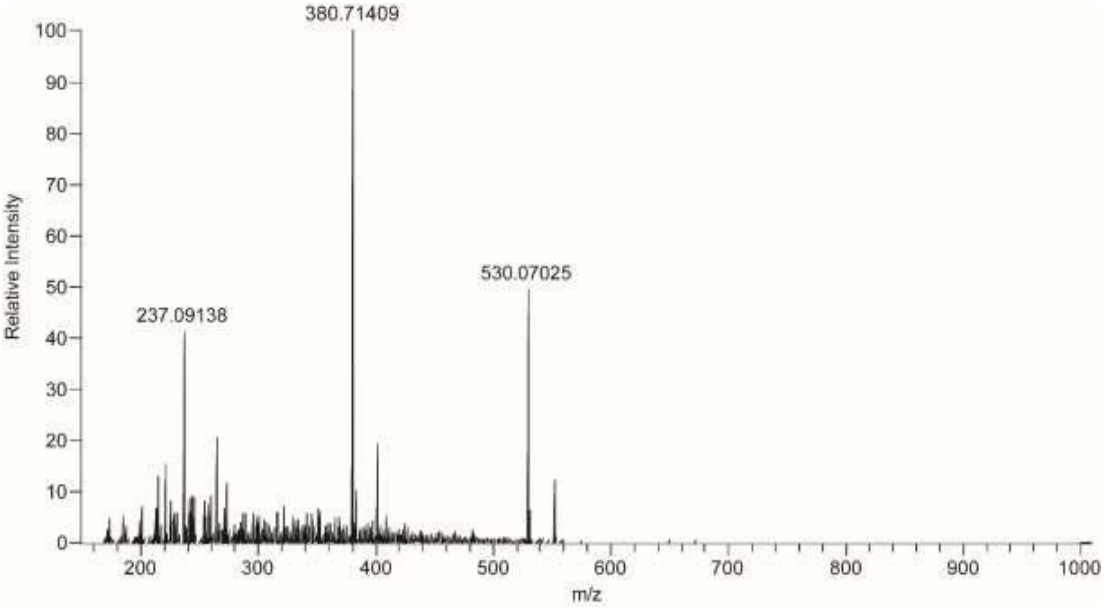

Figure 8 ESI negative ion mass spectrum of the unfractionated reaction mixture formed after incubation of Cj1416, MgCTP, and L-glutamine phosphate. The peak that corresponds to the mass of CDP-L-glutamine phosphate can be observed with an m/z of 530.07 for the (M-H)-species ($C_{14}H_{22}O_{13}N_5P_2$). Two other peaks are observed that correspond to the known compounds in the unfractionated reaction mixture, HEPES (m/z = 237.09) and triiodide anion from the synthesis of L-glutamine phosphate (m/z = 380.71).

When Cj1417 is subsequently added to the reaction mixture containing CDP-L-glutamine, the ^{31}P NMR resonances for CDP-L-glutamine disappear and are replaced by two new pairs of doublets at −0.43 ppm (β-P) and −10.24 ppm (α-P) that can be assigned to cytidine diphosphoramidate (Figure 7B and Figure 5C). These experiments demonstrate that Cj1416 catalyzes the formation of CDP-L-glutamine from CTP and L-glutamine phosphate (**2**) and that Cj1417 catalyzes the hydrolysis of CDP-L-glutamine to L-glutamate and cytidine diphosphoramidate.

The remaining issue to address for the functional characterization of Cj1417 is whether this enzyme is capable of catalyzing the hydrolysis of L-glutamine phosphate to L-glutamate and phosphoramidate (**2**). Cj1417 was therefore incubated with L-glutamine phosphate (**2**) at pH 8.0 for 90 min. The ^{31}P NMR spectrum (Figure 7C) of the reaction mixture demonstrated that ∼93% of the original L-glutamine phosphate (**2**) remained intact. Two other resonances that are consistent with the presence of a small amount of phosphate (3.08 ppm, 1.2%) and phosphoramidate (1.21 ppm, 5.5%) are observed. The ^{31}P NMR spectrum for chemically synthesized phosphoramidate (**2**) is shown in Figure 7D, where a resonance is observed at 1.19 ppm. On the basis of these results, it is clear that the preferred pathway for the synthesis of cytidine diphosphoramidate (**4**) is for Cj1416 to catalyze the displacement of pyrophosphate from CTP to form CDP-L-glutamine (**5**) and for Cj1417 to catalyze the hydrolysis of this intermediate to generate cytidine diphosphoramidate (**4**) as shown in Scheme 12C.

The kinetic constants for the catalytic activity of Cj1417 and Cj1416 were determined. At a fixed concentration of either 5.0 mM MgCTP or 2.0 mM L-glutamine

phosphate (2), the rates of the reaction catalyzed by Cj1416 were determined at 25 °C and pH 8.0 by monitoring the formation of products via anion exchange chromatography at 255 nm. The observed kinetic constants using L-glutamine phosphate (**2**) as the variable substrate are as follows: K_m = 120 ± 30 μM, k_{cat} = 57± 6 min^{-1}, and k_{cat}/K_m = (4.8 ± 1.3) × 10^5 M^{-1} min^{-1}. The observed kinetic constants using MgCTP as the variable substrate are as follows: K_m = 170 ± 35 μM, k_{cat} = 57± 6 min^{-1}, and k_{cat}/K_m = (3.4 ± 0.8) × 10^5 M^{-1} min^{-1}.

The kinetic constants for the hydrolysis of CDP-L-glutamine (**5**) catalyzed by Cj1417 were determined at 25 °C and pH 8.0 using a glutamate dehydrogenase coupled assay that monitors the formation of NADH at 340 nm. The kinetic constants were determined to be as follows: K_m = 28± 3 μM, k_{cat} = 34± 1.2 min^{-1}, and k_{cat}/K_m = (1.2 ± 0.2) × 10^6 M^{-1} min^{-1}. In an effort to determine the upper limit of the rate constant for the hydrolysis of L-glutamine phosphate (**2**) by Cj1417, 10 mM L-glutamine phosphate (**2**) was incubated with 20 μM Cj1417, and the reaction was monitored by ^{31}P NMR for 13 h. From this experiment, an upper limit of 1.6 h^{-1} was obtained for the hydrolysis of L-glutamine phosphate by Cj1417.

Previously, we have demonstrated that the first step in the biosynthesis of the MeOPN modification to the CPS of *C. jejuni* is catalyzed by Cj1418, where ATP is utilized to phosphorylate the amide nitrogen of L-glutamine (10). Here we have shown that Cj1416 catalyzes the displacement of pyrophosphate from MgCTP by L-glutamine phosphate (**2**), yielding CDP-L-glutamine (**5**). We have also established that the catalytic function of Cj1417 is to hydrolyze CDP-L-glutamine to L-glutamate and cytidine

diphosphoramidate (**4**). This investigation has thus unveiled the identities of two new nucleoside diphosphoramidate derivatives that are involved in the biosynthesis of MeOPN. It is likely that cytidine diphosphoramidate (**4**) will be subsequently phosphorylated at the hydroxyl group attached to C3 of the ribose ring prior to transfer of the phosphoramidate group to various carbohydrates of the CPS. On the basis of sequence similarity network analysis of the enzymes of unknown function contained within *C. jejuni*, we predict that Cj1415 will catalyze this reaction. Cj1415 is a member of cog0529, and the closest functionally characterized enzyme is CysC, an adenylyl-sulfate kinase, from *E. coli* (26% identity), an enzyme that catalyzes the ATP-dependent phosphorylation of the 3′-hydroxyl of adenylyl sulfate (16). The unique biosynthetic pathway for the assembly of the phosphoramidate functionality found in the CPS of *C. jejuni* offers many opportunities for the development of potent inhibitors that may ultimately be useful in the therapeutic control of this pathogenic organism.

3.4. References

1. Young, K. T., Davis, L. M., and Dirita, V. J. (2007) *Campylobacter jejuni*: Molecular Biology and Pathogenesis, *Nat. Rev. Microbiol. 5*, 665-679.
2. Jacobs, B. C., Rothbarth, P. H., van der Meché, F. G. A., Herbrink, P., Schmitz, P. I. M., de Klerk, M. A., and van Doorn, P. A. (1998) The Spectrum of Antecedent Infections in Gullain-Barre Syndrome: a Case-Controlled Study. *Neurology* 51, 1110−1115.
3. Acheson, D., and Allos, B. M. (2001) *Campylobacter jejuni* Infections: Update on Emerging Issues and Trends. *Clin. Infect. Dis*. 32, 1201− 1206.
4. Guerry, P., Poly, F., Riddle, M., Maue, A. C., Chen, Y.-H., and Monteiro, M. A. (2012) Campylobacter Polysaccharide Capsules: Virulence and Vaccines, *Front. Cell. Infect. Microbiol. 2*, 7.
5. Sørensen, M. C.; van Alphen, L. B.; Harboe, A.; Li, J.; Christensen, B. B.; Szymanski, C. M.; Brøndsted, L., (2011). Bacteriophage F336 Recognizes the Capsular Phosphoramidate Modification of *Campylobacter jejuni* NCTC 11168. *J. Bacteriol*. *193*, 6742-6749.
6. Karlyshev, A. V.; Champion, O. L., Churcher, C., Brisson J. R., Jarrell, H. C., Gilbert, M., Brochu, D., St. Michael, F.; Li, J.; Wakarchuk, W. W.; Goodhead, I.; Sanders, M.; Stevens, K.; White, B.; Parkhill, J.; Wren, B. W.; Szymanski, C. M., (2005) Analysis of *Campylobacter jejuni* Capsular Loci Reveals Multiple Mechanisms for the Generation of Structural Diversity and the ability to form Complex Heptoses. *Mol. Microbiol*. *55*, 90-103.

7. St. Michael, F.; Szymanski, C. M.; Li, J.;, Chan, K. H.; Khieu, N. H.; Larocque, S.; Wakarchuk, W. W.; Brisson, J. R.; Monteiro, M. A., (2002). The Structures of the Lipooligosaccharide and the Capsule Polysaccharide of *Campylobacter jejuni* Genome Sequenced Strain NCTC 11168. *Eur. J. Biochem. 269*, 5119-5136.
8. Karlyshev, A. V., Linton, D., Gregson, N. A., Lastovica, A. J., and Wren, B. W. (2000) Genetic and Biochemical Evidence of a *Campylobacter jejuni* Capsular Polysaccharide that Accounts for Penner Serotype Specificity, *Mol. Microbiol. 35*, 529-541.
9. van Alphen, L. B., Wenzel, C. Q., Richards, M. R., Fodor, C., Ashmus, R. A., Stahl, M., Karlyshev, A. V., Wren, B. W., Stintzi, A., Miller, W. G., Lowary, T. L., and Szymanski, C. M. (2014) Biological Roles of the O-Methyl Phosphoramidate Capsule Modification in *Campylobacter jejuni*, *PLoS One 9*, e87051.
10. Taylor, Z. W., Brown, H. A., Narindoshvili, T., Wenzel, C. Q., Szymanski, C. M., Holden, H. M., and Raushel, F. M. (2017) Discovery of a Glutamine Kinase Required for the Biosynthesis of the O-Methyl Phosphoramidate Modifications Found in the Capsular Polysaccharides of *Campylobacter jejuni*. *J. Am. Chem. Soc*. 139, 9463− 9466.
11. Massière, F., and Badet-Denisot, M.-A. (1998) The Mechanism of Glutamine-Dependent Amidotransferases, *Cell. Mol. Life Sci. 54*, 205-222.
12. Kurihara, S., Oda, S., Kato, K., Kim, H. G., Koyanagi, T., Kumagai, H., and Suzuki, H. (2005) A Novel Putrescine Utilization Pathway Involves γ-Glutamylated Intermediates of *Escherichia coli* K-12, *J. Biol. Chem. 280*, 4602-4608.

13. Kwak, B.-Y., Zhang, Y.-M., Yun, M., Heath, R. J., Rock, C. O., Jackowski, S., and Park, H.-W. (2002) Structure and Mechanism of CTP:Phosphocholine Cytidylyltransferase (LicC) from *Streptococcus pneumoniae*, *J. Biol. Chem. 277*, 4343-4350.
14. Wehrli, W., Verheyden, D., and Moffatt, J. (1965) Dismutation Reactions of Nucleoside Polyphosphates. II. Specific Chemical Syntheses of α-, β-, and γ-P^{32}-Nucleoside 5′-Triphosphates1. *J. Am. Chem. Soc*. 87, 2265−2277.
15. Watanabe, M., Sato, S., and Wakasugi, K. (1990) The Hydrolytic Property of Imidodiphosphate in Solid and in an Aqueous Medium. *Bull. Chem. Soc. Jpn*. 63, 1243−1245.
16. Leyh, T. S., Taylor, J. C., and Markham, G. D. (1988) The Sulfate Activation Locus of *Escherichia coli* K12: Cloning, Genetic, and Enzymatic Characterization. *J. Biol. Chem*. 263, 2409−2416.

4. CYTIDINE DIPHOSPHORAMIDATE KINASE: AN ENZYME REQUIRED FOR THE BIOSYNTHESIS OF THE O-METHYL PHOSPHORAMIDATE MODIFICATION IN THE CAPSULAR POLYSACCHARIDES OF *CAMPYLOBACTER JEJUNI*[*]

4.1. Introduction

Campylobacter jejuni, a Gram-negative pathogenic bacterium, is a leading cause of gastroenteritis worldwide (1,2) *C. jejuni*, while pathogenic in humans, is commensal in chickens, and thus contaminated poultry have become a common source of human infections (3). While most *C. jejuni* infections result in gastroenteritis, rare cases are linked to the occurrence of the autoimmune disease Guillain-Barré syndrome (4). Like many other organisms, *C. jejuni* produces a capsular polysaccharide (CPS) that aids in host colonization, evasion of immune responses, and serum resistance (5,6) Over 34 CPS gene clusters have been published, and it is believed that each strain produces a unique CPS (7). Currently, the structures of at least 10 *C. jejuni* capsular polysaccharides have been physically characterized (8). The CPS of *C. jejuni* NCTC 11168 consists of a four carbohydrate repeating unit that is decorated with a unique O-methyl phosphoramidate (MeOPN) modification (9,10). Approximately 70% of all *C. jejuni* strains contain the MeOPN moiety attached to their CPS. In the CPS of *C. jejuni*

[*] Reprinted with permission from "Cytidine Diphosphoramidate Kinase: An Enzyme Required for the Biosynthesis of the O-Methyl Phosphoramidate Modification in the Capsular Polysaccharides of *Campylobacter jejuni*" by Zane W. Taylor and Frank M. Raushel, *Biochemistry* (2018) *57* (15), pp 2238-2244, Copyright 2018 American Chemical Society

NCTC 11168, the 2-acetamido-2-deoxy-β-D-galactofuranose and D-glycero-α-L-gluco-heptopyranose sugars are derivatized with the methyl phosphoramidate group (Scheme 13).

Scheme 13 *C. jejuni* NCTC11168 Capsular Polysaccharide Structure

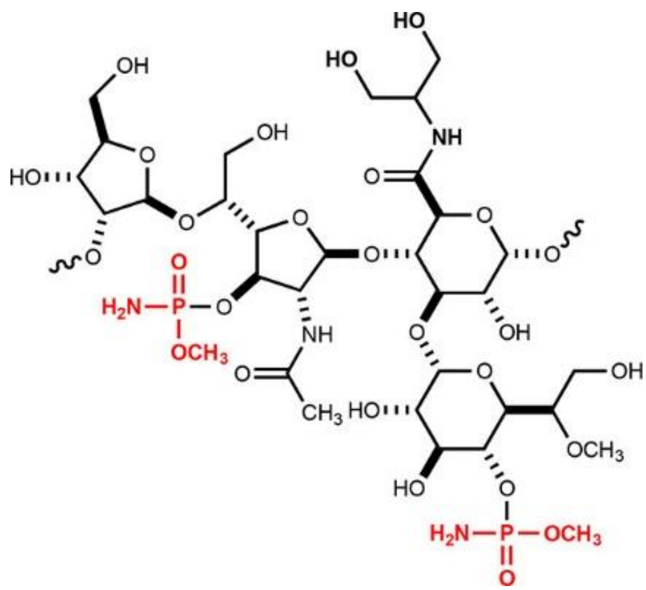

A cluster of 35 genes has been identified in *C. jejuni* NCTC 11168 that is primarily responsible for the biosynthesis and export of the CPS (11). Eight genes in this cluster (Cj1415 through Cj1422) have been predicted to be responsible for the biosynthesis and transfer of the MeOPN modification to the sugar backbone (10). Enzymes with the locus tags Cj1421 and Cj1422 have been implicated in the transfer of the phosphoramidate moiety to their respective sugar targets (10). Cj1422 is required for the attachment of the MeOPN group to D-glycero-α-L-*gluco*-heptopyranose, whereas

Cj1421 is needed for modification to 2-acetamido-2-deoxy-β-D-galactofuranose (10). Cj1419 and Cj1420 are annotated as SAM-dependent methyltransferases and are believed to be responsible for methylation of the phosphoramidate group (10). The other four enzymes, Cj1415, Cj1416, Cj1417, and Cj1418 are required for the biosynthesis of the phosphoramidate group of MeOPN, and if any of the four genes for these enzymes are deleted, all of the MeOPN modifications are lost (10).

Recently, we functionally characterized the first three enzymes in the biosynthesis of the phosphoramidate modification in *C. jejuni* (12,13). In the first reaction, Cj1418 catalyzes the adenosine triphosphate (ATP)-dependent phosphorylation of L-glutamine on the amide nitrogen to make L-glutamine phosphate (12). This product is utilized by Cj1416 to displace pyrophosphate from MgCTP to form cytidine diphosphate (CDP)-L-glutamine (13). Cj1417 then catalyzes the hydrolysis of CDP-L-glutamine to produce L-glutamate and cytidine diphosphoramidate (CDP-NH_2). These reactions are summarized in Scheme 14. Cj1415 is currently annotated as an adenylyl sulfate kinase from cog0529 (14). While most members of this family of enzymes are bifunctional adenylyl sulfate synthases/adenylyl sulfate kinases, the closest functionally characterized homologue to Cj1415 is the monofunctional CysC from *Escherichia coli* (14). CysC catalyzes the ATP-dependent phosphorylation of the 3′-hydroxyl group of adenylyl sulfate (APS), forming 3′-phosphoadenosine 5′-phosphosulfate (PAPS), a molecule that is ultimately used in the transfer of sulfate to various acceptors (Scheme 15). Because CysC is the closest functionally characterized homologue to Cj1415, we postulate that Cj1415 will phosphorylate the 3′-hydroxyl group of cytidine

diphosphoramidate (**1**) to synthesize a new cofactor for the transfer of phosphoramidate groups to various acceptors.

Scheme 14 Activities of Cj1418, Cj1416 and Cj1417

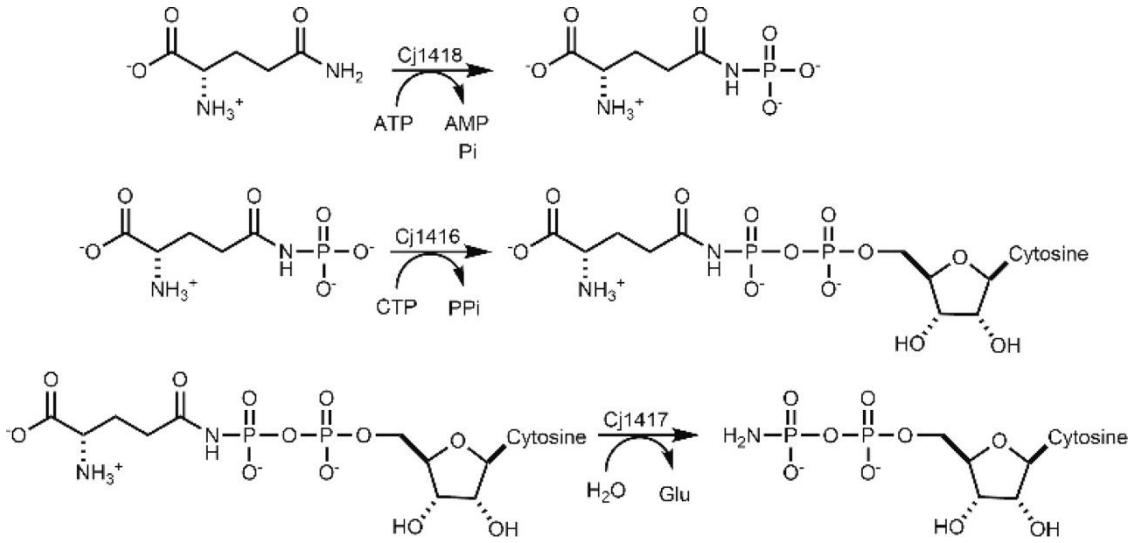

Scheme 15 Reaction Catalyzed by CysC

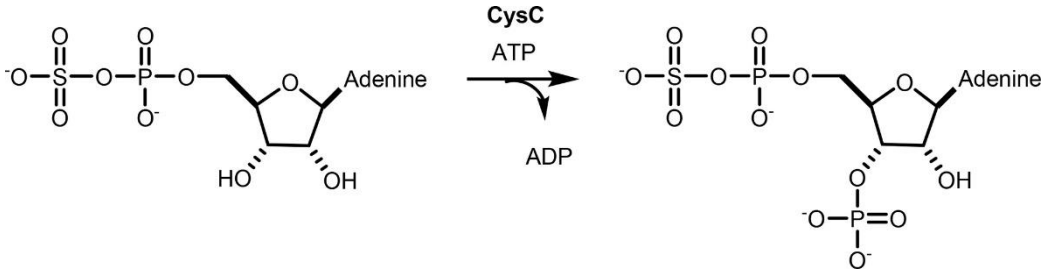

4.2. Materials and Methods

4.2.1. Materials

All chemicals and buffers were purchased from Sigma-Aldrich unless otherwise specified. CDP, uridine diphosphate (UDP), and cytidine triphosphate (CTP) were purchased from Alfa Aesar. Adenosine diphosphate (ADP) was purchased from TCI Chemicals. DpnI was obtained from New England Biolabs. Primestar HS polymerase was purchased from Takara Industries. The plasmid used for the expression of Cj1415 from *C. jejuni* NCTC 11168 was obtained from Professor Christine Szymanski of the University of Georgia.

4.2.2. Gene Expression and Enzyme Purification

The plasmid for the expression of Cj1415 (UniProt: Q0P8J9) with a C-terminal polyhistidine purification tag was used to transform Rosetta (DE3) *E. coli* cells by electroporation. Five-milliliter cultures of LB medium supplemented with 50 μg/mL kanamycin and 25 μg/mL chloramphenicol were inoculated with a single colony and grown overnight at 37 °C. These cultures were used to inoculate 1 L of LB medium (50 μg/mL kanamycin and 25 μg/mL chloramphenicol) and then incubated at 30 °C until an OD_{600} of ∼0.6−0.8 was reached. The cells were induced with 1.0 mM isopropyl β-thiogalactoside (IPTG), grown for 16 h at 16 °C, and then harvested by centrifugation at 6000 rpm at 4 °C. The resulting cell pellet was resuspended into loading buffer (50 mM HEPES/K^+, 300 mM KCl, 20 mM imidazole, pH 8.0) and lysed by sonication. The total

cell lysate was passed through a 0.45 μm filter before being loaded onto a prepacked 5 mL HisTrap HP (GE Healthcare) nickel affinity column. Protein was eluted with 50 mM HEPES/ K^+, pH 8.0, 300 mM KCl, and 400 mM imidazole over a gradient of 30 column volumes. Excess imidazole was removed by exchanging the buffers against 50 mM HEPES/K^+, pH 8.0, 100 mM KCl using a 20 mL (10 kDa molecular weight cutoff) concentrator (GE Healthcare). The purified protein was flash frozen and stored at −80 °C. Approximately 30 mg of purified protein was obtained per liter of cell culture.

4.2.3. Synthesis of Substrates

Cytidine diphosphoramidate (CDP-NH_2, **1**), uridine diphosphoramidate (UDP-NH_2, **6**), and adenosine diphosphoramidate (ADP-NH_2, **7**) were prepared chemically as previously described (15). 2′-Deoxy cytidine diphosphoramidate (2′-deoxy-CDP-NH_2, **2**) was made enzymatically with 2′-deoxy CTP (Roche) and L-glutamine phosphate,12 using Cj1416 and Cj1417 as catalysts (13). 2′-Deoxy CTP (10 mM), L-glutamine phosphate (10 mM) and $MgCl_2$ (15 mM) were incubated with Cj1416 (10 μM) and Cj1417 (10 μM) for 3 h at room temperature (100 mM HEPES pH 8.0). The enzymes were removed by filtration and the concentration of 2′-deoxy-CDP-NH_2 was determined by UV−visible spectroscopy.

CDP-methyl phosphate (CDP-OMe, **4**) and CDP-methyl phosphonate (CDP-Me, **5**) were made enzymatically using Cj1416 and MnCTP (13). In these reactions, methyl phosphate (15 mM) or methyl phosphonate (15 mM) was incubated with Cj1416 (15 μM) and CTP (15 mM) with $MgCl_2$ (15 mM) and $MnCl_2$ (4.0 mM) in 100 mM

HEPES/K^+, pH 8.0, 100 mM KCl. After 16 h, the reactions were quenched, and the target compounds were purified by anion exchange column chromatography (DEAE Sephadex) using a gradient of 10− 1000 mM triethylamonium bicarbonate (pH 8.0). The elution of the products from the column was monitored at 260 nm. The fractions were pooled, and the structures of the desired compounds were confirmed by ^{31}P NMR spectroscopy and ESI (negative) mass spectrometry. CDP-Me (**5**) was obtained in an isolated yield of ∼30%, and CDP-OMe (**4**) was obtained with a yield of ∼20% based on the starting concentration of CTP. The ^{31}P NMR spectrum of CDP-Me (**5**) showed two doublets at 17.92 (β-P) and −10.79 ppm (α-P), whereas the ^{31}P NMR spectrum for CDP-OMe (**4**) showed two doublets at −9.06 (βP) and −10.82 ppm (α-P). The ESI (negative) mass spectrum for CDP-Me (**5**) indicated an m/z of 400.03 (expected m/z for M − H = 400.03 for $C_{10}H_{17}N_3O_{10}P_2$), whereas the ESI (negative) mass spectrum for CDP-OMe (**4**) had an m/z of 416.02 (expected m/z for M − H = 416.02 for $C_{10}H_{17}N_3O_{11}P_2$). The structures of the compounds used in this investigation are presented in Scheme 16.

Scheme 16 Cj1415 Substrates

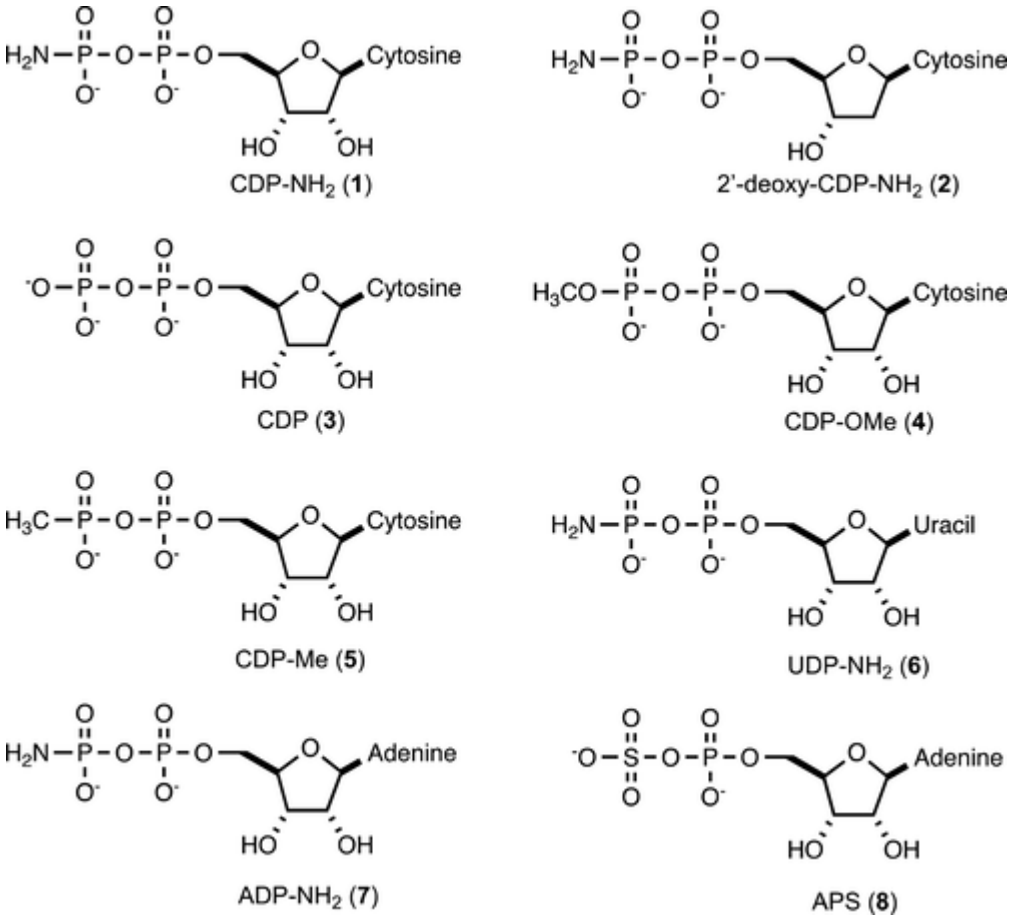

4.2.4. Determination of Kinetic Constants

The kinetic constants for wild-type Cj1415 were determined using a pyruvate kinase/lactate dehydrogenase coupled enzyme assay, following the oxidation of NADH at 340 nm at 25 °C with a SpectraMax340 UV−visible spectrophotometer (16). Assays were performed in 100 mM HEPES/K^+, pH 8.0, and 100 mM KCl. The coupling system contained 2.0 mM phosphoenol pyruvate, 0.3 mM NADH, 8 units/mL lactate dehydrogenase, and 8 units/mL pyruvate kinase. When determining the kinetic constants for CDP-NH_2 (20−200 μM), 2′-deoxy CDP-NH_2 (50−500 μM), ADP-NH_2 (1−10 mM), UDP-NH_2 (2.6−26 mM), CDP-OMe (200−2000 μM), and CDP-Me (360−3600 μM), a fixed concentration of 10 mM ATP was used. The kinetic constants for ATP (200−7000 μM) were determined with a fixed concentration of 400 μM CDP-NH_2. For these experiments, $MgCl_2$ was added in a 4.0 mM excess of the total nucleoside concentration. Kinetic constants for the consumption of CDP (0.5−15 mM) were determined using ^{31}P NMR spectroscopy because CDP interfered with the coupled enzyme assay. For these assays, each reaction mixture contained 10 mM ATP and a 4 mM excess of $MgCl_2$. The reactions were followed for 30 min, collecting a ^{31}P NMR spectrum every 5 min. With the S85A mutant of Cj1415, the kinetic constants for CDP-NH_2 (0.20−10 mM) were determined at a fixed concentration of ATP (10 mM). The kinetic constants for ATP (1−8 mM) were determined at a fixed concentration of CDP-NH_2 (15 mM). Kinetic constants for ATP, CDP-NH_2, dCDP-NH_2, CDP-OMe, and CDP-Me were determined using 200 nM Cj1415; CDP, ADP-NH_2, and UDP-NH_2 used 1, 2.1, and 10 μM of enzyme, respectively.

The kinetic parameters were determined by fitting the initial rates to eq 1 using GraFit 5, where υ is the initial velocity of the reaction, Et is the enzyme concentration, k_{cat} is the turnover number, [A] is the substrate concentration, and K_m is the Michaelis constant.

$$\upsilon/Et = k_{cat}(A)/(A + K_m) \quad (1)$$

4.2.5. ^{31}P NMR Spectroscopy

The product of the ATP-dependent phosphorylation of each substrate by Cj1415 was analyzed by ^{31}P NMR spectroscopy. Each reaction was conducted in 100 mM HEPES/K^+, pH 8.0, and 100 mM KCl at 25 °C and initially contained 5.0 mM ATP, 5.0 mM substrate, 14 mM $MgCl_2$, and 5 μM Cj1415. All reactions were quenched after 60 min with 15 mM EDTA, except for UDP-NH_2 (**6**) and ADP-NH_2 (**7**), which were quenched after 3 h. After the reactions were quenched, the pH was adjusted to 9.0 before the spectra were collected.

4.2.6. Cj1415 S85A Mutant

Ser85 in Cj1415 was determined to be a residue of interest based on previous reports that the homologous residue in CysC from *E. coli* is phosphorylated during catalysis (17). The pET 30b plasmid for the expression of wild-type Cj1415 with a C-terminal hexahistidine tag was used as a template for the construction of a plasmid for the expression of the S85A mutant. The forward primer (5′GTATGATGGTTATTGTCACTACGATTGCAATGTTTAATGAGATTTATG-3′)

and reverse primer (5 ′-
CATAAATCTCATTAAACATTGCAATCGTAGTGACAATAACCATCATAC-3′) were used to convert the serine codon (TCA) to alanine (GCA). Primestar HS polymerase was used to amplify the gene. The reaction used a three-step thermal cycle (98 °C for 10 s, 63 °C for 40 s, and 72 °C for 10 min) and continued through 30 cycles. After amplification, DpnI was used to digest the template DNA for 2 h at 37 °C. Following DpnI digestion, PCR cleanup (Qiagen) was performed, and the plasmid was transformed into *E. coli* BL21 (DE3) cells. Single colonies were selected, and the DNA sequence of the mutant gene was confirmed.

4.2.7. Cog0529 Sequence Similarity Network

The identification codes for cog0529 (1160 total sequences) were downloaded from Uniprot. The collected identifiers were used to generate a network using the Enzyme Function Initiative− Enzyme Similarity Tool through Option-D (18,19). The full network (each sequence is a node) was downloaded and used to generate a sequence similarity network using Cytoscape (20). Edges below a 50% identity threshold were removed, and each cluster was assigned an arbitrary number and color.

4.3. Results

4.3.1. Determination of the Catalytic Activity of Cj1415

CysC in *E. coli* catalyzes the final step in the biosynthesis of PAPS, the cofactor used for sulfuryl transfer in biological systems (14). Because the closest functionally characterized homologue to Cj1415 is CysC, adenylyl sulfate (APS, **8**) was tested as a substrate for this enzyme using ATP as the phosphoryl donor. Within the limits of the coupled enzyme assay, no activity could be detected using Cj1415 to catalyze the phosphorylation of APS. Because of its presumptive connection to the biosynthesis of the O-methyl phosphoramidate moiety in *C. jejuni*, Cj1415 was tested with cytidine diphosphoramidate (**1**) as a substrate because this compound has been demonstrated to be the final product in the collective reactions catalyzed by Cj1416, Cj1417, and Cj1418 (Scheme 14) (12,13). CDP-NH_2 (**1**) is an excellent substrate for Cj1415 with a turnover number of 2.2 s−1.

4.3.2. Characterization of the Cj1415 Catalyzed Reaction

The reaction between CDP-NH_2 and MgATP, as catalyzed by Cj1415, was analyzed by ^{31}P NMR spectroscopy. After an incubation period of approximately 1 h, the ^{31}P NMR spectrum shows that most of the ATP was converted to ADP and that a new resonance was observed at ~4.1 ppm (Figure 9A). In the ^{1}H-coupled spectrum, this resonance is a doublet with a coupling constant of 7.3 Hz, indicating that this phosphorus is coupled to a nonexchangeable proton. The molecular weight of the new product (**9**) was determined by ESI (negative ion) mass spectroscopy and shown to be 480.99. This value is consistent with the expected m/z of 480.99 for $C_9H_{17}N_4O_{13}P_3$. Based on the molecular structure of CDP-NH_2, the site of phosphorylation can correspond only to the 2′- or 3′-hydroxyl group of the ribose ring.

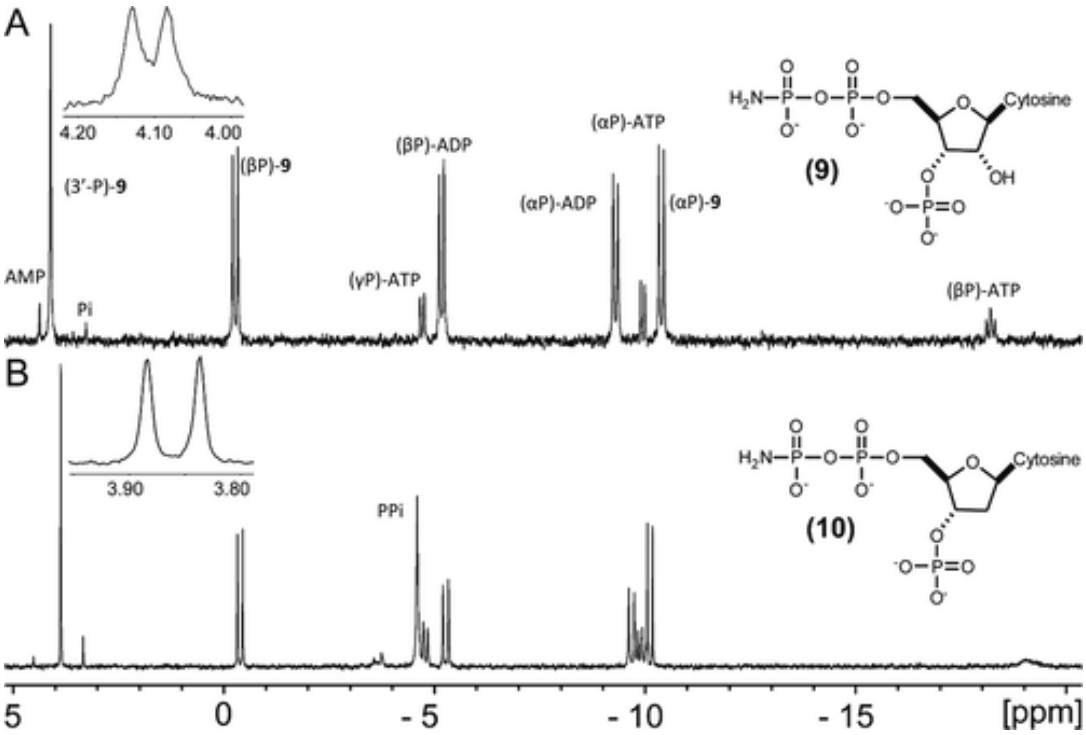

Figure 9 ^{31}P NMR spectra of the products in the reaction catalyzed by Cj1415. (A) Cj1415 (5 μM) was mixed with 5.0 mM MgATP and 5.0 mM CDP-NH_2 for 60 min at pH 8.0 before the reaction was quenched with 15 mM EDTA. (B) Cj1415 (5 μM) was mixed with 5.0 mM MgATP and 5.0 mM 2′-deoxy-CDP-NH_2 for 60 min before the reaction was quenched with 15 mM EDTA. The insets show the ^{1}H-coupled spectra for the resonances at 4.1 (A) and 3.85 ppm (B). Additional details are available in the text**.**

The 2′-deoxy derivative of CDP-NH_2 (**2**) was synthesized enzymatically and tested as a potential substrate for Cj1415. In the presence of MgATP, 2 ′-deoxy-CDP-NH_2 (**2**) was phosphorylated with a k_{cat} of 2.2 s^{-1} (Table 1). The ^{31}P NMR spectrum of the phosphorylated reaction product (Figure 9B) shows the presence of a new resonance at ~3.85 ppm that is a doublet, with a coupling constant of 7.8 Hz, in the absence of proton decoupling. The molecular weight of this product (**10**) was determined by negative ion ESI-MS and shown to be 465.00. This value is consistent with the expected m/z of 464.98 for $C_9H_{17}N_4O_{12}P_3$. Because the kinetic constants for the phosphorylation of CDP-NH_2 and 2′-deoxy-CDP-NH_2 are essentially identical, the site of phosphorylation is at the hydroxyl group attached to C3′ of the ribose ring. This result is fully consistent with the site of phosphorylation catalyzed by CysC. The reaction catalyzed by Cj1415 is summarized in Scheme 17.

Table 1 Kinetic Constants of Cj1415 at 25 ºC, pH 8.0

substrate		k_{cat} (s^{-1})	K_m (mM)	k_{cat}/K_m (M^{-1} s^{-1})
CDP-NH_2	(**1**)	2.2 ± 0.3	0.11 ± 0.01	20000 ± 3300
dCDP-NH_2	(**2**)	2.2 ± 0.2	0.39 ± 0.07	5600 ± 1100
CDP	(**3**)	0.64 ± 0.04	4.2 ± 0.7	150 ± 30
CDP-OMe	(**4**)	0.65 ± 0.06	1.35 ± 0.2	500 ± 100
CDP-Me	(**5**)	1.4 ± 0.1	0.83 ± 0.2	1700 ± 400
UDP-NH_2	(**6**)	0.023 ± 0.002	21 ± 3	1.1 ± 0.2
ADP-NH_2	(**7**)	0.08 ± 0.01	5.6 ± 0.8	14 ± 3
APS	(**8**)	< 0.01	n.d.	n.d.
CDP-NH_2[a]	(**1**)	1.6 ± 0.2	4.4 ± 0.4	360 ± 60
ATP		2.2 ± 0.3	1.5 ± 0.1	1500 ± 300
ATP[a]		1.6 ± 0.2	0.7 ± 0.1	2300 ± 500

[a]S85A mutant of Cj1415

Scheme 17 Reaction Catalyzed by Cj1415

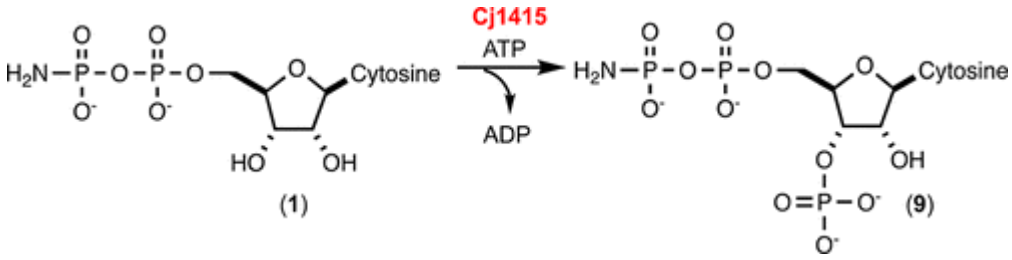

4.3.3. Substrate Specificity of Cj1415

The range of substrates accepted by Cj1415 was tested with five additional compounds. To determine if Cj1415 is selective for the cytosine base, uridine diphosphoramidate (**6**) and adenosine diphosphoramidate (**7**) were tested as substrates (Table 1). The values of k_{cat}/K_m for these two compounds are 3−4 orders of magnitude poorer than the value for CDP-NH_2, and thus, Cj1415 greatly prefers the cytosine base. Two other cytidine diphosphoramidate analogues were synthesized and assayed with Cj1415. Similar to CDP-NH_2, these analogues possess a single negative charge on the β-phosphorus group. CDP-methyl phosphate (**4**) and CDP-methyl phosphonate (**5**) were both found to be substrates for Cj1415. The values of k_{cat} are 30−60% comparable to CDP-NH_2, but the K_m values are about an order of magnitude greater than that for CDP-NH_2. CDP can be phosphorylated by Cj1415, but the value of k_{cat}/K_m is approximately two orders of magnitude poorer than that for CDP-NH_2. For all seven substrates discovered for Cj1415, the negative ion ESI mass spectra of the phosphorylated reaction products are fully consistent with the expected molecular structure.

4.3.4. Mutation of Serine-85

The closest functionally characterized homologue to Cj1415 is CysC from *E. coli* (14). Previous investigations with CysC have indicated the requirement for the phosphorylation of a serine residue as an obligatory reaction intermediate (17). The phosphorylated enzyme was isolated and shown to phosphorylate APS in the absence of added ATP (17). This serine residue is conserved in close CysC homologues and in

Cj1415. To determine if the corresponding residue in Cj1415 is required for catalytic activity, Ser-85 was mutated to an alanine residue (S85A). The value of k_{cat} for the S85A mutant is 73% of the value of the wild-type enzyme, but the value of K_m is 40 times greater, suggesting that this residue is not phosphorylated during catalysis but is perhaps interacting with the substrate in the active site (Table 1).

4.4. Discussion

4.4.1. Substrate Specificity

In this study, we established the substrate profile of Cj1415, an enzyme that functions in the biosynthesis of the cofactor used for the transfer of phosphoramidate to acceptor carbohydrates in *C. jejuni*. As anticipated, the product of the reaction catalyzed by Cj1417, cytidine diphosphoramidate (**1**), is the best substrate of those tested for Cj1415 and is phosphorylated on the C3′-hydroxyl group (Table 1). We also examined the catalytic activity with the corresponding adenine and uridine diphosphoramidate derivatives and confirmed that cytidine is the nucleotide preferred by Cj1415. CDP is a relatively poor substrate for Cj1415, and this result is likely to be a reflection of the two negative charges on the β-phosphoryl group, where CDP-NH_2 has only one. In addition to CDP-NH_2, the enzyme will also accept the substitution of $-CH_3$ or $-OCH_3$ for the $-NH_2$ functional group on the β-phosphorus substituent. We propose that this enzyme be called cytidine diphosphoramidate kinase (CDK).

4.4.2. Comparison with Adenylyl Sulfate Kinase

Cj1415 is a member of cog0529, and the sequence similarity network (SSN) is presented in Figure 10 at a percent identity cutoff of 50% (18). The only known catalytic activities from cog0529 are adenylyl sulfate kinase or a bifunctional adenylyl sulfate synthase and adenylyl sulfate kinase, which represent arbitrary Group 1 (Figure 10). At a 50% identity cutoff, Cj1415 is Group 2, which contains no functionally characterized enzymes. This cluster contains enzymes primarily from various *Campylobacter* and *Helicobacter* species. Groups 3−5 are not similar to adenylyl sulfate kinase or Cj1415 and thus likely represent other unique catalytic activities. Group 3 contains sequences only from *Desulfovibrio* species, indicating this group of enzymes may be specific to this bacterium.

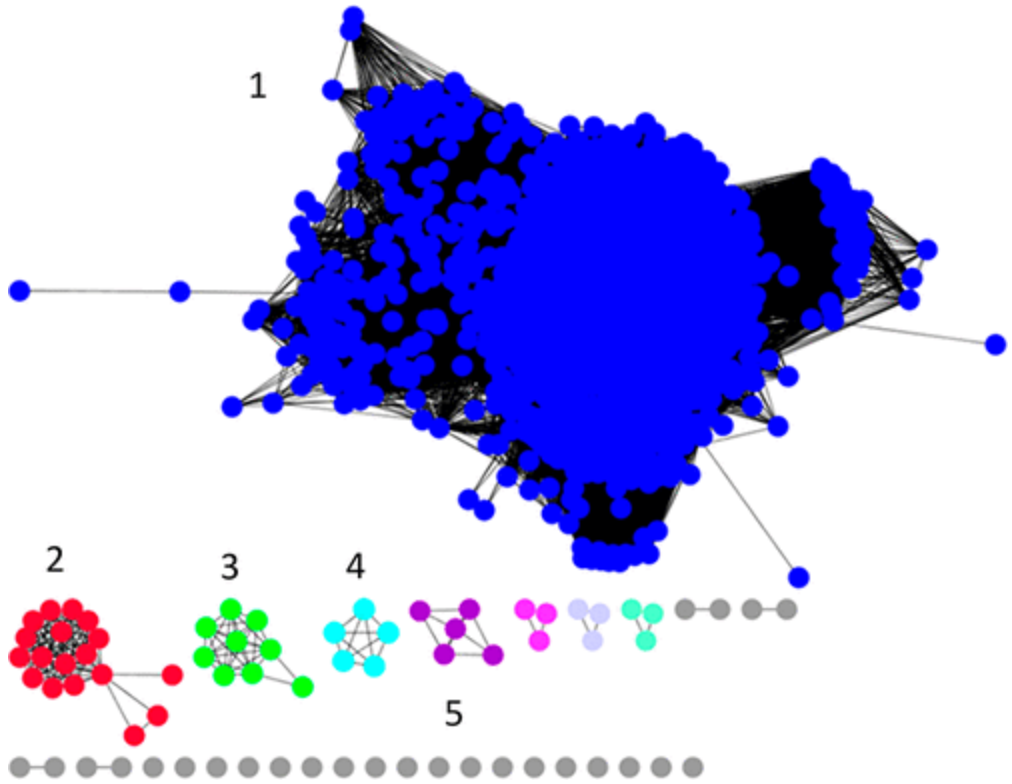

Figure 10 Sequence similarity network for proteins of cog0529 at a percent identity cutoff of 50%. All protein sequences for cog0529 obtained from Uniprot were used to create the network. Each node (colored sphere) represents a unique protein sequence, and each edge (black line) represents a connection between two sequences at the given percent identity cutoff. Group 1 contains known adenylyl sulfate kinases or bifunctional adenylyl sulfate kinase/adenylyl sulfate synthases. Group 2 contains Cj1415 and homologues from several *Campylobacter* and *Helicobacter* species. Groups 3–5 represent enzymes that are dissimilar from adenylyl sulfate kinases and Cj1415 and likely represent unique activities.

The closest functionally characterized homologue to Cj1415 is CysC from *E. coli* with a 26% identity. Two other monofunctional adenylyl sulfate kinases from *Arabidopsis thaliana* (UniProt Q43295) and *Penicillium chrysogenum* (UniProt Q12657) also share a 26% identity to Cj1415. A sequence alignment of these four proteins is presented in Figure 11. The three-dimensional structure of the *A. thaliana* enzyme was previously solved, and the adenylyl sulfate binding residues were identified (Figure 12). Comparing the residues in the active site of adenylyl sulfate kinase to Cj1415, there are three notable differences in residues that interact with the nucleoside base and the sulfate moiety of the bound adenylyl sulfate. In adenylyl sulfate kinase, there are two phenylalanine residues that interact with the adenine base; however, in Cj1415, these two residues are replaced by tyrosine and valine. These two residues may help to explain the specificity for cytosine over adenine (21). The sulfate of adenylyl sulfate in CysC is stabilized by an asparagine residue, which donates two hydrogen bonds to the substrate. In Cj1415, this residue is a methionine, a hydrogen bond acceptor. Methionine commonly forms hydrogen bonds with the backbone amide in a polypeptide chain (22). This change from a hydrogen bond donor to an acceptor in Cj1415 may help to explain why the amidate substrate is preferred over sulfate.

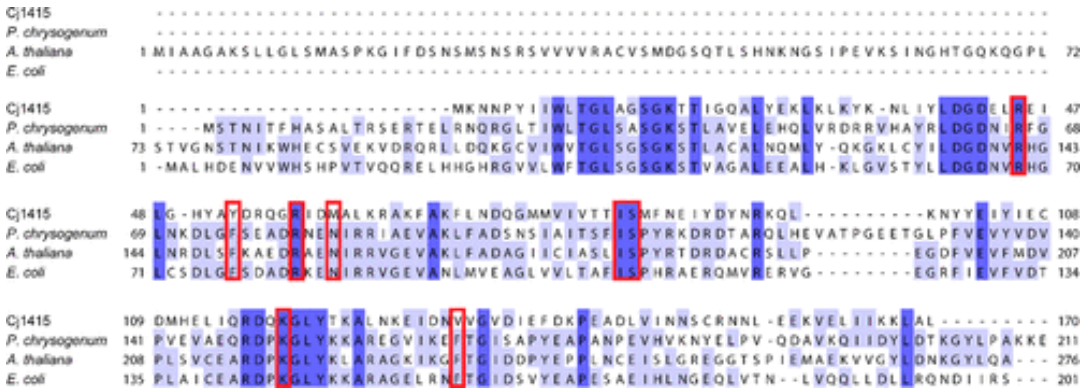

Figure 11 Sequence alignment of CysC homologues. Sequence alignment of *E. coli* CysC (UniProt P0A6J1), *Arabadopsis* CysC (UniProt Q43295), *Penicillium* CysC (UniProt Q12657), and Cj1415 (UniProt Q0P8J9). The annotated adenylyl sulfate binding residues are highlighted in red boxes (residues based on *Arabidopsis* crystal structure PDB id: 3UIE) (25).

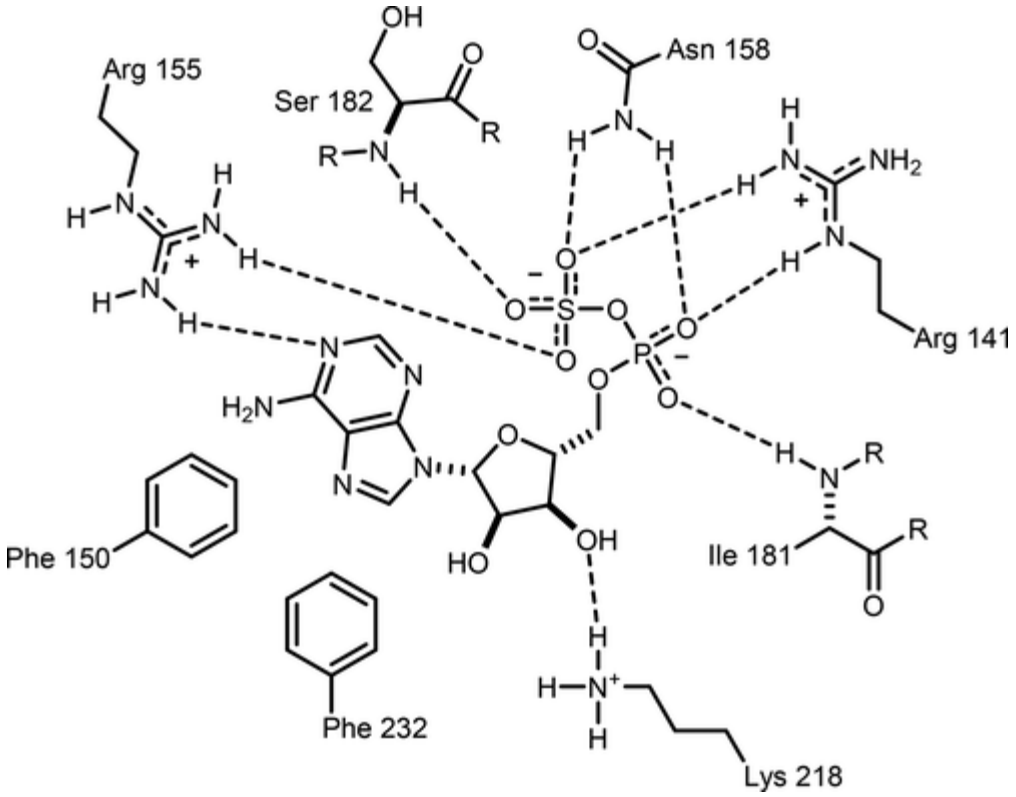

Figure 12 Active site of *Arabidopsis* adenylyl sulfate kinase (PDB id: 3UIE) (25). This image was adapted from the ligand interactions found within the Protein Data Bank for this structure. Potential hydrogen bonds are indicated by the dashed lines, where the distances between the two heteroatoms are ≤3.1 Å.

Previously, the *E. coli* CysC enzyme has been reported to require a phosphoserine enzyme intermediate (17). However, this residue has never been mutated, and a crystal structure is not available for the *E. coli* enzyme. Mutation of the *A. thaliana* and *P. chrysogenum* CysC homologues show that when this serine is mutated, there is no loss of catalytic activity (23,24). In the crystal structure of *A. thaliana* (Figure 12), this serine residue is in the active site but is removed from the 3′-hydroxyl group of adenylyl sulfate (25). While this residue is not forming a phosphorylated intermediate in Cj1415, its involvement in substrate binding can be seen in the increased K_m of CDP-NH_2 (Table 1).

We demonstrated that Cj1415, Cj1416, Cj1417, and Cj1418 collectively catalyze the biosynthesis of 3′-phosphocytidine-5′diphosphoamidate (**9**) using L-glutamine, CTP, and two molecules of ATP. The β-phosphoramidate group of **9** must ultimately be methylated and transferred to a specific carbohydrate that is incorporated into the growing capsular polysaccharide chain. However, at this point, it is unclear as to the timing of the methylation and phosphoryl transfer reactions in the biosynthesis of the capsular polysaccharide chain. From the appropriate gene cluster contained within *C. jejuni* 11168, it is highly likely that the enzymes Cj1419 and Cj1420 will be responsible for the transfer of the methyl group of SAM to the appropriate substrate and that Cj1421 and Cj1422 will catalyze the transfer of the phosphoramidate or the methylated phosphoramidate group to either an NDP-functionalized sugar or the growing capsular polysaccharide itself. Experiments are currently underway to unravel the substrate profiles for Cj1419, Cj1420, Cj1421, and Cj1422.

4.5. References

1. Young, K. T., Davis, L. M., and Dirita, V. J. (2007) *Campylobacter jejuni*: Molecular Biology and Pathogenesis. *Nat. Rev. Microbiol*. 5, 665−679.
2. Guerry, P., Poly, F., Riddle, M., Maue, A. C., Chen, Y.-H., and Monteiro, M. A. (2012) Campylobacter Polysaccharide Capsules: Virulence and Vaccines. *Front. Cell. Infect. Microbiol.* 2,1 −7.
3. Lee, M. D., and Newell, D. G. (2006) Campylobacter in Poultry: Filling an Ecological Niche. *Avian Dis*. 50,1−9.
4. Poropatich, K. O., Walker, C. L. F., and Black, R. E. (2010) Quantifying the Association between Campylobacter Infection and Guillain-Barré Syndrome: A Systematic Review. *J. Health Popul. Nutr*. 28, 545−552.
5. Roberts, I. S. (1996) The Biochemistry and Genetics of Capsular Polysaccharide Production in Bacteria. *Annu. Rev. Microbiol*. 50, 285− 315.
6. Bacon, D. J., Szymanski, C. M., Burr, D. H., Silver, R. P., Alm, R. A., and Guerry, P. (2001) A Phase-Variable Capsule is Involved in Virulence of *Campylobacter jejuni* 81−176. *Mol. Microbiol*. 40, 769− 777.
7. Liang, H., Zhang, A., Gu, Y., You, Y., Zhang, J., and Zhang, M. (2016) Genetic Characteristics and Multiple-PCR Development for Capsular Identification of Specific Serotypes of *Campylobacter jejuni*. *PLoS One* 11, e0165159.
8. Poly, F., Serichatalergs, O., Schulman, M., Ju, J., Cates, C. N., Kanipes, M., Mason, C., and Guerry, P. (2011) Discrimination of Major Capsular Types of *Campylobacter jejuni* by Multiplex PCR. *J. Clin. Microbiol*. 49, 1750−1757.

9. Michael, F. S., Szymanski, C. M., Li, J., Chan, K. H., Khieu, N. H., Larocque, S., Wakarchuk, W. W., Brisson, J.-R., and Monteiro, M. A. (2002) The Structures of the Lipooligosaccharide and Capsule Polysaccharide of *Campylobacter jejuni* Genome Sequenced Strain NCTC 11168. *Eur. J. Biochem.* 269, 5119−5136.
10. McNally, D. J., Lamoureux, M. P., Karlyshev, A. V., Fiori, L. M., Li, J., Thacker, G., Coleman, R. A., Khieu, N. H., Wren, B. W., Brisson, J.-R., Jarrell, H. C., and Szymanski, C. M. (2007) Commonality and Biosynthesis of the O-Methyl Phosphoramidate Capsule Modification in *Campylobacter jejuni*. *J. Biol. Chem*. 282, 28566−28576.
11. Karlyshev, A. V., Linton, D., Gregson, N. A., Lastovica, A. J., and Wren, B. W. (2000) Genetic and Biochemical Evidence of a *Campylobacter jejuni* Capsular Polysaccharide that Accounts for Penner Serotype Specificity. *Mol. Microbiol*. 35, 529−541.
12. Taylor, Z. W., Brown, H. A., Narindoshvili, T., Wenzel, C. Q., Szymanski, C. M., Holden, H. M., and Raushel, F. M. (2017) Discovery of a Glutamine Kinase Required for the Biosynthesis of the O-Methyl Phosphoramidate Modifications Found in the Capsular Polysaccharides of *Campylobacter jejuni*. *J. Am. Chem. Soc*. 139, 9463− 9466.
13. Taylor, Z. W., Brown, H. A., Holden, H. M., and Raushel, F. M. (2017) Biosynthesis of Nucleoside Diphosphoramidates in *Campylobacter jejuni*. *Biochemistry* 56, 6079−6082.

14. Leyh, T. S., Taylor, J. C., and Markham, G. D. (1988) The Sulfate Activation Locus of *Escherichia coli* K12: Cloning, Genetic, and Enzymatic Characterization. *J. Biol. Chem*. 263, 2409−2416.
15. Wehrli, W., Verheyden, D., and Moffatt, J. (1965) Dismutation Reactions of Nucleoside Polyphosphates. II. Specific Chemical Syntheses of α-, β-, and γ-P^{32}-Nucleoside 5′-Triphosphates1. *J. Am. Chem. Soc*. 87, 2265−2277.
16. Technikova-Dobrova, Z., Sardanelli, A. M., and Papa, S. (1991) Spectrophotometric Determination of Functional Characteristics of Protein Kinases with Coupled Enzymatic Assay. *FEBS Lett*. 292, 69−72.
17. Satishchandran, C., Hickman, Y. N., and Markham, G. D. (1992) Characterization of the Phosphorylated Enzyme Intermediate Formed in the Adenosine 5′-Phosphosulfate Kinase Reaction. *Biochemistry* 31, 11684−11688.
18. Atkinson, H. J., Morris, J. H., Ferrin, T. E., and Babbitt, P. C. (2009) Using Sequence Similarity Networks for Visualization of Relationships Across Diverse Protein Superfamilies. *PLoS One* 4, e4345.
19. Gerlt, J. A., Bouvier, J. T., Davidson, D. B., Imker, H. J., Sadkhin, B., Slater, D. R., and Whalen, K. L. (2015) Enzyme Function Initiative Enzyme Similarity Tool (EFI-EST): A web tool for generating protein sequence similarity networks. *Biochim. Biophys. Acta, Proteins Proteomics* 1854, 1019−1037.
20. Shannon, P., Markiel, A., Ozier, O., Baliga, N. S., Wang, J. T., Ramage, D., Amin, N., Schwikowski, B., and Ideker, T. (2003) Cytoscape: A Software Environment for

Integrated Models of Biomolecular Interaction Networks. *Genome Res*. 13, 2498−2504.

21. Copeland, K. L., Anderson, J. A., Farley, A. R., Cox, J. R., and Tschumper, G. S. (2008) Probing Phenylalanine/Adenine π-Stacking Interactions in Protein Complexes with Explicitly Correlated and CCSD(T) Computations. *J. Phys. Chem*. B 112, 14291−14295.
22. Biswal, H. S., Gloaguen, E., Loquais, Y., Tardivel, B., and Mons, M. (2012) Strength of NH···S Hydrogen Bonds in Methionine Residues Revealed by Gas-Phase IR/UV Spectroscopy. *J. Phys. Chem. Lett*. 3, 755−759.
23. Lillig, C. H., Schiffmann, S., Berndt, C., Berken, A., Tischka, R., and Schwenn, J. D. (2001) Molecular and Catalytic Properties of Arabidopsis thaliana Adenylyl Sulfate (APS)-Kinase. *Arch. Biochem. Biophys*. 392, 303−310.
24. MacRae, I. J., Segel, I. H., and Fisher, A. J. (2000) Crystal Structure of Adenosine 5′-Phosphosulfate Kinase from *Penicillium chrysogenum*. *Biochemistry* 39, 1613−1621.
25. Ravilious, G. E., Nguyen, A., Francois, J. A., and Jez, J. M. (2012) Structural Basis and Evolution of Redox Regulation in Plant Asenosine-5′-phosphosulfate Kinase. *Proc. Natl. Acad. Sci. U.S.A.* 109, 309−314.

5. SUBSTRATE SPECIFICITY AND CHEMICAL MECHANISM FOR THE REACTION CATALYZED BY GLUTAMINE KINASE*

5.1. Introduction

Campylobacter jejuni, a Gram-negative pathogenic bacterium, is a leading cause of gastroenteritis in the US (1). While *C. jejuni* is pathogenic toward humans, this organism is commensal toward chickens, and as a result, contaminated poultry is a common source of human infection. Like many other Gram-negative bacteria, *C. jejuni* produces a capsular polysaccharide (CPS), which is composed of unusually modified sugars, that envelops the organism. The capsular polysaccharides help protect the organism from the environment and are important for the invasion and colonization of the host organisms (2). Numerous strains of *C. jejuni* have been identified, and it is currently believed that each strain produces a unique capsular polysaccharide (3,4). An O-methyl phosphoramidate (MeOPN) modification was discovered in the CPS of the NCTC11168 strain of *C. jejuni* (4,5). This modification to the CPS is most unusual since phosphorus−nitrogen bonds are quite rare in nature (5)

The gene cluster for the biosynthesis of the CPS for the NCTC11168 strain of *C. jejuni* capsule has been identified, and eight of the 35 genes in this cluster appear to be linked with the presence of the MeOPN modification in the capsular polysaccharide (5,6) Of the eight enzymes that appear to be required for the biosynthesis of the MeOPN

* Reprinted with permission from "Substrate Specificity and Chemical Mechanism for the Reaction Catalyzed by Glutamine Kinase" by Zane W. Taylor, Alexandra R. Chamberlain, and Frank M Raushel, *Biochemistry* (2018) *57* (37), pp 5447-5455, Copyright 2018 American Chemical Society

modification, two are predicted to be phosphoramidate transferases (Cj1421 and Cj1422) and two are annotated as SAM-dependent methyltransferases (Cj1419 and Cj1420). The other four enzymes (Cj1415, Cj1416, Cj1417, and Cj1418) are directly responsible for the formation of the phosphoramidate moiety. Previously, we have characterized the four enzymes responsible for the formation of the phosphoramidate (7−9). The first enzyme, Cj1418, is a novel glutamine kinase that catalyzes the ATP-dependent phosphorylation of L-glutamine (**1**) to form L-glutamine phosphate (**2**) (8). L-Glutamine phosphate is subsequently used by Cj1416, a CTP−phosphoglutamine cytidylyltransferase, to displace pyrophosphate from CTP to generate CDP-L-glutamine (**3**) (7). Cj1417, a γ-glutamyl-CDP-amidate hydrolase, hydrolyzes CDP-L-glutamine to form L-glutamate and cytidine diphosphoramidate (**4**) (7). Cj1415, a cytidine diphosphoramidate kinase, catalyzes the phosphorylation of the 3′ hydroxyl group of cytidine diphosphoramidate (9). The phosphoramidate moiety of the 3′-phospho 5′-cytidine diphosphoramidate cofactor (**5**) is likely transferred to the capsule and methylated or, alternatively, methylated and then transferred to the capsule. The reactions are summarized in Scheme 18.

Scheme 18 Biosynthesis of 3'-Phospho-5'-cytidine Diphosphoramidate in *C. jejuni* NCTC 11168

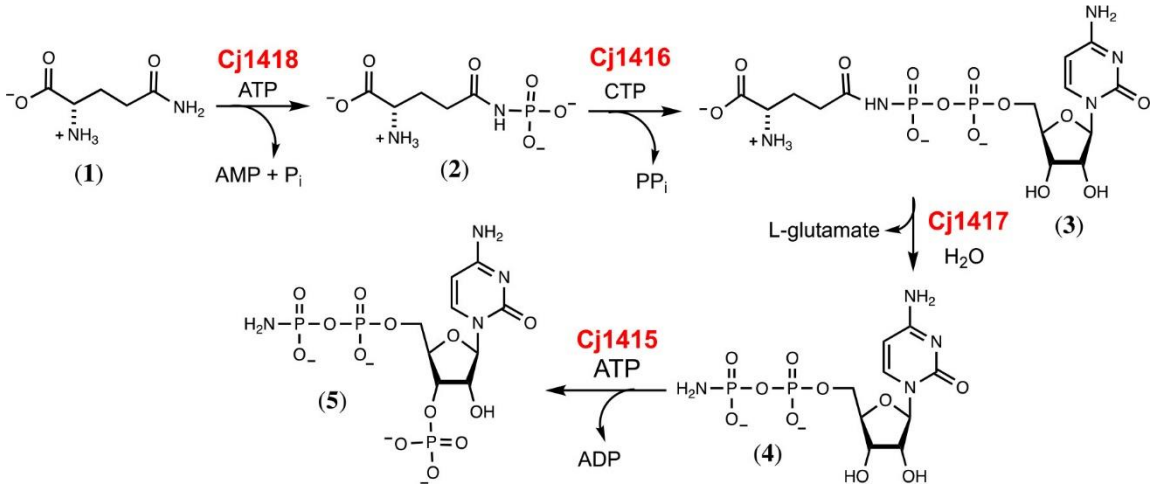

Of these four enzymes, glutamine kinase (Cj1418), is perhaps the most interesting mechanistically, as it is responsible for the synthesis of the phosphoramidate bond. Very few enzymes have been shown previously to catalyze the formation of P−N bonds; however, two strategies exist. Creatine kinase and arginine kinase catalyze the ATP-dependent phosphorylation of their respective substrates and generate ADP as a product (10,11). Alternatively, enzymes that are related to tRNA synthetases can also be used to generate phosphoramidate bonds through a mechanism similar to adenylylation (12). Cj1418 belongs to a family of kinases that employ an unusual reaction mechanism. Phospho(enol)pyruvate synthase catalyzes the ATP-dependent phosphorylation of pyruvate, generating PEP, AMP, and phosphate (13). Pyruvate phosphate dikinase catalyzes the ATP-dependent phosphorylation of phosphate and pyruvate to generate AMP, pyrophosphate, and PEP (14). Finally, rifampin phosphotransferase catalyzes the phosphorylation of rifampin with the formation of Pi and AMP (15,16). All three enzymes share a similar protein architecture and contain an ATP-grasp domain, a phospho-histidine domain, and a specialized substrate binding domain (16−18). These three domains can be identified in Cj1418, where residues 1−219 comprise the predicted ATP-grasp domain, residues 220−693 is likely the specialized substrate-binding domain for L-glutamine, and residues 694− 767 form the predicted phospho-histidine domain (17).

This enzyme family catalyzes the phosphorylation of substrates via a mechanism that requires three distinct chemical steps. In the first step, the enzyme utilizes a histidine residue to attack ATP at the β-phosphoryl group to liberate AMP and a

pyrophosphorylated enzyme intermediate. In the next step, the pyrophosphorylated enzyme is hydrolyzed to form inorganic phosphate and a phosphorylated enzyme intermediate. In the final step, the phosphorylated enzyme intermediate transfers the phosphate to the acceptor substrate. These transformations are summarized in Scheme 19 for the reaction catalyzed by Cj1418.

Scheme 19 Proposed Reaction Mechanism for the Formation of L-Glutamine Phosphate by Cj1418

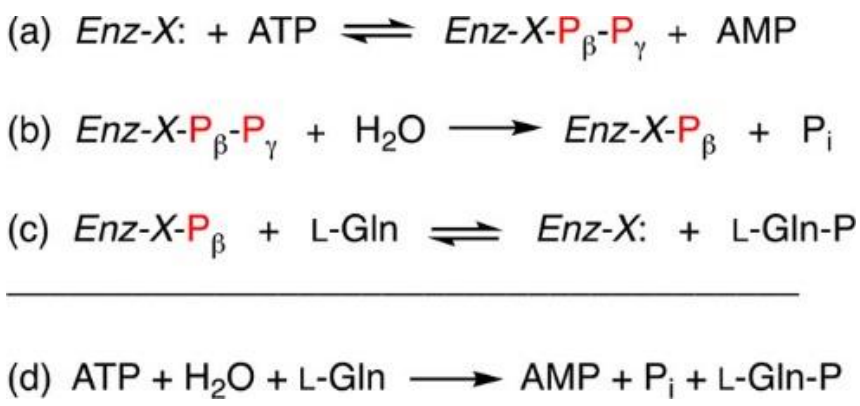

In this investigation, we have addressed the reaction mechanism and substrate profile for the reaction catalyzed by glutamine kinase. The formation of the pyrophosphorylated and phosphorylated covalent reaction intermediates have been interrogated by utilization of positional isotope exchange (PIX) and molecular isotope exchange (MIX) techniques (19,20). The active site histidine residue has been identified by mutagenesis, and the enzyme has been shown to catalyze the phosphorylation of the hydroxamate and hydrazide derivatives of glutamate and aspartate.

5.2. Materials and Methods

5.2.1. Materials

All buffers and salts were purchased from SigmaAldrich, unless otherwise specified. L-Glutamine (**1**), γ-L-glutamyl hydroxamate (**7**), β-L-aspartyl hydroxamate (**9**), AMP-morpholidate (**10**), and phosphorus pentachloride were purchased from Sigma-Aldrich. γ-L-Glutamyl hydrazide (**8**) was obtained from Santa Cruz Biotechnology. ^{18}O-Labeled water (97 atom %) was obtained from Cambridge Isotope Laboratories. [^{15}N-Amide]-L-glutamine was obtained from Merck, Sharp and Dohme, Canada. D-Glutamine (98% pure) was purchased from Acros Organics. The restriction enzyme DpnI was obtained from New England Biolabs. Primestar HS Polymerase was purchased from Takara Industries. The plasmid used for the expression of Cj1418 from *C. jejuni* NCTC 11168 was obtained from Professor Christine Szymanski of the University of Georgia.

5.2.2. Purification of Glutamine Kinase

The plasmid used for the expression of Cj1418 (UniProt: Q0P8J6) with an N-terminal poly histidine purification tag was used to transform Rosetta (DE3) *Escherichia coli* cells by electroporation. Cultures (5 mL) of LB medium supplemented with 50 μg/mL kanamycin and 25 μg/mL chloramphenicol were inoculated with a single colony and grown overnight at 30 °C. These cultures were used to inoculate 1 L of LB medium (50 μg/mL kanamycin and 25 μg/mL chloramphenicol) and then incubated at 30 °C until an OD_{600} of ∼0.6−0.8 was reached. The cells were induced with 1.0 mM isopropyl β-

thiogalactoside (IPTG), grown for 16 h at 16 °C, and then harvested by centrifugation at 6000 rpm at 4 °C. The resulting cell pellet was resuspended into loading buffer (50 mM HEPES/KOH, 300 mM KCl, 20 mM imidazole, pH 8.0) and lysed by sonication. The total cell lysate was passed through a 0.45 μm filter before being loaded onto a prepacked 5 mL HisTrap HP (GE Healthcare) nickel affinity column. Protein was eluted with 50 mM HEPES/KOH, pH 8.0, 300 mM KCl, and 400 mM imidazole over a gradient of 30 column volumes. Excess imidazole was removed by exchanging the buffer against 50 mM HEPES/KOH, pH 8.0, 100 mM KCl, using a 20 mL (10 kDa molecular weight cutoff) concentrator (GE Healthcare). The protein was concentrated to a volume of 3 mL and loaded onto a GE Healthcare HiLoad 16/600 Sephadex 120 mL size exclusion column and eluted with 10 mM HEPES/ KOH (pH 8.0) and 100 mM KCl. Fractions were assayed for catalytic activity, pooled, concentrated, and stored at −80 °C until needed.

5.2.3. Construction of H737N Mutant of Glutamine Kinase

His-737 from Cj1418 was mutated to asparagine. The plasmid used for the expression of wild-type Cj1418 with an N-terminal hexa-histidine tag was used as a template for the construction of the plasmid for the expression of the H737N mutant. The forward (5′-GGGGGTGCTAATTCAAATATGGCCATTCGTGC-3′) and reverse primers (5′-GCACGAATGGCCATATTTGAATTAGCACCCCC-3′) were used to convert the histidine codon (CAT) at residue 737 to asparagine (AAT). Primestar HS polymerase was used to amplify the gene. The reaction used a three-step thermal cycle

(98 °C for 10 s, 55 °C for 40 s, and 72 °C for 10 min) and continued through 30 cycles. After amplification, DpnI was used to digest the template DNA for 2 h at 37 °C. Following DpnI digestion, PCR cleanup (Qiagen) was performed and the plasmid transformed into *E. coli* BL21 (DE3) cells. Single colonies were selected, and the DNA sequence of the mutant gene was confirmed.

5.2.4. Determination of Kinetic Constants

The kinetic constants for Cj1418 were determined using a pyruvate kinase/lactate dehydrogenase/myokinase coupled enzyme assay by following the oxidation of NADH at 340 nm at 25 °C with a SpectraMax340 UV−visible spectrophotometer. Assays were performed in 100 mM HEPES/KOH, pH 8.0, and 100 mM KCl. The coupling system contained 2.0 mM PEP, 0.3 mM NADH, 14 mM MgCl2, 10 mM ATP, 8 units/mL lactate dehydrogenase, 8 units/mL adenylate kinase, and 8 units/mL pyruvate kinase (PK). The kinetic constants for D-glutamine (2.0−20 mM), γ-L-glutamyl hydroxamate (0.4−4.0 mM), γ-L-glutamyl hydrazide (2.0−20 mM), and β-L-aspartyl hydroxamate (5.0−40 mM) were all assayed using 250 nM Cj1418. The kinetic constants were determined by fitting the initial rates to eq 1 using GraFit 5, where ν is the initial velocity of the reaction, Et is the enzyme concentration, k_{cat} is the turnover number, A is the substrate concentration, and K_m is the Michaelis constant.

$$\nu / E_t = k_{cat}(A)/(A + K_m) \quad (1)$$

5.2.5. Synthesis of [$^{18}O_4$]-Phosphate

The synthesis of [$^{18}O_4$]Pi (**11**) was carried out as reported previously (21). The reaction was conducted in a 10 mL round-bottom flask that was placed in an ice bath. The reaction utilized 1.0 g of water containing 97% ^{18}O, and 2.5 g of PCl_5. PCl_5 was slowly added to the water and then heated to 100 °C and allowed to stir for an additional 2 h. After heating, the reaction was cooled to room temperature, the pH was adjusted to 7.0, and aliquots were flash frozen and stored at −80 °C. The ^{31}P NMR spectrum of the product indicated that 93% of the phosphate contained four ^{18}O atoms and 7% contained three ^{18}O atoms, for an overall ^{18}O content of 98%.

5.2.6. Synthesis of β-[$^{18}O_4$]-ATP

The procedure for the synthesis of ^{18}O-labeled ATP where the β-phosphoryl group contains four ^{18}O atoms was modified from a previously reported method (22,23). AMP morpholidate (**10**, 1.0 g) (Sigma) and the tributylammonium salt of [$^{18}O_4$]-phosphate were stirred in dry DMSO (20 mL) at room temperature for 3 days. The reaction was diluted with water (100 mL) and then loaded onto a column of DEAE Sephadex. The β-[$^{18}O_4$]-ADP (**12**) was eluted from the column using a linear gradient of triethylammonium bicarbonate (300 mL from 0.01 to 1.0 M) and then concentrated by rotary evaporation. The labeled ADP (20 mM) was incubated with pyruvate kinase (3 units/ mL) and 25 mM phospho(enol)pyruvate (PEP) in 50 mM HEPES/KOH, pH 8.0 for 16 h in a volume of 50 mL. The reaction mixture was loaded onto a column of DEAE Sephadex and eluted with triethylammonium bicarbonate (600 mL from 0.01 to 1 M).

The fractions containing β-[$^{18}O_4$]-ATP (**13**) were identified by the absorbance at 260 nm and ^{31}P NMR spectroscopy. Excess triethylamine was removed by evaporation, and the product was stored at −80 °C. The reactions are summarized in Scheme 20.

Scheme 20 Chemical Synthesis of β-[$^{18}O_4$]-ADP and Enzymatic Syntheses of β-[$^{18}O_4$]-ATP and Hydroxylamine O-Phosphate Ester

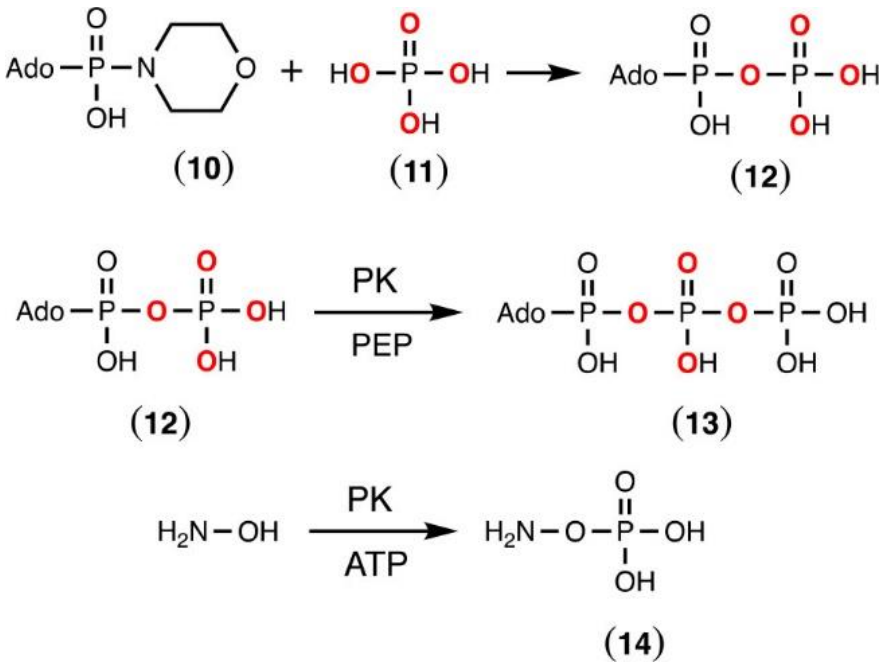

5.2.7. Synthesis of Hydroxylamine O-Phosphate Ester

O-Phosphorylated hydroxylamine (**14**) was synthesized using pyruvate kinase (24). Pyruvate kinase (4 units/mL) was incubated with 20 mM ATP, 25 mM hydroxylamine, 30 mM zinc acetate, and 100 mM ammonium bicarbonate (pH 8.0). The reaction was monitored by ^{31}P NMR spectroscopy until all of the ATP was converted to ADP. Once complete, the reaction mixture was diluted with water and loaded onto a DEAE Sephadex anion exchange resin and eluted with a linear gradient of triethylammonium bicarbonate (0.01−1.0 M). Fractions containing the O-phosphorylated hydroxylamine were identified by ^{31}P NMR spectroscopy, concentrated, flash frozen, and then stored at −20 °C.

5.2.8. Positional Isotope Exchange (PIX)

A reaction mixture containing 5 mM β-[$^{18}O_4$]-ATP (**13**), 7 mM $MgCl_2$, and 10 μM Cj1418 in 100 mM KCl, 100 mM HEPES/KOH, 50 mM CHES/KOH, pH 8.0, was incubated at 25 °C. At various times, 500 μL of the reaction mixture was removed and quenched with 15 mM EDTA, and the pH was adjusted to 9.5 before ^{31}P NMR analysis. Samples that were not analyzed immediately were flash frozen and stored at −20 °C. Aliquots were collected at 0, 1, 4, 8, 12, and 15 h, and the reaction velocities were determined using eq 2, where X is the fraction of change of the original ATP pool, and F is the fraction of the equilibrium value for positional isotope exchange in the ATP pool at time t (25).

$$\upsilon_{ex} = (X/\ln(1-X))(ATP_0/t)(\ln(1-F)) \quad (2)$$

5.2.9. Molecular Isotope Exchange (MIX)

The reaction mixture containing 10 mM L-glutamine phosphate and 10 mM [^{15}N-amide]-L-glutamine was incubated with 5 mM $MgCl_2$ and 20 μM Cj1418 for 12 h in 100 mM HEPES/ KOH, 100 mM KCl (pH 8.0) at 25 °C. The reaction products were analyzed by ^{15}N and ^{31}P NMR spectroscopy. [^{15}N-Amide]-L-glutamine phosphate was made enzymatically as previously described (8).

5.3. Results

5.3.1. Substrate Specificity of Cj1418

Cj1418 has previously been identified as a glutamine kinase that catalyzes the ATP-dependent phosphorylation of L-glutamine (8). However, the substrate profile for this enzyme has not been adequately determined. In addition to L-glutamine, 15 structural analogues of L-glutamine were tested as potential substrates for Cj1418 (Scheme 21). Of the compounds tested, only L-glutamine (**1**), D-glutamine (**6**), γ-L-glutamyl hydroxamate (**7**), γ-L-glutamyl hydrazide (**8**), and β-L-aspartyl hydroxamate (**9**) exhibited substrate activity based on the formation of AMP and Pi (Scheme 22). The kinetic constants for the phosphorylation of these compounds by Cj1418 are summarized in Table 2.

Scheme 21 Substrates Tested with Cj1418

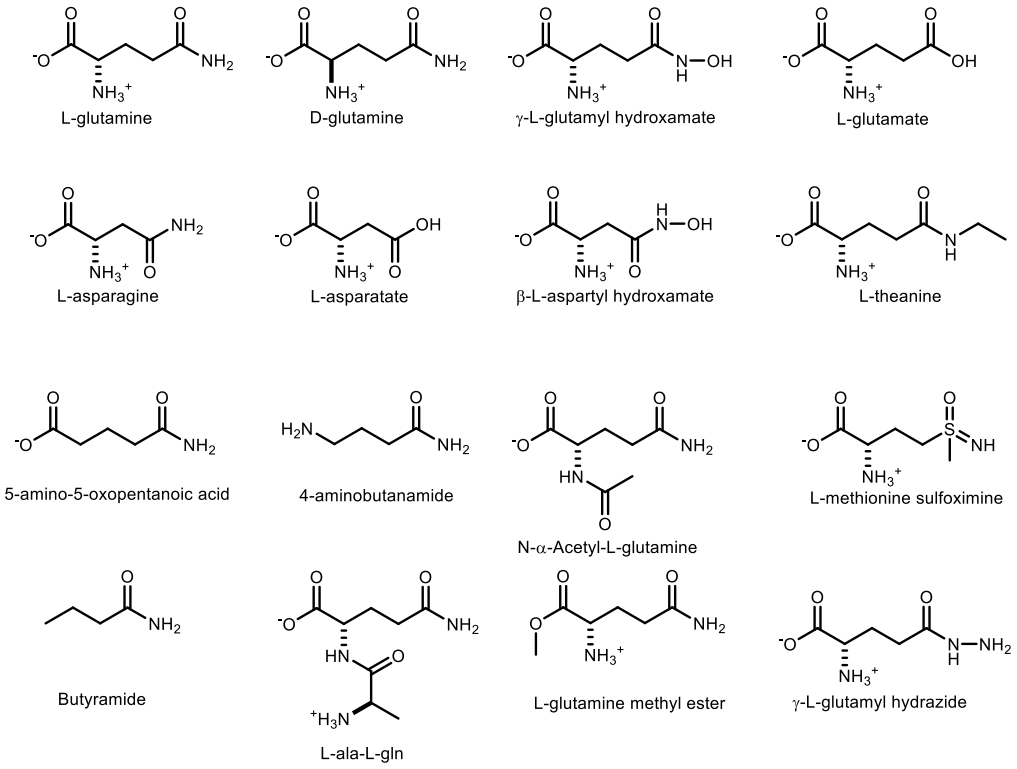

Scheme 22 Alternate Substrates for Cj1418

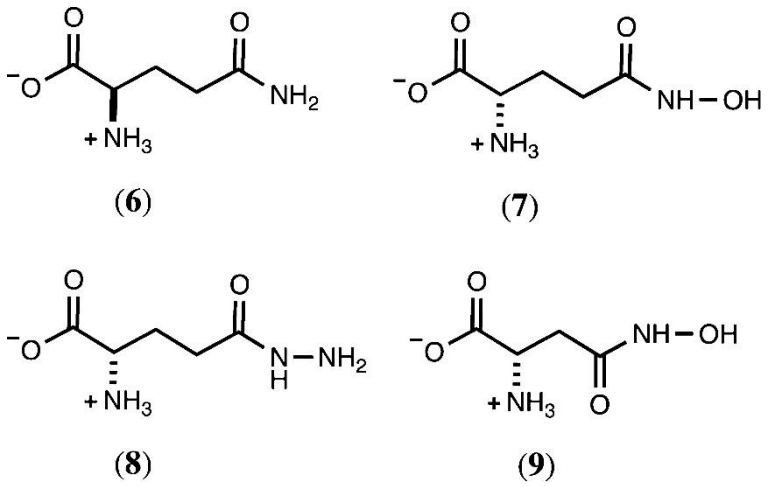

Table 2 Kinetic constants for Cj1418 at 25 °C, pH 8.0, and 10 mM MgATP.

substrate	k_{cat} (s^{-1})	K_m (mM)	k_{cat}/K_m (M^{-1} s^{-1})
L-glutamine (**1**)	2.5 ± 0.3	0.64 ± 0.06	3900 ± 800
D-glutamine (**6**)	1.5 ± 0.1	10.5 ± 1.8	140 ± 30
γ-L-glutamyl hydroxamate (**7**)	2.1 ± 0.2	1.5 ± 0.4	1400 ± 360
γ-L-glutamyl hydrazide (**8**)	0.41 ± 0.05	17.2 ± 3.8	24 ± 6
β-L-aspartyl hydroxamate (**9**)	nd[ab]	nd[ab]	1.2 ± 0.2[b]

[a]nd, not determined.
[b]A plot of reaction rate versus substrate concentration was linear up to a concentration of 40 mM

5.3.2. Characterization of Reaction Products

The reaction products for the phosphorylation of the alternate substrates **6**− **9** were analyzed by ^{31}P NMR spectroscopy (Figure 13−Figure 16). The product for the reaction with D-glutamine (**6**) exhibited two new resonances (−3.65 and −4.28 ppm) with the same chemical shifts as reported previously for the reaction of Cj1418 with L-glutamine and formation of L-glutamine phosphate (**2**) (8). These two resonances represent the *syn*- and *anti*-conformers of D-glutamine phosphate (Figure 13). With the hydroxamate derivative of L-glutamate (**7**), two new resonances were observed at 5.91 ppm (major) and 6.33 ppm (minor) ppm after the addition of ATP and Cj1418 (in addition to those for AMP and Pi). However, this product was unstable and a new resonance was observed at 7.92 ppm after ∼24 h. The degradation product was shown to be hydroxylamine-O-phosphate (**14**) by direct comparison of authentic **14** by ^{31}P NMR (Figure 14). This result is consistent with the enzymatic phosphorylation of **7** on the hydroxyl group and the initial formation of compound **15** (Scheme 23). Formation of **14** is proposed to occur via the intramolecular attack of the α-amino group of **15** with the C5 carbonyl group and generation of pyroglutamic acid (**16**) as shown in Scheme 23. The ^{13}C NMR spectrum of the reaction mixture confirmed the formation of pyroglutaminic acid (Figure 17A).

With the hydrazide derivative of L-glutamine (**8**), two new ^{31}P NMR resonances were observed with chemical shifts of 5.66 ppm (major) and 5.47 ppm (minor) (Figure 15A). This product was unstable (**17**) and subsequently converted to phosphate (Figure 15B). The ^{13}C NMR spectrum is consistent with the formation of pyroglutamate (Figure

17B). The fate of the hydrazine is unknown. The reaction product with the hydroxamate of aspartate (**9**) exhibited two new ^{31}P NMR resonances with chemical shifts of 6.07 ppm (major) and 6.44 ppm (minor) (Figure 16A). However, unlike the phosphorylated hydroxamate from L-glutamate (**15**), the phosphorylated hydroxamate product (**18**) from L-aspartate is stable (Figure 16B). Presumably, this is a direct consequence of the fact that nucleophilic attack by the α-amino group of **16** is hindered by the steric strain imposed by the formation of a β-lactam.

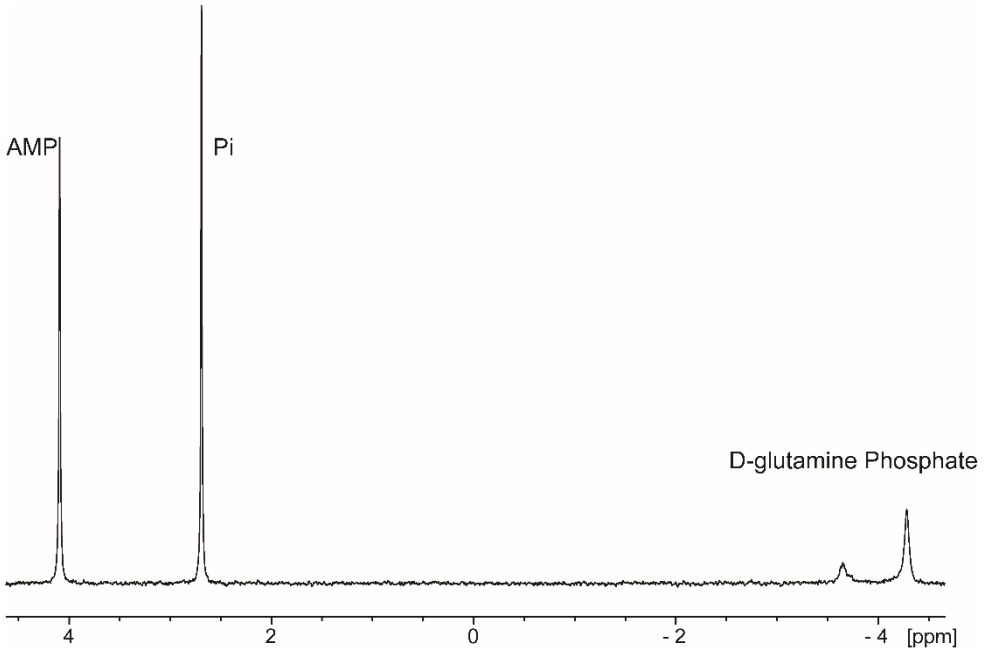

Figure 13 ^{31}P NMR of the reaction product formed from D-glutamine and ATP by the action of Cj1418. The reaction mixture was incubated for 3 h and contained 10 mM D-glutamine, 10 mM ATP, 14 mM $MgCl_2$ 10 µM Cj1418, 100 mM KCl, and 100 mM HEPES, pH 8.0. Two resonances (-3.65 and -4.28 ppm) are observe for the *syn*- and *anti*- conformations of D-glutamine phosphate, in addition to resonances for AMP (4.09 ppm) and phosphate (2.69 ppm).

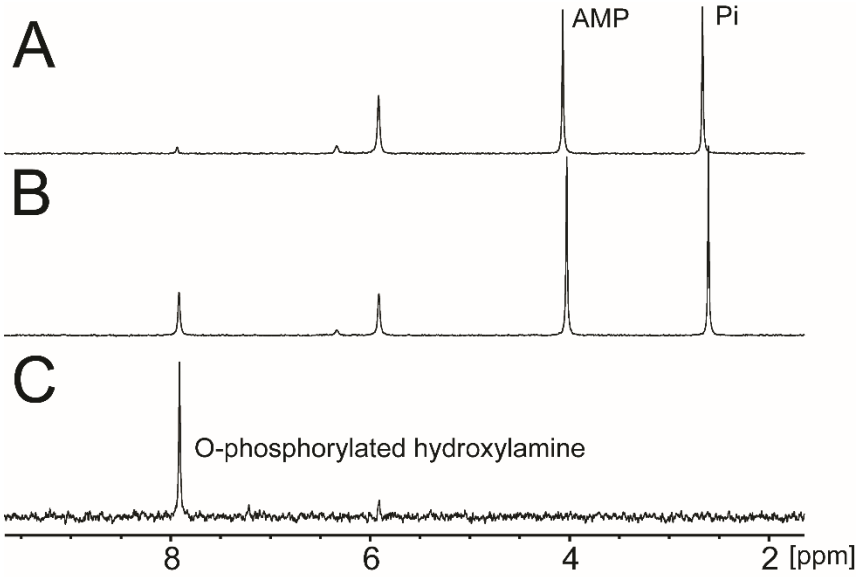

Figure 14 Formation and degradation of γ-L-glutamyl hydroxamate *O*-phosphate (15). Reactions contained 10 mM γ-L-glutamyl hydroxamate (7), 10 mM ATP, 14 mM $MgCl_2$, 100 mM HEPES, pH 8.0 and 10 µM Cj1418. (A) ^{31}P NMR spectrum of the reaction mixture after an incubation period of 3 h. (B) ^{31}P NMR spectrum of the same reaction mixture as seen in part A, but the spectrum was collected after 24 hours. (C) Standard of *O*-phosphorylated hydroxylamine (14).

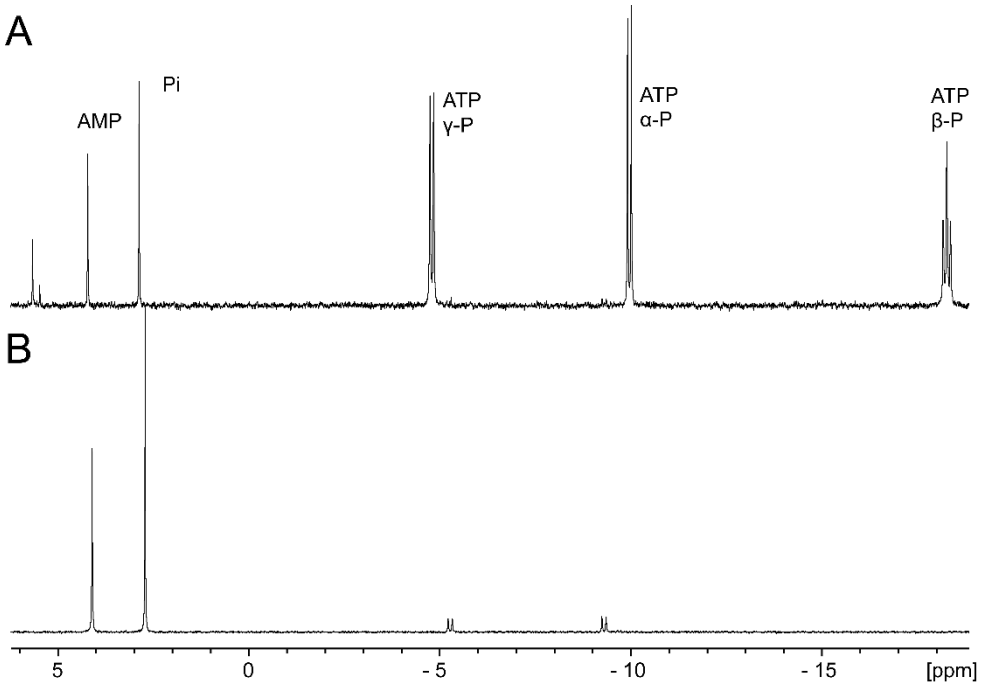

Figure 15 Formation and degradation of γ-L-glutamyl hydrazide Cj1418 product. Reactions contained 10 mM γ-L-glutamyl hydrazide, 10 mM ATP and 14 mM $MgCl_2$ and 10 µM Cj1418. (A) ^{31}P NMR spectrum of a reaction mixture that was incubated for 30 min in 100 mM HEPES 100 mM KCl (pH 8.0). (B) ^{31}P NMR of the same reaction as seen in part A, but spectrum was collected after 24 h of incubation. (C) ^{13}C NMR of a reaction in 500 mM ammonium bicarbonate (pH 8.0) after 24 h of incubation. Resonances labeled "A" are AMP, "P" are pyroglutamic acid, "H" are starting material, and "B" is bicarbonate buffer.

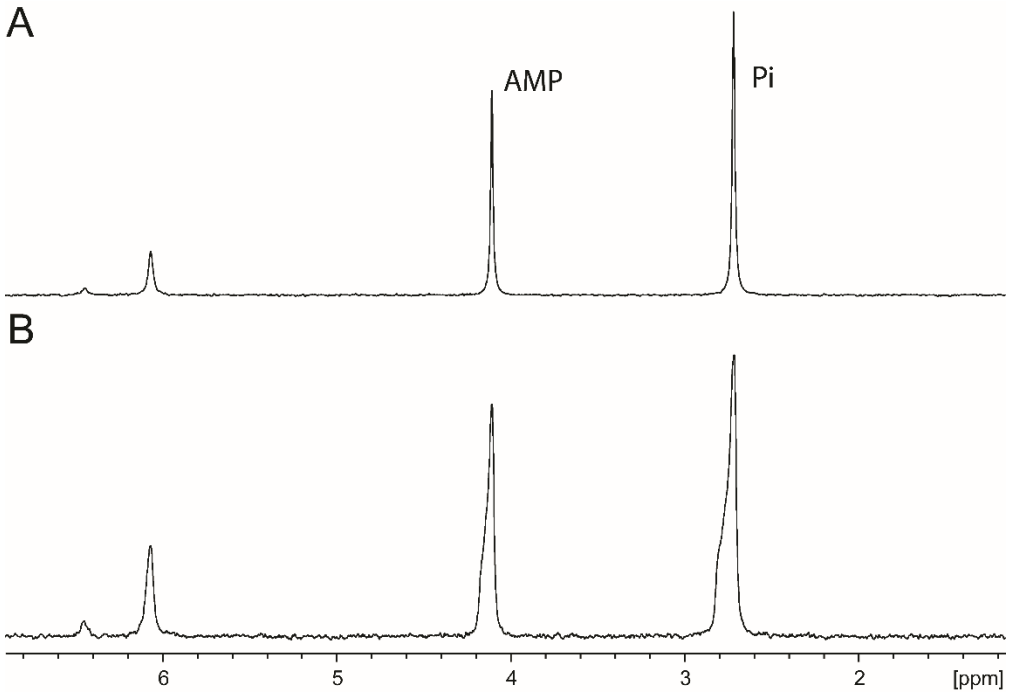

Figure 16 ^{31}P NMR of β-L-aspartyl hydroxamate *O*-phosphate. 10 mM β-L-aspartyl hydroxamate, 10 mM ATP and 14 mM MgCl were incubated for three with 10 µM Cj1418 in 100 mM KCl and 100 mM HEPES pH 8.0. (A) Spectrum was collected 12 h after the addition of Cj1418. (B) Spectrum was collected 36 h after the addition of Cj1418. Two resonances (6.07 and 6.45 ppm) are observed for β-L-aspartyl hydroxamate (as well as resonances for AMP (4.11 ppm) and phosphate (2.72 ppm).

Scheme 23 Reaction Products for the Phosphorylation of **7**, **8**, and **9** by Cj1418

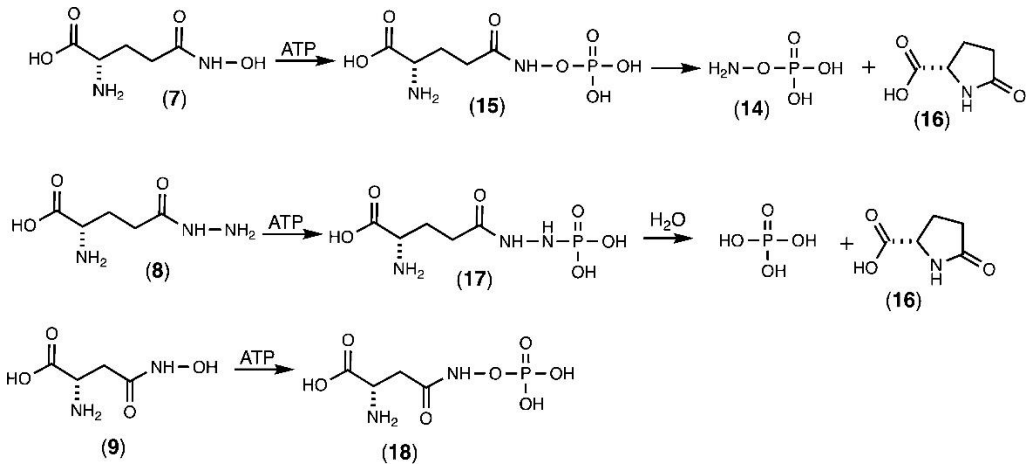

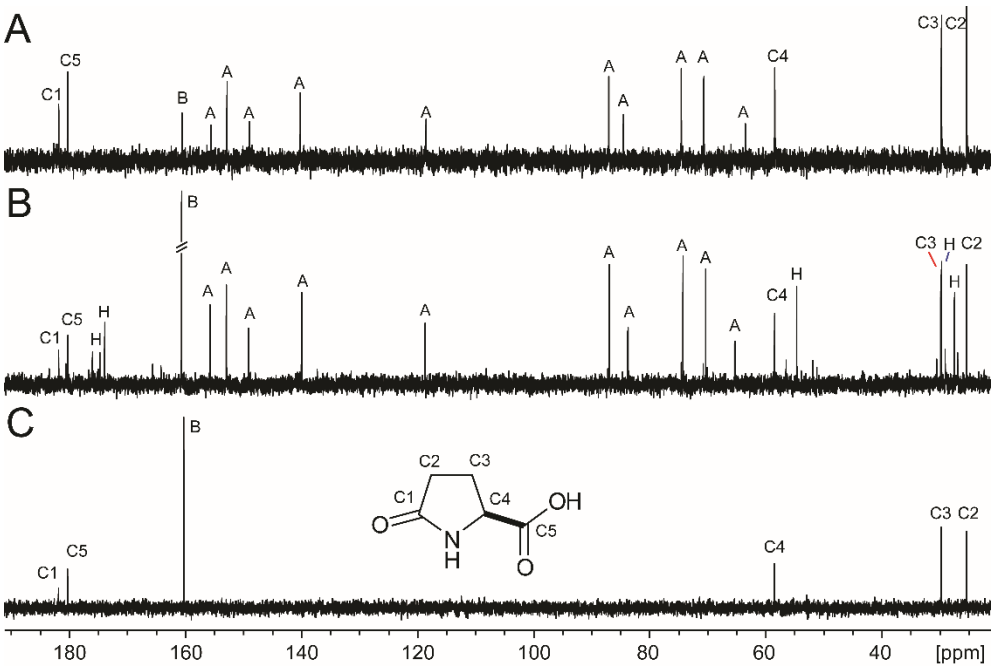

Figure 17 ^{13}C NMR Spectra of γ-L-glutamyl hydroxamate *O*-phosphate and γ-L-glutamyl hydrazide Cj1418 product, after their degradation. Peaks labeled "A" are AMP, "B" are bicarbonate buffer, "H" is starting material, and "C1-5" are pyroglutamic acid. (A) Spectrum of a reaction mixture containing 20 mM γ-L-glutamyl hydroxamate (7), 20 mM ATP in 50 mM ammonium bicarbonate (pH 8.0) after 72 hours of incubation. (B) Spectrum of a reaction mixture containing 10 mM γ-L-glutamyl hydrazide 10 mM ATP in 500 mM ammonium bicarbonate (pH 8.0) after 24 hours of incubation. (C) Spectrum of pyroglutamic acid in bicarbonate buffer, the five peaks for pyroglutamic acid are labeled C1-5.

5.3.3. Characterization of Reaction Products with L-Glutamine

It was previously demonstrated that Cj1418 catalyzes the formation of AMP, Pi, and L-glutamine phosphate from ATP, water, and L-glutamine (8). The proposed mechanism of action (Scheme 19) assumes that the β-phosphoryl group of ATP is ultimately found as L-glutamine phosphate, whereas the γ-phosphoryl group is found as Pi. However, the previous characterization of the reaction products did not differentiate between the β- and γ-phosphoryl groups in the two reaction products (8). To unambiguously determine the origin of the two products from ATP, the reaction was first conducted in 100% [^{16}O]-H_2O and then in 50% [^{18}O]-H_2O. For the product Pi, there is a single phosphorus resonance when the reaction was conducted in unlabeled water (Figure 18A) but two phosphorus resonances, separated by ~0.023 ppm from one another, when the reaction was conducted in a mixture of ^{16}O- and ^{18}O-H_2O (Figure 18B). The upfield resonance is for the phosphate with a single ^{18}O label, and the downfield resonance is for phosphate without an ^{18}O label (26). The ^{31}P NMR spectrum of the reaction products clearly indicates that only the Pi product was labeled with ^{18}O.

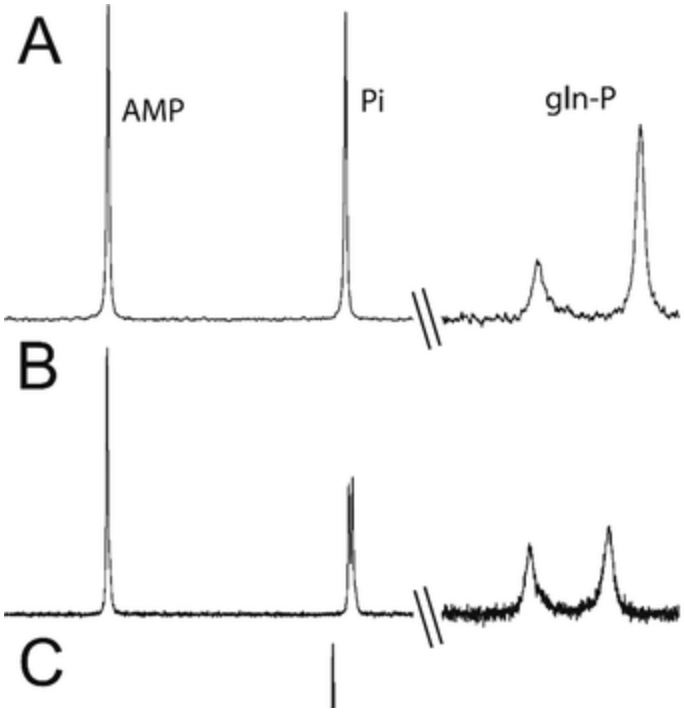

Figure 18 ^{31}P NMR spectra of the products in the reaction catalyzed by Cj1418. (A) ^{31}P NMR spectrum after incubation of Cj1418 (5 μM) with L-glutamine (5 mM) and MgATP (5 mM) at pH 8.0. Resonances at −3.66 and −4.31 ppm are from L-glutamine phosphate, 2.43 ppm is from phosphate, and 3.91 ppm is from AMP. (B) Same reaction conditions as for spectrum A, but the reaction was conducted in 50% [^{18}O]-H_2O. The ^{31}P NMR resonance for phosphate is shifted upfield by 0.023 ppm due to the incorporation of a single atom of ^{18}O in the phosphate product. (C) Same reaction conditions as for spectrum A, except that unlabeled ATP was mixed with 50% of β-[$^{18}O_4$]-ATP (13). The ^{31}P NMR spectrum for L-glutamine phosphate exhibits four resonances. There are two resonances each for the *syn*- and *anti*-conformers that are separated by 0.072 ppm due to the incorporation of 3 atoms of ^{18}O. In the spectra, the ^{31}P NMR resonance for AMP appears at 3.91 ppm. In spectrum C, the ^{31}P NMR resonance for AMP exhibits two resonances separated by 0.024 ppm due to the presence of a single atom of ^{18}O from the enzymatic cleavage of the bond between the β-P and α/β-bridging oxygen in the labeled ATP used in this reaction.

In a second experiment, the Cj1418-catalyzed reaction was conducted with L-glutamine and a 50/50 mixture of β-[$^{18}O_4$]-ATP (**13**) and unlabeled ATP. In the ^{31}P NMR spectrum of the reaction products, a single resonance is observed for phosphate, and four resonances are observed for the L-glutamine phosphate product (Figure 18C). One pair of resonances is for the unlabeled product (*syn*- and *anti*- conformations) and the other for the product labeled with ^{18}O. The separation in the chemical shifts for the two pairs of resonances is 0.072 ppm, consistent with the incorporation of three ^{18}O atoms, as expected from the labeled ATP used in this experiment (26). These two experiments clearly indicate that the β-phosphoryl group is ultimately found in L-glutamine phosphate and that the γ-phosphoryl group is ultimately found as phosphate. This confirms part of the mechanism proposed in Scheme 19.

5.3.4. Importance of His-737 as an Enzyme Nucleophile

The closest homologues of Cj1418 include PEP synthase, pyruvate phosphate dikinase, and rifampin phosphotransferase (13,15,16,18). Each of these enzymes has been structurally characterized and shown to be pyrophosphorylated on a conserved histidine residue that originates from either a central or C-terminal domain of the protein (16,18). The multiprotein sequence alignment of Cj1418 (residues 694−767) with the phospho-histidine domains of these proteins (Figure 19) identifies His-737 as the residue that is likely to be pyrophosphorylated in the reaction mechanism of Cj1418 (Scheme 19). This residue was mutated to asparagine (H737N) and the mutant assayed for its ability to phosphorylate glutamine; however, no activity was detected ($k_{cat} \leq 0.001\ s^{-1}$). This result is consistent with His-737 as being the nucleophile that attacks the β-phosphoryl group of ATP with formation of a pyrophosphorylated enzyme intermediate.

Figure 19 Sequence alignment of the phospho-histidine domains of Cj1418 (residues 694-767), pyruvate phosphate dikinase (PPDK from *Clostridium symbiosum*, residues 379-508), phosphenolpyruvate synthase (PEPS from *E. coli*, residues 386-457) and rifampin phosphotransferase (RIF from *Listeria monocytogenes*, residues 758-864). The characterized phospho-histidine residues (PPDK: His-455, PEPS: His-421, and RIF: His-825) and the predicted phospho-histidine residue from Cj1418 (His737) are highlighted in red. Phosphohistidine domains were identified using InterPro protein sequence, analysis and classification, and the sequence alignment was generated using Clustal Omega.

5.3.5. Detection of Pyrophosphorylated Intermediate

In the proposed reaction mechanism for Cj1418, the first step is initiated by the nucleophilic attack of the enzyme (likely His737) on the β-phosphoryl group of ATP to generate a covalent pyrophosphorylated intermediate and AMP (Scheme 19A). The significance of this first step was addressed by measurement of the positional isotope exchange (PIX) reaction using β-[$^{18}O_4$]ATP (**13**) in the absence of added L-glutamine (19,20). To observe a PIX reaction with Cj1418, the formation of the Enz-X-PP_i intermediate must be reversible and the α-phosphoryl group of AMP bound in the active site must be free to rotate. The positional exchange of the ^{18}O label is outlined in Scheme 24. As the reaction proceeds, the ^{18}O that originally occupies the α/β-bridge position in the labeled ATP (**13**) will equilibrate with the ^{16}O in the two α-nonbridge positions to form **19** and **20**. At equilibrium, 1/3 of the ^{18}O label will remain in the α/βbridge position and 2/3 will be in the two α-nonbridge positions.

Scheme 24 Positional Isotope Exchange Reaction with Cj1418 and β-[$^{18}O_4$]-ATP

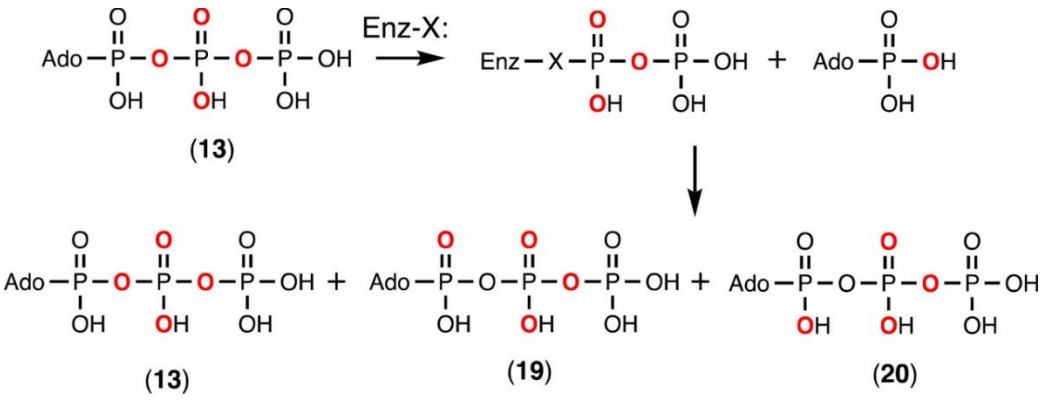

The PIX reaction was followed by ^{31}P NMR spectroscopy since the incorporation of ^{18}O into ATP results in a perturbation in the chemical shift for phosphorus, and the magnitude of the shift is dependent on whether the 18-oxygen occupies a bridge or nonbridge position within the polyphosphate moiety of ATP (26). It has been previously shown that ^{18}O in the α/β-bridge position of ATP will cause a +0.017 ppm upfield chemical shift perturbation for the α- and β-phosphoryl groups (26). In the α-nonbridge position, there will be a +0.028 ppm upfield shift perturbation for a single 18-oxygen (26). Thus, as the α/β-bridge oxygen in the β-[$^{18}O_4$]-ATP scrambles, there will be a change in the chemical shift of the β-phosphate of approximately −0.017 ppm and an increase in the chemical shift for the α-phosphate by ∼0.011 ppm (0.028− 0.017 ppm).

The PIX reaction was initiated by incubation of 5 mM β-[$^{18}O_4$]-ATP (**13**) and 10 μM Cj1418. Aliquots were removed, the reaction was quenched with EDTA, and the products were analyzed by ^{31}P NMR spectroscopy. The ^{31}P NMR spectra of the α- and β-phosphoryl groups of the labeled ATP, before the addition of the Cj1418 and after 8 h, are presented in Figure 20. For the β-phosphoryl group, the ^{31}P NMR spectrum (Figure 20C) indicates that, in the original β-[$^{18}O_4$]-ATP, 86% is labeled with 2 nonbridge and 2 bridge ^{18}O atoms (denoted as 2,2), 7% contain 2 nonbridge and 1 bridge ^{18}O atoms (2,1), and 7% contain 1 nonbridge and 2 nonbridge (1,2) ^{18}O atoms. For the α-phosphoryl group, the ^{31}P NMR spectrum (Figure 20A) indicates, that in the original β-[$^{18}O_4$]-ATP, 96% contains 1 bridge ^{18}O atoms (0,1) and 4% contains no label (0,0). The average ^{18}O content of the 4 oxygen atoms attached to the β-phosphoryl group is 96%. After 8 h, the fraction of the ATP with 2 nonbridge and 2 bridge ^{18}O atoms at the β-phosphoryl group

(2,2), relative to that fraction of ATP with 2 nonbridge and 1 bridge ^{18}O (2,1), has been reduced from 92% to 58% (Figure 20D). For the α-phosphoryl group, the fraction of ATP with 1 bridge ^{18}O atom (0,1), relative to that with 1 nonbridge ^{18}O atom, has decreased from 100% to 38% (Figure 20B). The rate of the PIX reaction (vPIX) was calculated using eq 2, and the data for additional time points are collected in Table 3. The average ratio of the PIX rate to the rate for the loss of ATP (v_{PIX}/v_{chem}) is 1.6 ± 0.3. In the presence of 5 mM AMP, there was no measurable increase in the rate of the PIX reaction under these conditions. The observation of the positional isotope exchange reaction is consistent with the formation of a pyrophosphorylated enzyme in the absence of added L-glutamine.

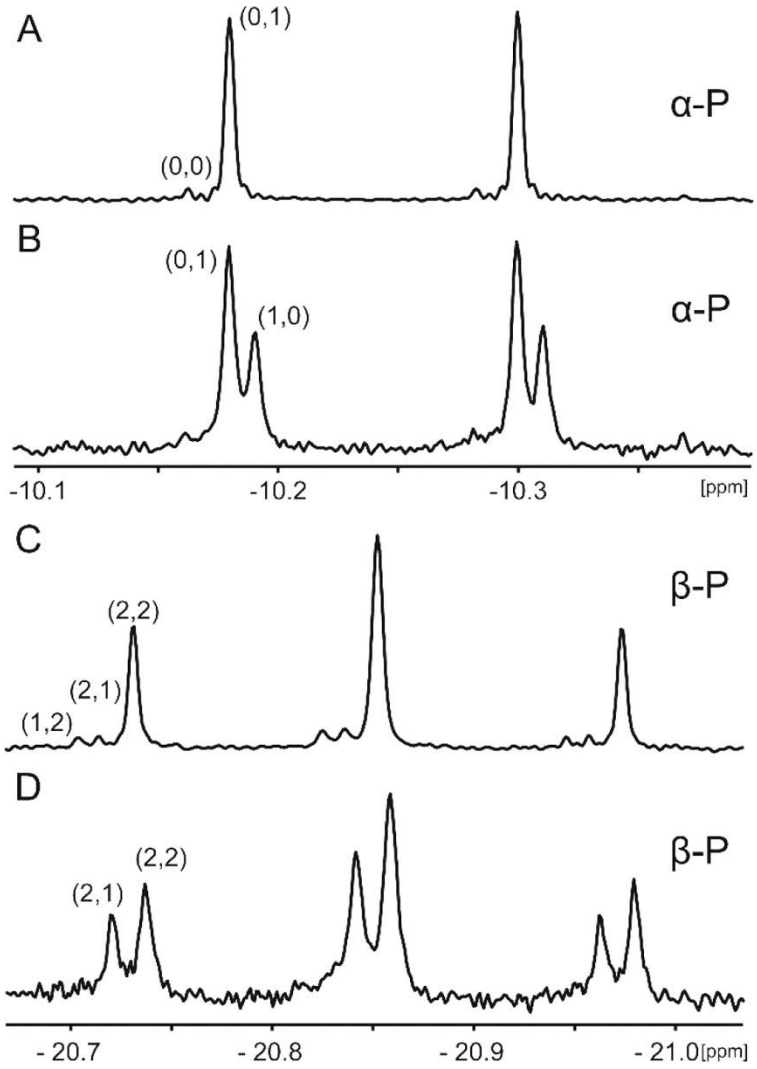

Figure 20 ^{31}P NMR spectra of ^{18}O-labeled ATP before and after the addition of Cj1418. (A) Spectrum of the α-phosphoryl group of [$^{18}O_4$]-ATP (13) before the addition of Cj1418. (B) Spectrum of the α-phosphoryl group of the ATP after 8 h of incubation with Cj1418. (C) Spectrum of the β-phosphoryl group of [$^{18}O_4$]-ATP (13) before the addition of Cj1418. (D) β-Phosphoryl group of the ATP after incubation with Cj1418 for 8 h. Additional details are provided in the text. The first number in parentheses indicates the number of nonbridging ^{18}O atoms attached to the respective phosphoryl group in ATP, and the second indicates the number of bridging ^{18}O atoms.

Table 3 Positional isotope exchange for the α- and β-phosphoryl groups with β-[$^{18}O_4$]-ATP.

Time (h)	% α-P (0,1)	% α-P (1,0)	% β-P (2,2)	% β-P (2,1)	F	ATP (mM)	X	υ_{ex} (mM hr^{-1})	υ_{chem} (mM hr^{-1})	$\upsilon_{ex}/\upsilon_{Chem}$
0	100	0	92	8		5.00				
1	86	14	82	18	0.19	4.41	0.11	0.99	0.59	1.68
4	75	25	68	32	0.39	3.91	0.21	0.55	0.27	2.04
8	62	38	58	42	0.57	3.03	0.39	0.41	0.25	1.64
12	51	49	53	47	0.69	2.21	0.55	0.33	0.23	1.43
15	48	52	48	52	0.76	1.66	0.66	0.29	0.22	1.32

5.3.6. Detection of Phosphorylated Intermediate

In Scheme 19, we have proposed that the pyrophosphorylated enzyme (Enz-X-P_β-P_γ) is hydrolyzed to generate a phosphorylated enzyme intermediate (Enz-X-P_β), and in the last step, this intermediate is utilized to phosphorylate L-glutamine. If this last step is reversible, then a molecular isotope exchange reaction (MIX) can be used to provide experimental support for the formation of Enz-X-P_β. This exchange reaction is illustrated in Scheme 25. In the MIX experiment, Cj1418 was incubated with 10 mM [^{15}N-amide]-L-glutamine (**21**) and 10 mM of unlabeled L-glutamine phosphate (**2**) in the absence of added ATP. The products of the reaction mixture were examined by both ^{31}P and ^{15}N NMR spectroscopy after a period of 12 h. In Figure 21A is the ^{31}P NMR spectrum of the L-glutamine-P (**2**) prior to the addition of Cj1418 and the [^{15}Namide]-L-glutamine (**21**). Two resonances are observed at −3.56 and −3.91 ppm, representing the *syn*- and *anti*-conformations of the product. After the addition of Cj1418 and [^{15}N-amide]-L-glutamine, four new resonances are observed, representing L-glutamine-P where the two phosphorus resonances are now coupled to ^{15}N (compound **22**). In the corresponding ^{15}N NMR spectra (Figure 21C), a single ^{15}N-resonance is observed at 111.92 ppm for the amide nitrogen of the labeled L-glutamine (**21**). After incubation with L-glutamine-P and Cj1418, four new resonances are observed from 146.06 and 142.18 ppm. These resonances represent the *syn*- and *anti*-conformations of the L-glutamine-P products and coupling with ^{31}P of 19 Hz.

Scheme 25 Molecular Isotope Exchange Reaction for Cj1418

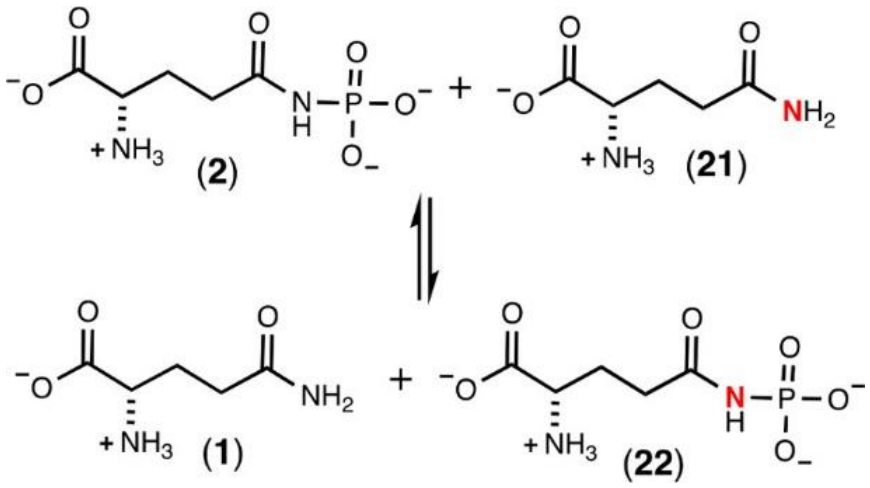

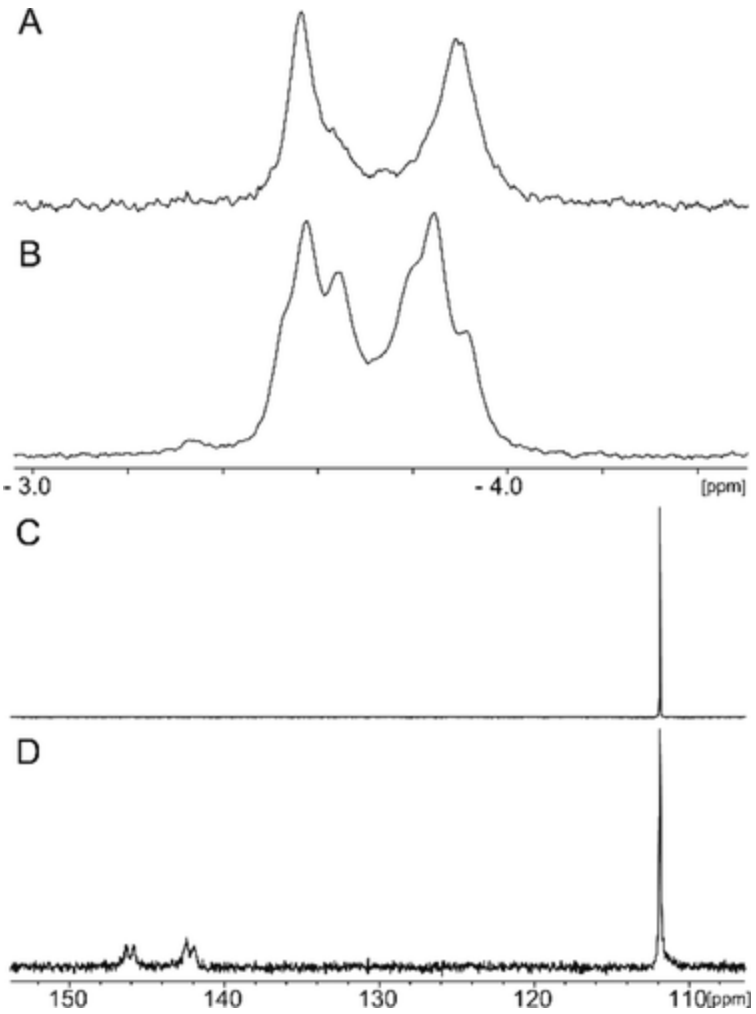

Figure 21 ^{31}P and ^{15}N NMR spectra for the MIX reaction with Cj1418. (A) ^{31}P NMR spectrum of L-glutamine phosphate. (B) ^{31}P NMR spectrum after 10 μM Cj1418 was incubated with 10 mM L-glutamine phosphate (**2**) and 10 mM [^{15}N-amide]-L-glutamine (**21**) for 12 h. (C) ^{15}N NMR spectrum of [^{15}N-amide]-L-glutamine (**21**). (D) ^{15}N NMR spectrum after 10 μM Cj1418 was incubated with 20 mM [^{15}N-amide]-L-glutamine and 20 mM L-glutamine phosphate (**2**) for 12 h.

5.4. Discussion

5.4.1. Mechanism of Action

The proposed mechanism of action for L-glutamine kinase is presented in Scheme 19. In this mechanism, a nucleophile in the active site first attacks the β-phosphoryl group of ATP to form a pyrophosphorylated enzyme intermediate (Enz-X-P_β-P_γ) and AMP. The pyrophosphorylated intermediate is subsequently hydrolyzed to generate a phosphorylated intermediate (Enz-X-P_β) and Pi. In the last step, the phosphorylated intermediate is used to phosphorylate L-glutamine on the amide nitrogen. Using amino acid sequence alignments with the closest functional homologues to Cj1418 and site-directed mutagenesis experiments, we have demonstrated that His-737 is the most likely residue in the active site of this enzyme to function as the primary nucleophile.

In the proposed mechanism, the γ-phosphoryl group of ATP is converted to phosphate and the β-phosphoryl group is ultimately used to phosphorylate L-glutamine. An alternative mechanism could have been written with the opposite outcome for these two phosphoryl groups of ATP. However, we have now demonstrated using β-[$^{18}O_4$]-ATP that the β-phosphoryl group is exclusively utilized to phosphorylate L-glutamine. This result was confirmed by conducting the Cj1418-catalyzed reaction in [^{18}O]-H_2O, where the only labeled product was inorganic phosphate.

Positional isotope exchange (PIX) and molecular isotope exchange (MIX) experiments were used to further support the formation of the pyrophosphorylated (Enz-

X-P_β-P_γ) and phosphorylated enzyme intermediates (Enz-X-P_β) in the overall reaction mechanism. In the PIX experiment, β-[$^{18}O_4$]-ATP was incubated with the enzyme in the absence of L-glutamine in an attempt to observe the migration of the α/β-bridge oxygen to the α-nonbridge positions in ATP (Scheme 24). As conducted, the PIX reaction can only occur if the enzyme is pyrophosphorylated by ATP in the absence of L-glutamine, and this reaction must be reversible. In essence, the experiment measures the partitioning of the [Enz-X-$P_\beta P_\gamma$•AMP] complex. When this complex reverts back to Enz-X and ATP, a PIX reaction will be observed if the α-phosphoryl group of AMP is able to rotate in the active site. The PIX rate will then be governed by the rate at which the ATP can be reformed and dissociate from the active site into solution.

The partitioning forward is potentially governed by two related events. The AMP may dissociate from the active site or the pyrophosphorylated enzyme may be hydrolyzed to the phosphorylated enzyme. The dissociation of AMP is essentially irreversible since the initial concentration of AMP is equivalent to the enzyme concentration used in this experiment (10 μM). We attempted to enhance the PIX rate by adding unlabeled AMP to the reaction mixture (20). If the partitioning forward was governed by AMP dissociation, then increasing the concentration of AMP would enhance the steady-state concentration of the [Enz-X-P_β-P_γ•AMP] complex and the overall PIX rate would increase. However, the addition of AMP had no effect on the PIX rate, and no ATP was directly formed from the added unlabeled AMP. This result indicates that the partitioning forward is actually governed by the rate at which the [Enz-X-P_β-P_γ•AMP] complex is hydrolyzed to [Enz-X-P_β•P_γ]. Thus, the experimentally

determined partitioning ratio (v_{PIX}/v_{chem}) of 1.6 for the [Enz-X-P_β-P_γ•AMP] complex indicates that ATP is reformed and dissociates from the active site 1.6 times faster than this complex is hydrolyzed to irreversibly form [Enz-X-P_β•Pi•AMP].

It should also be noted that the average rate constant for the PIX reaction (obtained from the average value for v_{ex} in Table 3) is relatively small at ~54 h^{-1} (0.54 mM h^{-1}/0.01 mM enzyme). Since the dissociation of AMP and the hydrolysis of the pyrophosphorylated enzyme intermediate are essentially irreversible, the enzyme must somehow be recycled back to free enzyme. This can only occur via the hydrolysis of the [Enz-X-P_β] complex to [Enz-X]. The rate constant for the net loss of ATP in the absence of L-glutamine (obtained from the average value of v_{chem} in Table 3) is 31 h^{-1} (0.31 mM h^{-1}/0.01 mM enzyme). The k_{cat} for the overall reaction (2.5 s^{-1}) in the presence of L-glutamine is 2.9×10^4-fold faster than this value. This clearly indicates that L-glutamine is much better than water in reacting with the [Enz-X-P_β] intermediate. PIX experiments have previously been used to characterize the pyrophosphorylated enzyme intermediate formed in the reaction catalyzed by pyruvate phosphate dikinase (20).

Experimental support for the [Enz-X-P_β] intermediate was obtained with the MIX experiment where the free enzyme (Enz-X) was phosphorylated with L-glutamine phosphate in the absence of any added nucleotide (Scheme 25). The phosphorylated enzyme intermediate was subsequently captured by the ^{15}N-labeled L-glutamine to generate the ^{15}N-labeled L-glutamine phosphate (22). This exchange reaction can only occur with the formation of the [Enz-X-P] intermediate.

5.4.2. Substrate Specificity

We have identified four additional substrates for Cj1418 in addition to L-glutamine. These new substrates include the hydroxamate derivatives of L-glutamate (**7**) and L-aspartate (**9**), the hydrazide of L-glutamate (**8**), and D-glutamine (**6**). Other compounds were tested as alternative substrates such as L-glutamate and L-asparagine; however, neither of these compounds exhibited any detectable activity. L-Glutamine derivatives with either the α-amino or α-carboxy groups removed were not substrates; however, D-glutamine was shown to be a substrate, and thus the stereochemistry at the α-carbon is not vital. The second best substrate for Cj1418 is γ-glutamyl hydroxamate (**7**) and formation of an unstable O-phosphorylated derivative (**15**). Previously, compound **15** has been shown to be an inhibitor of γ-L-glutamyl-L-cysteine synthetase where a highly reactive isocyanate intermediate was proposed via a Lossen rearrangement (27). With Cj1418, we did not obtain any evidence for the formation of an isocyanate derivative from **7**. However, the ^{13}C and ^{31}P NMR spectra clearly indicate the formation of pyroglutamic acid (**16**) and the hydroxyl amine O-phosphate ester (**14**). In contrast, the phosphorylated derivative of β-aspartyl hydroxamate (**18**) appears to be relatively stable under the reaction conditions. The hydrazide derivative of L-glutamate (**9**) is also a substrate that produces a relatively unstable phosphorylated product (**18**). The final products were determined to be phosphate and L-pyroglutamate (**16**). The formation of phosphate presumably arises from the nonenzymatic hydrolysis of the hydrazide derivative of phosphate. However, this intermediate was not observed directly in the ^{31}P NMR spectrum of the reaction mixture.

5.5. Conclusions

Here we have determined the substrate profile for L-glutamine kinase, an enzyme that functions in the formation of the O-methyl phosphoramidate modification in the capsular polysaccharide in *C. jejuni*. We have proposed a chemical reaction mechanism for the phosphorylation of L-glutamine and have provided kinetic evidence for the formation of pyrophosphorylated and phosphorylated enzyme intermediates in this transformation.

5.6. References

1. Young, K. T., Davis, L. M., and Dirita, V. J. (2007) *Campylobacter jejuni*: Molecular Biology and Pathogenesis. *Nat. Rev. Microbiol*. 5, 665−679.
2. Roberts, I. S. (1996) The Biochemistry and Genetics of Capsular Polysaccharide Production in Bacteria. *Annu. Rev. Microbiol*. 50, 285− 315.
3. Karlyshev, A. V., Champion, O. L., Churcher, C., Brisson, J.-R., Jarrell, H. C., Gilbert, M., Brochu, D., St Michael, F., Li, J., Wakarchuk, W. W., Goodhead, I., Sanders, M., Stevens, K., White, B., Parkhill, J., Wren, B. W., and Szymanski, C. M. (2005) Analysis of *Campylobacter jejuni* Capsular Loci Reveals Multiple Mechanisms for the Generation of Structural Diversity and the Ability to form Complex Heptoses. *Mol. Microbiol*. 55, 90−103.
4. Michael, F. S., Szymanski, C. M., Li, J., Chan, K. H., Khieu, N. H., Larocque, S., Wakarchuk, W. W., Brisson, J. -R., and Monteiro, M. A. (2002) The Structures of the Lipooligosaccharide and Capsule Polysaccharide of *Campylobacter jejuni* Genome Sequenced Strain NCTC 11168. *Eur. J. Biochem*. 269, 5119−5136.
5. McNally, D. J., Lamoureux, M. P., Karlyshev, A. V., Fiori, L. M., Li, J., Thacker, G., Coleman, R. A., Khieu, N. H., Wren, B. W., Brisson, J.-R., Jarrell, H. C., and Szymanski, C. M. (2007) Commonality and Biosynthesis of the O-Methyl Phosphoramidate Capsule Modification in *Campylobacter jejuni*. *J. Biol. Chem*. 282, 28566−28576.
6. Karlyshev, A. V., Linton, D., Gregson, N. A., Lastovica, A. J., and Wren, B. W. (2000) Genetic and Biochemical Evidence of a *Campylobacter jejuni* Capsular

Polysaccharide that Accounts for Penner Serotype Specificity. *Mol. Microbiol*. 35, 529−541.

7. Taylor, Z. W., Brown, H. A., Holden, H. M., and Raushel, F. M. (2017) Biosynthesis of Nucleoside Diphosphoramidates in *Campylobacter jejuni*. *Biochemistry* 56, 6079−6082.
8. Taylor, Z. W., Brown, H. A., Narindoshvili, T., Wenzel, C. Q., Szymanski, C. M., Holden, H. M., and Raushel, F. M. (2017) Discovery of a Glutamine Kinase Required for the Biosynthesis of the O-Methyl Phosphoramidate Modifications Found in the Capsular Polysaccharides of *Campylobacter jejuni*. *J. Am. Chem. Soc*. 139, 9463−9466.
9. Taylor, Z. W., and Raushel, F. M. (2018) Cytidine Diphosphoramidate Kinase: An Enzyme Required for the Biosynthesis of the O-Methyl Phosphoramidate Modification in the Capsular Polysaccharides of *Campylobacter jejuni*. *Biochemistry* 57, 2238− 2244.
10. Morrison, J. F., Griffiths, D. E., and Ennor, A. H. (1957) The Purification and Properties of Arginine Phosphokinase. *Biochem. J.* 65, 143−153.
11. Ennor, A. H., Rosenberg, H., and Armstrong, M. D. (1955) Specificity of Creatine Phosphokinase. *Nature* 175, 120.
12. Roush, R. F., Nolan, E. M., Löhr, F., and Walsh, C. T. (2008) Maturation of an *Escherichia coli* Ribosomal Peptide Antibiotic by ATP-Consuming N-P Bond Formation in Microcin C7. *J. Am. Chem. Soc*. 130, 3603−3609.

13. Cooper, R. A., and Kornberg, H. L. (1967) The Mechanism of the Phosphoenolpyruvate Synthase Reaction. *Biochim. Biophys. Acta, Gen. Subj*. 141, 211−213.
14. Evans, H. J., and Wood, H. G. (1968) The Mechanism of the Pyruvate, Phosphate Dikinase Reaction. *Proc. Natl. Acad. Sci. U. S. A.* 61, 1448−1453.
15. Stogios, P. J., Cox, G., Spanogiannopoulos, P., Pillon, M. C., Waglechner, N., Skarina, T., Koteva, K., Guarné, A., Savchenko, A., and Wright, G. D. (2016) Rifampin Phosphotransferase is an Unusual Antibiotic Resistance Kinase. *Nat. Commun.* 7, 11343.
16. Qi, X., Lin, W., Ma, M., Wang, C., He, Y., He, N., Gao, J., Zhou, H., Xiao, Y., Wang, Y., and Zhang, P. (2016) Structural Basis of Rifampin Inactivation by Rifampin Phosphotransferase. *Proc. Natl. Acad. Sci. U. S. A.* 113, 3803−3808.
17. Finn, R. D., Attwood, T. K., Babbitt, P. C., Bateman, A., Bork, P., Bridge, A. J., Chang, H.-Y., Dosztányi, Z., El-Gebali, S., Fraser, M., Gough, J., Haft, D., Holliday, G. L., Huang, H., Huang, X., Letunic, I., Lopez, R., Lu, S., Marchler-Bauer, A., Mi, H., Mistry, J., Natale, D. A., Necci, M., Nuka, G., Orengo, C. A., Park, Y., Pesseat, S., Piovesan, D., Potter, S. C., Rawlings, N. D., Redaschi, N., Richardson, L., Rivoire, C., Sangrador-Vegas, A., Sigrist, C., Sillitoe, I., Smithers, B., Squizzato, S., Sutton, G., Thanki, N., Thomas, P. D., Tosatto, S. C. E., Wu, C. H., Xenarios, I., Yeh, L.-S., Young, S.-Y., and Mitchell, A. L. (2017) InterPro in 2017 Beyond Protein Family and Domain Annotations. *Nucleic Acids Res*. 45, D190−D199.

18. Lim, K., Read, R. J., Chen, C. C. H., Tempczyk, A., Wei, M., Ye, D., Wu, C., Dunaway-Mariano, D., and Herzberg, O. (2007) Swiveling Domain Mechanism in Pyruvate Phosphate Dikinase. *Biochemistry* 46, 14845−14853.

19. Rose, I. A. (2006) Positional Isotope Exchange Studies of Enzyme Mechanisms. *Adv. Enzymol*. 50, 361.

20. Wang, H. C., Ciskanik, L., Dunaway-Mariano, D., Von der Saal, W., and Villafranca, J. J. (1988) Investigations of the Partial Reactions Catalyzed by Pyruvate Phosphate Dikinase. *Biochemistry* 27, 625−633.

21. Melby, E. S., Soldat, D. J., and Barak, P. (2011) Synthesis and Detection of Oxygen-18 Labeled Phosphate. *PLoS One* 6, e18420.

22. Wehrli, W., Verheyden, D., and Moffatt, J. (1965) Dismutation Reactions of Nucleoside Polyphosphates. II. Specific Chemical Syntheses of α-, β-, and γ-P^{32}-Nucleoside 5′-Triphosphates1. *J. Am. Chem. Soc*. 87, 2265−2277.

23. Midelfort, C. F., and Rose, I. A. (1976) A Stereochemical Method for Detection of ATP Terminal Phosphate Transfer in Enzymatic Reactions. Glutamine synthetase. *J. Biol. Chem*. 251, 5881−5887.

24. Cottam, G. L., Kupiecki, F. P., and Coon, M. J. (1968) A Study of the Mechanism of O-Phosphorylhydroxylamine Synthesis Catalyzed by Pyruvate Kinase. *J. Biol. Chem*. 243, 1630−1637.

25. Litwin, S., and Wimmer, M. J. (1979) Correction of Scrambling Rate Calculation for Loss of Substrate. *J. Biol. Chem*. 254, 1859.

26. Cohn, M., and Hu, A. (1978) Isotopic ((^{18})O) shift in (^{31})P Nuclear Magnetic Resonance Applied to a Study of Enzyme-Catalyzed Phosphate Phosphate Exchange and Phosphate (Oxygen) Water Exchange Reactions. *Proc. Natl. Acad. Sci. U. S. A.* 75, 200−203.

27. Katoh, M., Hiratake, J., and Oda, J. I. (1998) ATP-Dependent Inactivation of *Escherichia coli* γ-Glutamylcysteine Synthetase by L-Glutamic Acid γ-Monohydroxamate. *Biosci., Biotechnol., Biochem*. 62, 1455−1457.

6. MANGANESE-INDUCED SUBSTRATE PROMISCUITY IN THE REACTION CATALYZED BY PHOSPHOGLUTAMINE CYTIDYLYLTRANSFERASE FROM *CAMPYLOBACTER JEJUNI*[*]

6.1. Introduction

Campylobacter jejuni, a Gram-negative pathogenic bacteria, is the leading cause of bacterial gastroenteritis worldwide (1,2). Like many Gram-negative bacteria, *C. jejuni* produces a capsular polysaccharide (CPS), which helps improve the overall fitness and pathogenicity of this organism (3) Approximately 70% of all *C. jejuni* strains contain an O-methyl phosphoramidate (MeOPN) modification to the capsular polysaccharide (CPS) (4). This decoration is unique to the genus *Campylobacter*, and phosphorus nitrogen bonds are relatively rare in nature (5). In the NCTC 11168 strain of *C. jejuni*, several gene knockout studies have been conducted and eight genes appear to be responsible for the biosynthesis of the MeOPN modification to the CPS (4). The role of MeOPN was examined using mutants that lacked this modification of its CPS, and it was shown that MeOPN contributes to serum resistance and evasion of host immune responses (6).

Of the eight genes directly linked to the presence of MeOPN, four have previously been characterized. The first enzyme in the pathway, Cj1418, represents a novel L-glutamine kinase that catalyzes the ATP-dependent phosphorylation of L-

[*] Reprinted with permission from "Manganese-Induced Substrate Promiscuity in the Reaction Catalyzed by Phosphoglutamine Cytidylyltransferase from *Campylobacter jejuni*" by Zane W. Taylor and Frank M. Raushel, *Biochemistry* (2019) *58* (16), pp 2144-2151, Copyright 2019 American Chemical Society

glutamine, resulting in L-glutamine phosphate (**1**) (7,8). The second enzyme, Cj1416, uses L-glutamine phosphate and MgCTP to form CDP-L-glutamine (**2**) (9). CDP-L-glutamine is then hydrolyzed by Cj1417 to generate L-glutamate and cytidine diphosphoramidate (**3**) (9). Finally, Cj1415 catalyzes the phosphorylation of the 3′-hydroxyl group of cytidine diphosphoramidate to make 3′-phosphocytidine 5′-diphosphoramidate (**4**), a cofactor that shares similarity with 3′phosphoadenosine 5′-phosphosulfate (PAPS), which is used in the transfer of sulfate to various acceptors (10). The remaining four enzymes, Cj1419, Cj1420, Cj1421, and Cj1422, are likely responsible for the transfer of the phosphoramidate moiety from 3′-phosphocytidine 5′-diphosphoramidate to a carbohydrate substrate and subsequent methylation to generate the O-methyl phosphoramidate product.

Throughout the characterization of the first four steps in the formation of 3′-phospho-5′-cytidine diphosphoramidate (**4**) as illustrated in Scheme 26, alternative pathways for the biosynthesis of the phosphoramidate cofactor were postulated. In these other transformations, Cj1416 was initially proposed to use phosphoramidate (**5**) as a substrate with a nucleotide triphosphate (NTP) to form the corresponding NDP-amidate (**3**). Cj1416 was initially assayed for its ability to catalyze the formation of an NDP-amidate using phosphoramidate and the Mg^{2+} complexes of various nucleotide triphosphates (9). However, no significant activity with phosphoramidate was detected with any of the NTPs tested in the presence of Mg^{2+}, but catalytic activity was detected when Mn^{2+} was used as the divalent cation (Scheme 27). This promiscuous catalytic activity with Cj1416 and MnCTP was unexpected, but other nucleotide utilizing

enzymes have previously been shown to alter their substrate profile when different divalent cations have been substituted for Mg^{2+}. Pyruvate kinase, for example, catalyzes the Mg^{2+}-dependent phosphorylation of pyruvate with ATP. If Zn^{2+} is used in place of Mg^{2+}, the enzyme is able to phosphorylate hydroxylamine to form hydroxylamine phosphate (11). DNA polymerase has been shown to use Mn^{2+}, but significantly more errors are made in copying DNA, compared with the fidelity observed with Mg^{2+} (12,13). Error-prone PCR uses the enhanced Mn^{2+}-dependent error rate to generate libraries of mutants for enzyme evolution investigations (14). Dihydroxyacetone kinase catalyzes the phosphorylation of dihydroxyacetone with MgATP, but in the presence of Mn^{2+}, the enzyme acts as a cyclase, catalyzing the cyclization of flavin adenine dinucleotide (FAD) to riboflavin 4′,5′-cyclic phosphate and AMP (15).

Scheme 26 Biosynthesis of 3'-Phospho-5'-cytidine Diphosphoramidate

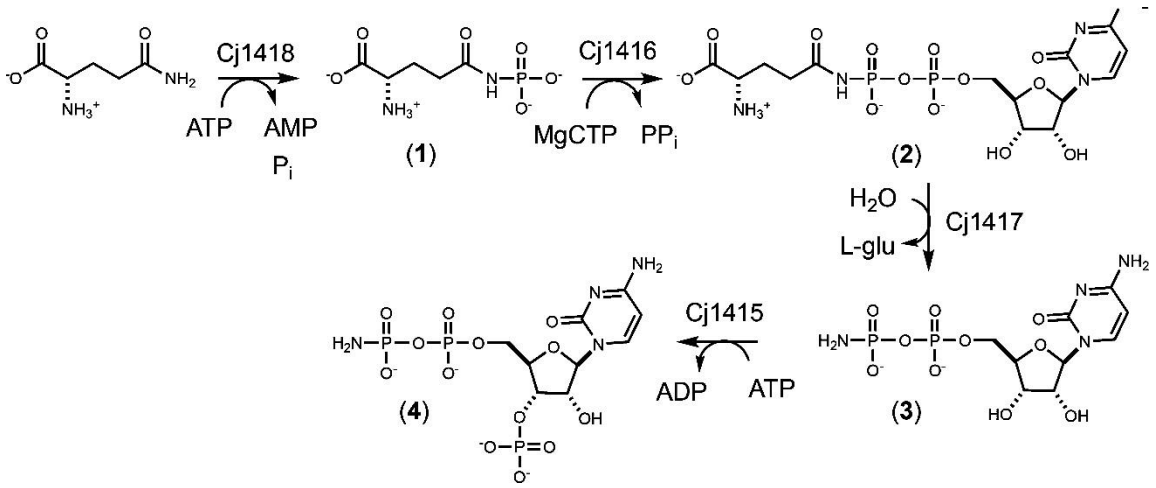

Scheme 27 Formation of Cytidine Diphosphoramidate by Cj1416 and MnCTP

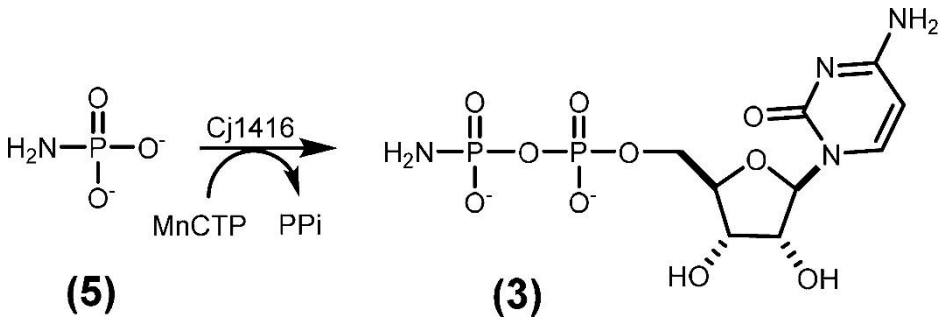

In this article, we have more fully characterized the expansion in the substrate profile of Cj1416 when the reaction is catalyzed in the presence of MnCTP. We have shown that Cj1416 can catalyze the formation of 12 different reaction products when MnCTP is used as one of the substrates. The products have been characterized by ^{31}P NMR spectroscopy and ESI (negative mode) mass spectrometry.

6.2. Materials and Methods

6.2.1. Materials

All buffers and salts were purchased from SigmaAldrich, unless otherwise specified. Phosphate, methyl phosphonate, arsenate, ethanolamine phosphate, 3-phospho-D-glycerate, racemic glycerol-1-phosphate, glycerol-2-phosphate, and L-serine phosphate were purchased from Sigma Aldrich. Phosphoramidate (**5**), L-glutamine phosphate (**1**), and (R/S)-serinol phosphate (**14**) were synthesized as reported previously (7,16,17). Methyl phosphate (**7**) was synthesized by adding dichloromethyl phosphate to water. The plasmid (pET30b) for the expression of Cj1416 from *C. jejuni* NCTC 11168 was obtained from Professor Christine Szymanski of the University of Georgia.

6.2.2. Purification of CTP/Phosphoglutamine Cytidylyltransferase

The plasmid used for the expression of Cj1416 (UniProt ID: Q0P8J8) with a C-terminal poly histidine purification tag was used to transform Rosetta (DE3) *Escherichia coli* cells by electroporation. Cultures (5 mL) of LB medium supplemented with 50

μg/mL kanamycin and 25 μg/mL chloramphenicol were inoculated with a single colony and grown overnight at 37 °C. These cultures were used to inoculate 1 L of LB medium containing 50 μg/mL kanamycin and 25 μg/mL chloramphenicol and then incubated at 30 °C until an OD_{600} of ∼0.6−0.8 was achieved. Gene expression was induced with 1.0 mM isopropyl β-thiogalactoside (IPTG), grown for 16 h at 16 °C, and then harvested by centrifugation at 6300g at 4 °C. The resulting cell pellet was resuspended in loading buffer (50 mM HEPES/K^+, 300 mM KCl, 20 mM imidazole, pH 8.0) and lysed by sonication. Cell debris was removed by centrifugation at 26000g and then passed through a 0.45 μm filter before being loaded onto a prepacked 5 mL HisTrap HP (GE Healthcare) nickel affinity column. Protein was eluted with 30 column volumes using a gradient of 20− 400 mM imidazole in 50 mM HEPES/K^+, pH 8.0, and 300 mM KCl. Excess imidazole was removed by exchanging the buffer against 50 mM HEPES/K^+, pH 8.0, and 100 mM KCl, using a 20 mL (10 kDa molecular weight cutoff) of a concentrator (GE Healthcare). The enzyme was divided into smaller aliquots, frozen in liquid nitrogen, and stored at −80 °C until needed.

6.2.3. ^{31}P NMR Experiments

^{31}P NMR analysis was performed on a Bruker Ascend 400 MHz instrument with phosphoric acid as the reference at 0.0 ppm. Reactions (600 μL) contained 2.5 mM CTP, 5.0 mM substrate, and 5.0 mM $MnCl_2$ in 100 mM HEPES/K^+ and 100 mM KCl, pH 8.0, with 15 μM Cj1416 for 8 h at 30 °C while shaking. Control reactions were conducted under the same conditions with no added enzyme. After incubation, 50 μL of 1 M KOH

was added to the reaction mixture. The samples were vortexed, and the oxidized manganese was removed by centrifugation at 18000g in a microcentrifuge for 5 min. The reaction mixtures were centrifuged two more times to remove all of the remaining manganese. After the third centrifugation, 10 mM EDTA and 100 μL of D_2O were added to the sample and the product was analyzed by ^{31}P NMR spectroscopy.

6.2.4. Reaction Rates

The rates of the reactions catalyzed by Cj1416 were determined by measuring the change in substrate and product concentrations using anion exchange chromatography and following the reaction on an FPLC by monitoring the wavelength of 255 nm. The column used was a prepackaged 1 mL HiTrap Q HP column from GE Healthcare. A sample of 600 μL was prepared, which contained 1.0 mM CTP, 4.0 mM $MnCl_2$, 10 mM of the substrate to be tested, and 5.0 μM Cj1416 in 100 mM HEPES/K^+ and 100 mM KCl, pH 8.0. Samples of 100 μL were injected onto the column every 12.5 min. A total of 17 column volumes were used to elute the sample using a gradient of 0−17% 10 mM triethanolamine, 2 M KCl, pH 8.0, with a flow rate of 2.0 mL min^{-1}. CMP, CDP, and CTP standards were used to determine their relative elution times as 5.5, 7.1, and 8.3 min, respectively.

6.2.5. Negative ESI Mass Spectrometry

Electrospray ionization mass spectrometry (ESI-MS) experiments were performed using a Thermo Scientific Q Exactive Focus. The sample was directly infused

at a flow rate of 10 μL/min. The Q Exactive Focus HESI source was operated in full MS in the negative mode. The mass resolution was tuned to 17500 fwhm at m/z 200. The spray voltage was set to 3.30 kV, and the sheath gas and auxiliary gas flow rates were set to 7 and 0 arbitrary units, respectively. The transfer capillary temperature was held at 250 °C, and the S-Lens RF level was set at 50 V. Exactive Series 2.8 SP1/Xcalibur 4.0 software was used for data acquisition and processing.

Samples for negative mode ESI mass spectrometry were prepared as follows, unless otherwise stated. Reaction of 1.0 mL containing 5.0 mM CTP, 9.0 mM $MnCl_2$, 10 mM substrate, and 30 μM Cj1416 were incubated together in 100 mM HEPES/K^+ and 100 mM KCl, pH 8.0, for 16 h, while shaking. Samples were then centrifuged for 5 min at 15500g in a microcentrifuge. The supernatant solution was loaded onto an anion exchange column, and the product eluted with a total of 35 column volumes using a gradient of 0−35% of 1.0 M ammonium bicarbonate, pH 8.0. At a high pH, the initial products formed using 3-phospho-D-glycerate (**11**), glycerol-1phosphate (**12**), or glycerol-2-phosphate (**13**) degrade to a cyclic phosphate species and CMP. Unfractionated reactions using these three substrates were submitted for ESI analysis. All conditions were the same as before, except ammonium acetate (pH 8.0) was used in place of the HEPES buffer.

6.3. Results and Discussion

6.3.1. Substrate Specificity of Cj1416

Cj1416 was previously characterized as a CTP/phosphoglutamine cytididylyltransferase, which catalyzes the formation of CDP-L-glutamine (**2**) from L-glutamine phosphate (**1**) and MgCTP (Scheme 26) (9). When Cj1416 was incubated with MgCTP and phosphoramidate (**5**) and the reaction followed by anion exchange chromatography, no significant activity could be detected (k_{cat} <1h^{-1}). Since Cj1416 appeared inactive with phosphoramidate using Mg^{2+} as a cofactor, Mn^{2+} was substituted as a potential divalent cation for the enzyme. Incubation of Cj1416 with MnCTP and phosphoramidate resulted in the consumption of CTP and formation of PP_i and cytidine diphosphoramidate (**3**), as demonstrated by changes in the FPLC chromatogram (Figure 22) and ^{31}P NMR spectroscopy. The ^{31}P NMR spectrum of the reaction products revealed the appearance of two new resonances at −0.40 and −10.15 ppm, consistent with the formation of cytidine diphosphoramidate and an additional singlet (−5.01 ppm) from the PP_i reaction product (Figure 23).

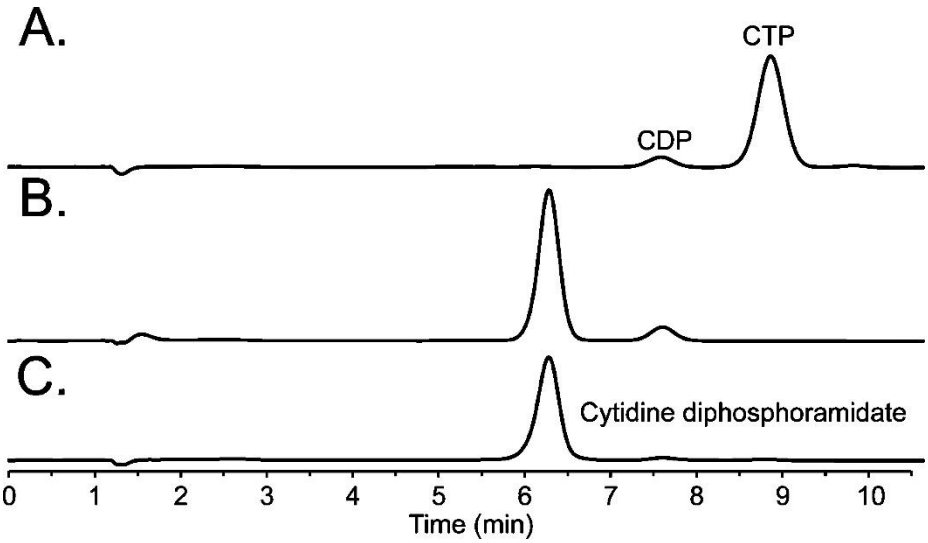

Figure 22 Anion exchange chromatograms for the reaction of MnCTP and phosphoramidate (5). (A) Control sample containing 1.0 mM CTP, 4.0 mM $MnCl_2$, and 10 mM phosphoramidate in 100 mM HEPES/K^+, pH 8.0, and 100 mM KCl. (B) Same reaction mixture as in part A, plus the addition of 5.0 μM Cj1416. (C) Authentic cytidine diphosphoramidate standard.

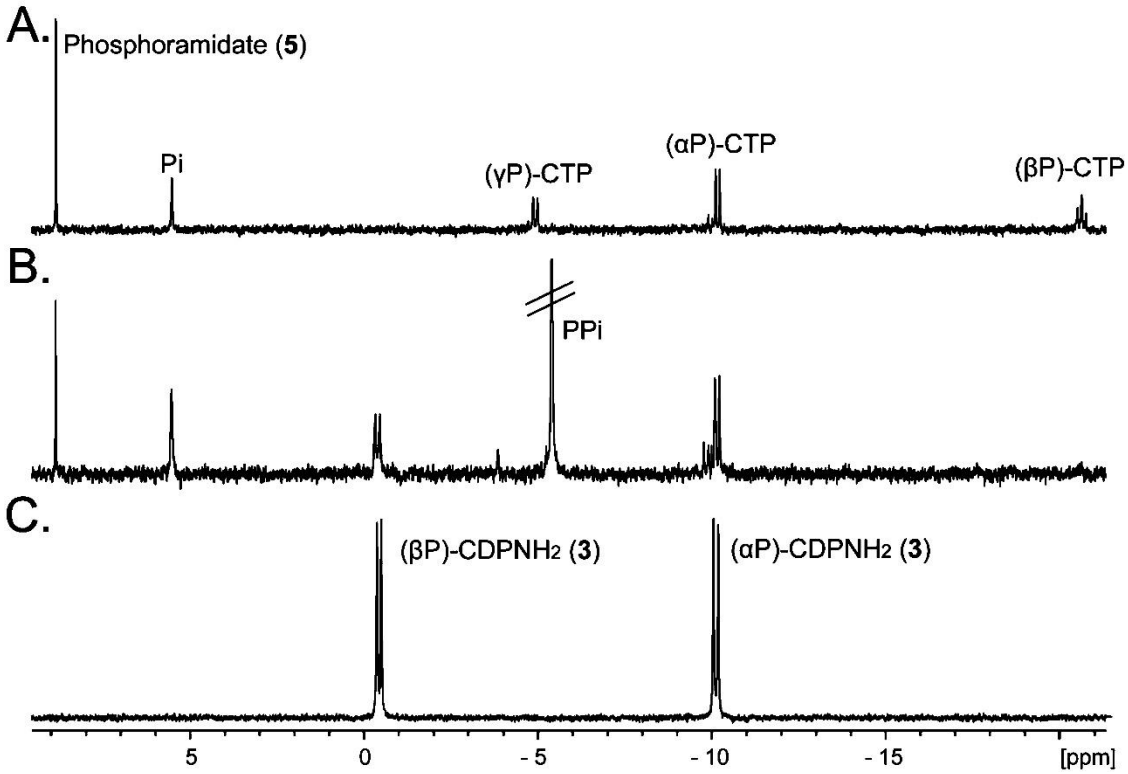

Figure 23 ^{31}P NMR spectra for the reaction of MnCTP and phosphoramidate (5). (A) ^{31}P NMR spectrum for the reaction mixture containing 2.5 mM CTP, 5.0 mM phosphoramidate, and 5.0 mM $MnCl_2$ in 100 mM HEPES/K^+ and 100 mM KCl, at pH 8.0 for 8 h at 30 °C. The pH was adjusted to 12 to oxidize the manganese. The mixture was centrifuged, and then 10 mM EDTA was added. (B) Same reaction conditions as in part A, except 15 μM Cj1416 was added. (C) Control sample of authentic cytidine diphosphoramidate (3).

Since Cj1416 is able to catalyze the formation of cytidine diphosphoramidate (**3**) using MnCTP, the breadth of this promiscuous activity with other substrates was explored. Methyl phosphate (**7**) and methyl phosphonate (**8**) were both assayed as possible substrates, since they are each similar in size and shape to phosphoramidate (**5**). Cj1416 catalyzed the formation of the O-methyl ester of CDP (**17**) and CMP methyl phosphonate (**18**). In total, 35 different compounds were assayed for catalytic activity with Cj1416 and MnCTP (Scheme 28). Of these 35 compounds, 12 showed product formation when analyzed by ^{31}P NMR spectroscopy after an incubation period of 8 h with 15 μM Cj1416 and 2.5 mM MnCTP (Scheme 29). The apparent rate constants for the reaction of Cj1416 with 1.0 mM MnCTP and 10 mM substrate are presented in Table 4.

Scheme 28 Substrates Tested with Cj1416

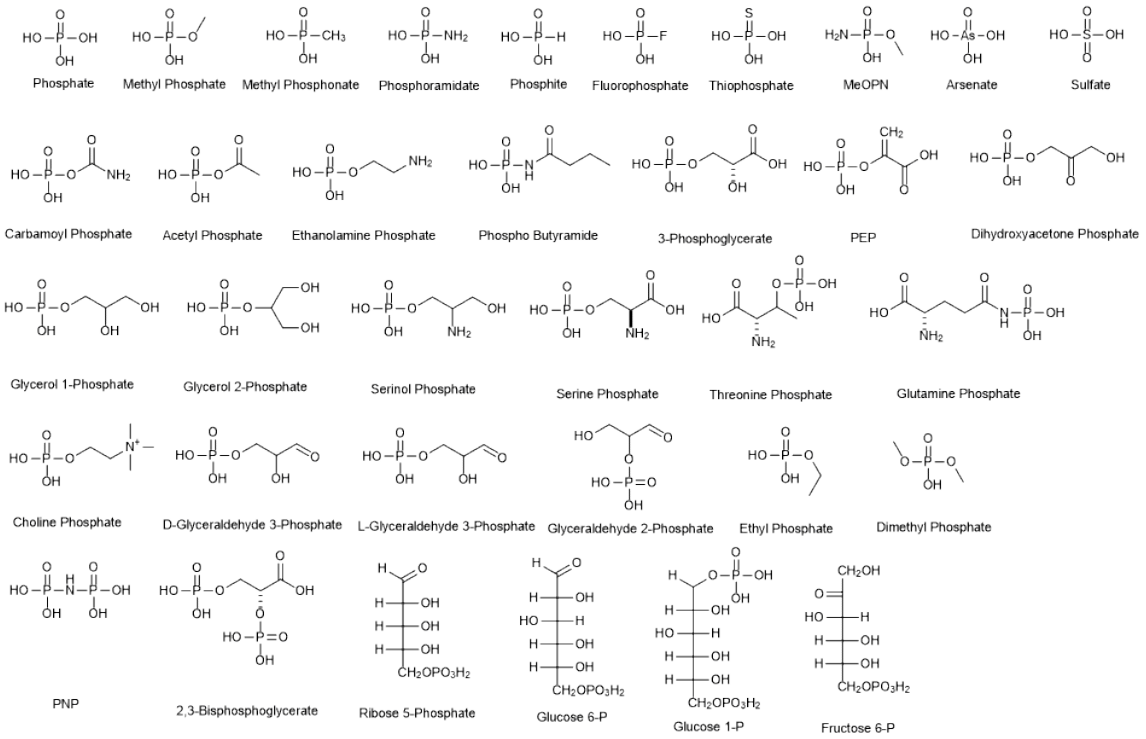

Scheme 29 Compounds Identified as Substrates with MnCTP and Cj1416

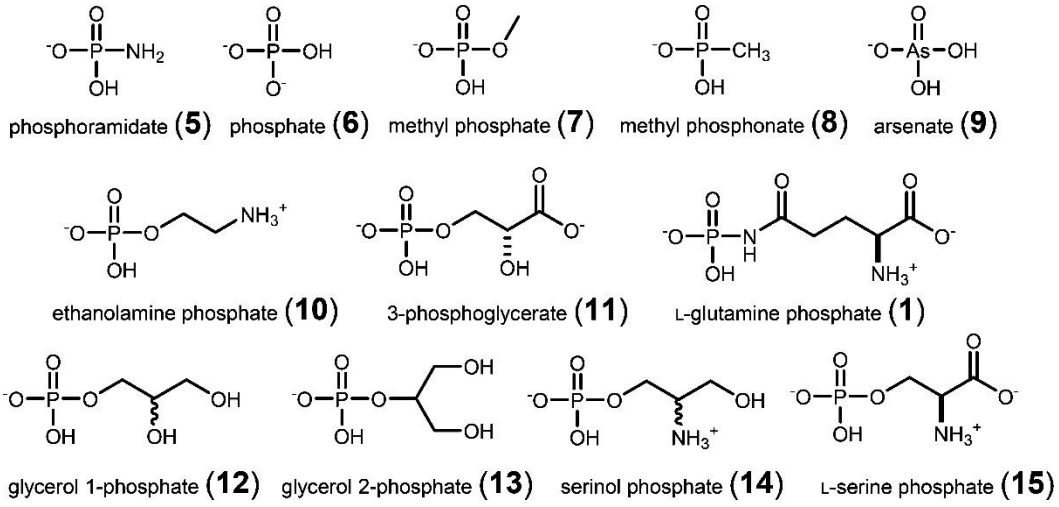

Table 4 Cj1416 and MnCTP Relative Rates, ^{31}P NMR Chemical Shifts and Observed $[M-H]^-$

Substrate	Expected $[M-H]^-$	Observed $[M-H]^-$	Rate Constant	α-^{31}P (ppm)	β-^{31}P (ppm)
phosphoramidate (**5**)	401.02	401.02	36 ± 2 h^{-1}	-10.15	-0.40
phosphate (**6**)	402.01	402.01	11 ± 1 h^{-1}	-9.85	-5.33
methyl phosphate (**7**)	416.02	416.02	4 ± 0.3 h^{-1}	-10.53	-8.84
methyl phosphonate (**8**)	400.03	400.03	9 ± 1 h^{-1}	-10.59	18.18
arsenate (**9**)	446.96	322.04	11 ± 1 h^{-1}	4.51[a]	NA
ethanolamine phosphate (**10**)	445.05	445.05	1 ± 0.2 h^{-1}	-10.58	-9.91
3-phospho-D-glycerate (**11**)	490.02	490.02	220 ± 20 h^{-1}	4.51[a]	18.88[b]
L-glutamine phosphate (**1**)	530.06	530.06	21 ± 2 h^{-1}	-10.79	-15.64
(*R/S*)-glycerol-1-phosphate (**12**)	476.04	476.04	4 ± 0.7 h^{-1}	4.51[a]	19.16[b]
glycerol-2-phosphate (**13**)	476.04	476.04	5 ± 0.5 h^{-1}	4.51[a]	19.16[b]
(*R/S*)-serinol phosphate (**14**)	475.06	475.06	1 ± 0.2 h^{-1}	-10.56	-9.96
L-serine phosphate (**15**)	489.04	489.04	11 ± 2 h^{-1}	-10.47	-10.11

[a]The α-phosphoryl group is for CMP

[β]Cyclic degradation products

NA: Not applicable for arsenate.

6.3.2. Characterization of Cj1416 Reaction Products

The predicted initially formed products for Cj1416 with MnCTP and the substrates in Scheme 29 are shown in Scheme 30. The Cj1416-catalyzed reaction products, cytidine diphosphoramidate (**3**), CDP-L-glutamine (**2**), CDP (**16**), and CDP-ethanolamine (**20**) using phosphoramidate (**5**), L-glutamine-P (**1**), phosphate (**6**), and ethanolamine-P (**10**) are consistent with their previously published ^{31}P NMR spectra (Figure 23and Figure 24) (9,18). The chemical shifts for four other reaction products, O-methyl CDP (**17**), CMP methyl phosphonate (**18**), CDP-L-serine (**25**), and CDP-serinol (**24**), are also consistent with their predicted structures (Figure 25). The remaining four substrates, 3-phospho-D-glycerate (**11**), (R/S)-glycerol-1-phosphate (**12**), glycerol 2-phosphate (**13**), and arsenate (**9**), all exhibited ^{31}P NMR spectra that were inconsistent with the predicted products.

Scheme 30 Initial Reaction Products Formed by Cj1416 Using MnCTP and the Substrates Shown in Scheme 29.

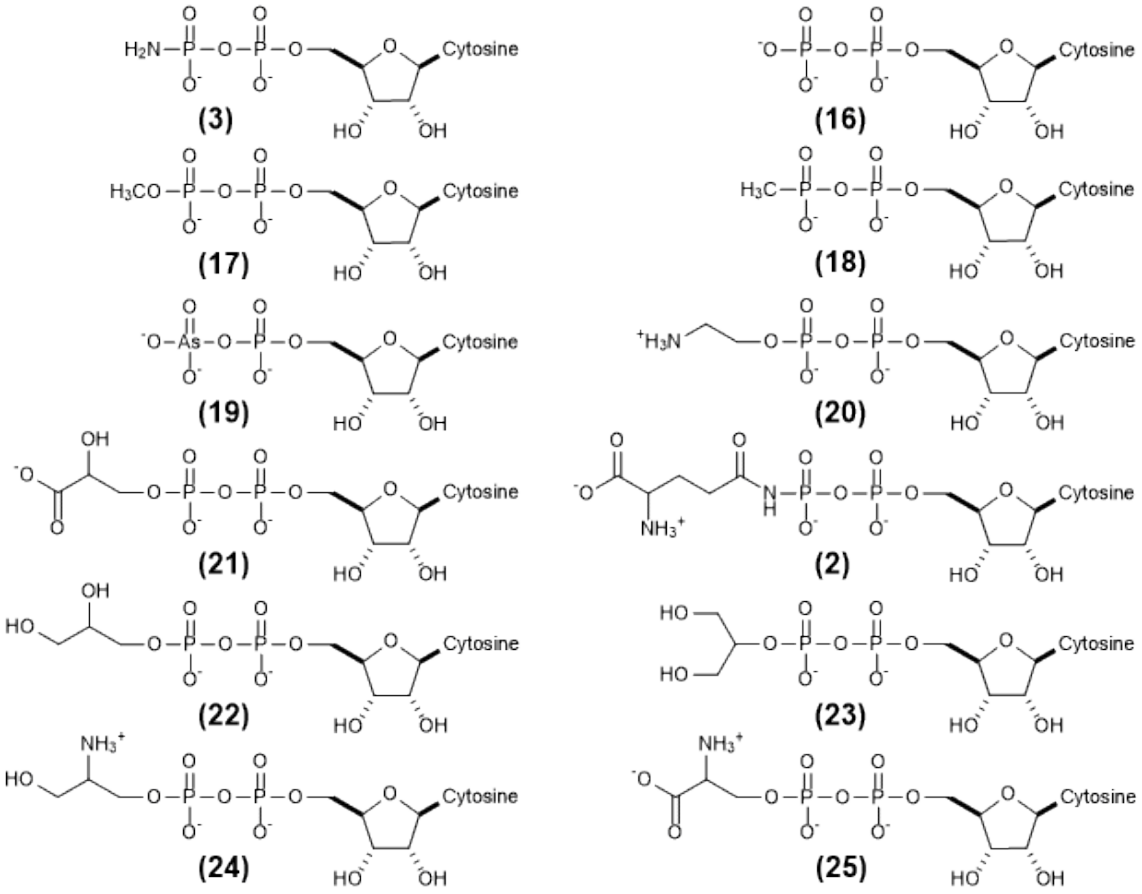

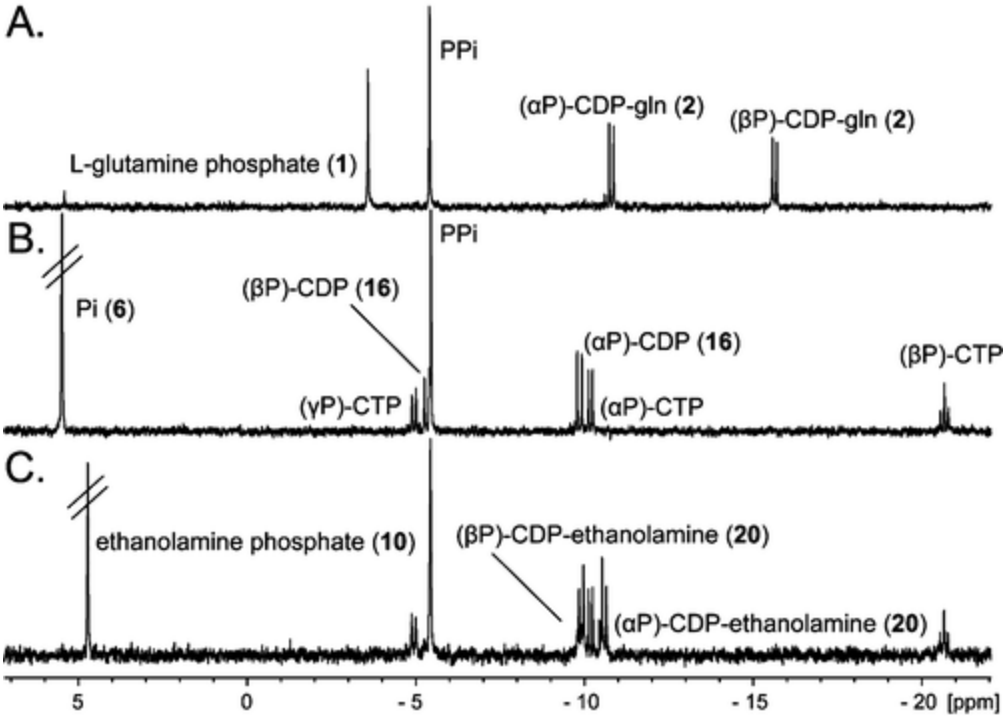

Figure 24 ^{31}P NMR spectra of the Cj1416-catalyzed reaction products. Samples initially contained 2.5 mM CTP, 5.0 mM substrate, and 5.0 mM $MnCl_2$ in 100 mM HEPES/K^+, pH 8.0, and were incubated for 8 h at 30 °C while shaking with 15 μM Cj1416. The pH was adjusted to 12 to oxidize the manganese. After removal of manganese by centrifugation, 10 mM EDTA was added to the sample to sequester any remaining Mn^{2+}. (A) L-Glutamine phosphate and the formation of L-glutamine CDP (2). (B) Phosphate and formation of CDP (16). (C) Ethanolamine phosphate and formation of ethanolamine CDP (20).

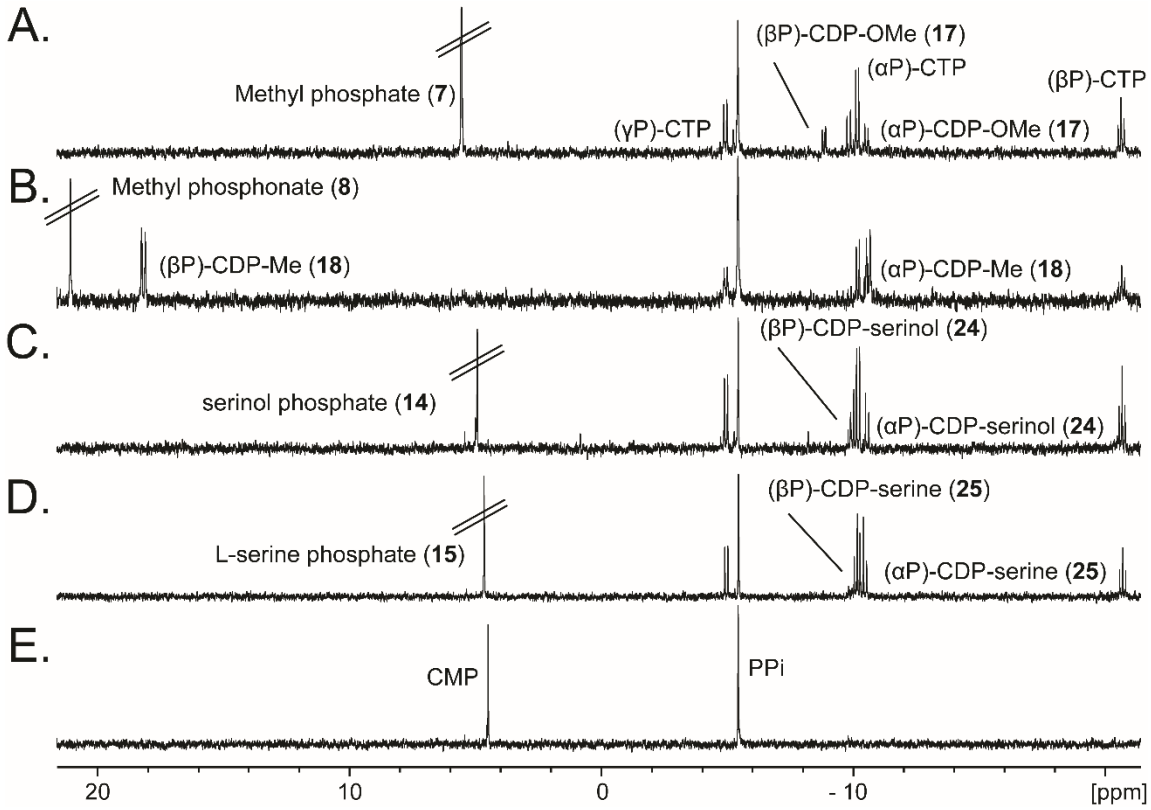

Figure 25 ^{31}P NMR of Cj1416 Products. Samples contained 2.5 mM CTP, 5.0 mM substrate and 5.0 mM $MnCl_2$ in 100 mM HEPES/KOH, 100 mM KCl at pH 8.0 with for 8 h at 30 °C while shaking. The pH was adjusted to12 to oxidize manganese. After removal of manganese by centrifugation 10 mM EDTA was added to the sample. (A) Methyl phosphate (7) and formation of O-methyl ester CDP (17). (B) Methyl phosphonate (8) and the formation of CMP-methyl phosphonate (18). (C) (*R/S*)-serinol phosphate (14) and the formation of CDP-serinol (24). (D) L-serine phosphate (15) and the formation of CDP-L-serine (25). (E) Arsenate (9) and the formation of CMP.

In the reaction with arsenate, a new ^{31}P NMR resonance is consistent with the formation of PP_i, indicating that there was a turnover of MnCTP. However, CMP-arsenate (**19**) was not detected, but CMP was observed. The formation of pyrophosphate is consistent with arsenate being a substrate for the enzyme, but the CMP-arsenate product is anticipated to be unstable and degrades to CMP and arsenate (Figure 25). The FPLC chromatograph of the reaction mixture is also consistent with rapid formation of the CMP degradation product. With (R/S)-glycerol-1-phosphate (**12**), glycerol-2-phosphate (**13**), and 3-phospho-D-glycerate (**11**), all of the initially anticipated products were predicted to have a pair of doublets in their ^{31}P NMR spectra due to ^{31}P–^{31}P spin coupling. However, for these three reaction products, new singlets are observed at 4.51 ppm (for CMP) and at ~19 ppm (Figure 26). The proton coupled ^{31}P NMR spectrum of the 3-phospho-D-glycerate reaction product that resonates at 4.51 is a triplet, consistent with the formation of CMP and another resonance at 18.88 ppm, consistent with the formation a cyclic phosphate product as illustrated in Scheme 31. The observed cyclic degradation products are believed to be formed during the procedure to remove the manganese from the reaction mixture. The initial formation of CDP-3-D-glycerate is observed in the FPLC chromatogram when MnCTP is incubated with 3-phospho-D-glycerate in the presence of Cj1416 (Figure 27). Other examples of five-membered cyclic phosphate species have previously been made chemically using a high pH (19,20).

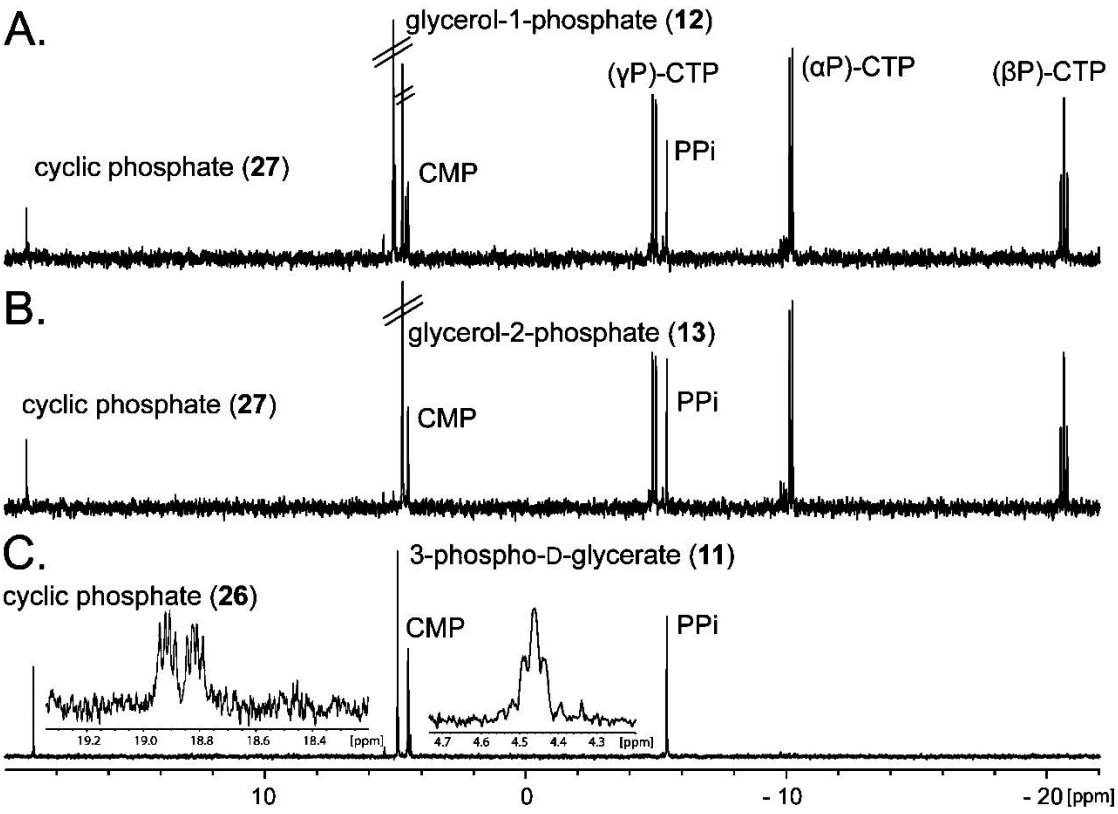

Figure 26 ^{31}P NMR spectra. ^{31}P NMR of a reaction containing 2.5 mM CTP, 5.0 mM substrate, and 5.0 mM $MnCl_2$ in 100 mM HEPES/KOH and 100 mM KCl at pH 8.0 for 8 h at 30 °C while shaking with 15 µM Cj1416. The pH was adjusted to 12 to oxidize manganese. After the removal of manganese by centrifugation, 10 mM EDTA was added to the sample. (A) Glycerol-1-phosphate and the formation of CMP and cyclic glycerol phosphate (27). (B) Glycerol-2-phosphate and the formation of CMP and cyclic glycerol phosphate (27). (C) 3-Phospho-D-glycerate and the formation of cyclic 3-phospho-D-glycerate (26). Insets show the ^{31}P–^{1}H coupled spectra.

Scheme 31 Cyclic Degradation Products

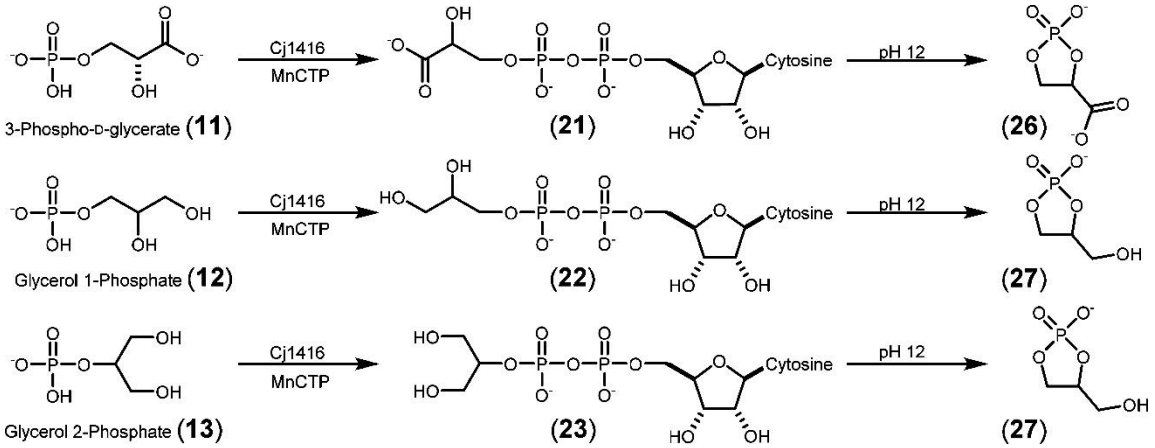

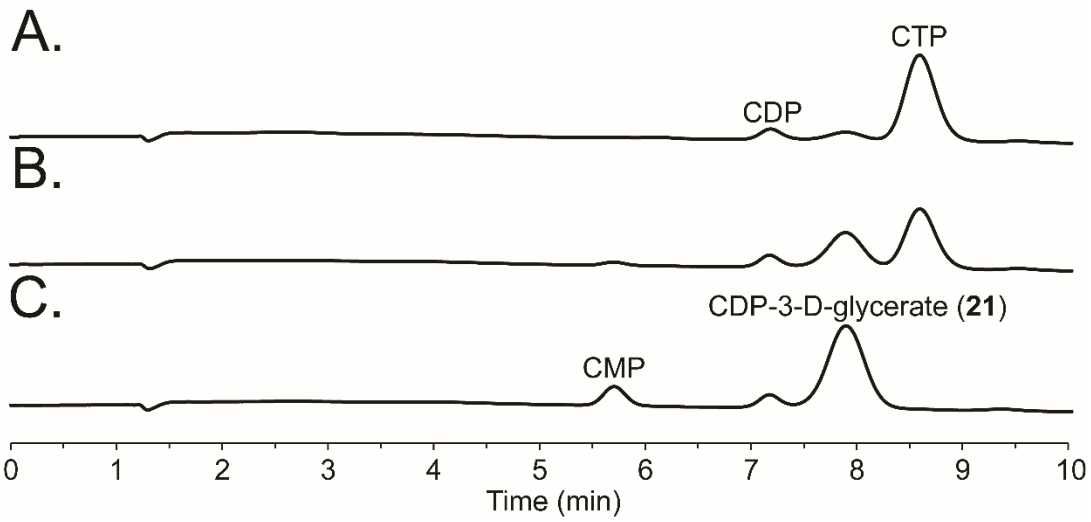

Figure 27 Anion exchange chromatograms for the reaction of 1.0 mM MnCTP and 10 mM 3-phospho-D-glycerate (11). (A) Sample immediately following the addition of 5 µM Cj1416. (B) Sample after incubation with Cj1416 for 25 min. (C) Sample after 1 h when all CTP has been consumed. The formation of CDP-3-D-glycerate is observed with an elution time of ~7.9 min and the degradation product, CMP is observed at a retention time of ~5.7 min.

ESI-negative mode mass spectrometry was used to analyze all of the Cj1416-catalyzed reaction products using MnCTP as the nucleotide substrate (Table 4). Table 4 shows the predicted and observed masses for each of the 12 products. The spectra for CDP-glycerol (**22**) and CDP-2-glycerol (**23**) both show a mass of 476.04, which is consistent with the formation of their respective CDP-glycerol products. With CDP-2-glycerol (**23**), masses of 152.99 and 322.04 are consistent with the cyclic phosphate (**27**) degradation product and CMP, respectively. The 3-phosphoglycerate reaction indicates a mass of 490.02, which is consistent with the formation of CDP-3-D-glycerate (**21**). The mass spectrum is also consistent with the formation of CMP (322.04) and the cyclic phosphate species (166.97) (**26**). This confirms our prediction that CDP-glycerol, CDP-2-glycerol, and CDP-3-D-glycerate are the enzymatic products and that the degradation products occur due to the high pH, to which the samples were exposed.

6.3.3. Cj1416 Relative Rates

The rates observed with MnCTP and Cj1416 are relatively slow. In the presence of MnCTP, L-glutamine phosphate is utilized with an apparent k_{cat} of 21 ± 2 h^{-1}, compared to a k_{cat} of 3400 ± 400 h^{-1} with MgCTP, resulting in a >100-fold reduction in rate (9). With phosphoramidate and MnCTP, the apparent k_{cat} is 36 ± 2h^{-1} but no significant activity (k_{cat} <1h^{-1}) was detected with MgCTP as the cosubstrate. The most surprising substrate was 3-phospho-D-glycerate (**11**). An apparent k_{cat} of 220 ± 20 h^{-1} was observed with this substrate and MnCTP, and thus the promiscuous activity of 3-phospho-D-glycerate with MnCTP is an order of magnitude faster than the activity of the

physiological substrate L-glutamine phosphate when MnCTP is used as the nucleotide. When 3-phospho-D-glycerate was examined with MgCTP as the cofactor, no significant activity was observed (k_{cat} <1h $^{-1}$), thus demonstrating a >200-fold increase in rate with Mn^{2+} as a divalent cation, compared to Mg^{2+}.

6.3.4. Manganese-Induced Promiscuity of Cj1416

The effects of various divalent cations on enzyme catalysis have previously been studied. In many cases, the effects of divalent cations have been addressed in terms of reaction rates, but promiscuity has rarely been examined. DNA polymerase is well-known to exhibit promiscuity when Mg^{2+} is replaced by Mn^{2+}. The promiscuous activity has been exploited in error-prone PCR procedures to generate random mutations in genes of interest. A physical explanation for how Mn^{2+} induces this effect on DNA polymerase is unknown. DNA polymerases generally require two metals for catalysis; "metal A" helps to lower the pK_a of the 3′-hydroxyl group of the primer and coordinates the α-phosphoryl group of the incoming nucleotide, while "metal B" is coordinated to the incoming nucleotide and helps negate the negative charge of the triphosphate moiety of the substrate (12). It is unclear which one of these two metals in DNA polymerase is responsible for the Mn^{2+} promiscuity. Magnesium and manganese are similar in several ways; both metals utilize an octahedral coordination geometry, have a similar ionic radius (Mg^{2+} 0.86 Å, Mn^{2+} 0.81 Å), and have a similar effect on the pKa of coordinated water (Mg^{2+} 11.4, Mn^{2+} 11.5) (21). However, if the average covalent bond length is examined in all high-resolution Mg^{2+} and Mn^{2+} protein crystal structures, Mg^{2+} has an

average bond length of 2.09 Å and Mn^{2+} has an average bond length of 2.22 Å.22 The higher average bond length may help Mn^{2+} form distorted octahedral geometries, which can broaden or relax ligand preferences (21). The substitution of divalent cations is now known to have an effect on the substrate profile of Cj1416. Cj1416 can form a minimum of 12 unique reaction products from MnCTP. CDP-ethanolamine is a known natural product and is used in the formation of phosphatidylethanolamine, a common lipid, and CDP-1-glycerol is used in teichoic acid biosynthesis (23). CDP-2-glycerol is another known natural product from *Streptococcus pneumonia* (24). Cj1416 is capable of forming all three of these natural products, two of which are unavailable commercially. Additionally CDP-serine, CDP-serinol, and CDP-3-D-glycerate are all structurally similar to CDP-glycerol and may function as potential inhibitors or as mechanistic probes for enzymes that use CDP-glycerol. Another reaction catalyzed by Cj1416 and MnCTP is the formation of CDP from CTP and phosphate. If ^{18}O-labeled phosphate is used as an alternate substrate, Cj1416 can be used to form β-[$^{18}O_4$]-CDP, which can subsequently be used to synthesize β-[$^{18}O_4$]-CTP. Typically, β-[$^{18}O_4$]-CDP is made using morpholidate chemistry in dry DMSO with ^{18}O-labeled phosphate. Labeled nucleotides of this type can be used to probe the details of enzyme-catalyzed reactions using the methodologies of positional isotope exchange (PIX) and molecular isotope exchange (MIX).

6.4. References

1. Young, K. T., Davis, L. M., and Dirita, V. J. (2007) *Campylobacter jejuni*: Molecular Biology and Pathogenesis. *Nat. Rev. Microbiol*. 5, 665−679.
2. García-Sánchez, L., Melero, B., Rovira, J., and Rodríguez-Lázaro, D. (2018) Campylobacter in the Food Chain. *Adv. Food Nutr. Res*. 86, 215−252.
3. Roberts, I. S. (1996) The Biochemistry and Genetics of Capsularpolysaccharide Production in Bacteria. *Annu. Rev. Microbiol*. 50, 285−315.
4. McNally, D. J., Lamoureux, M. P., Karlyshev, A. V., Fiori, L. M., Li, J., Thacker, G., Coleman, R. A., Khieu, N. H., Wren, B. W., Brisson, J.-R., Jarrell, H. C., and Szymanski, C. M. (2007) Commonality and Biosynthesis of the O-Methyl Phosphoramidate Capsule Modification in *Campylobacter jejuni*. *J. Biol. Chem*. 282, 28566−28576.
5. Petkowski, J. J., Bains, W., and Seager, S. (2019) Natural Products Containing 'Rare' Organophosphorus Functional Groups. *Molecules* 24, 866−932.
6. van Alphen, L. B., Wenzel, C. Q., Richards, M. R., Fodor, C., Ashmus, R. A., Stahl, M., Karlyshev, A. V., Wren, B. W., Stintzi, A., Miller, W. G., Lowary, T. L., and Szymanski, C. M. (2014) Biological Roles of the O-Methyl Phosphoramidate Capsule Modification in *Campylobacter jejuni*. *PLoS One* 9 (1), e87051.
7. Taylor, Z. W., Brown, H. A., Narindoshvili, T., Wenzel, C. Q., Szymanski, C. M., Holden, H. M., and Raushel, F. M. (2017) Discovery of a Glutamine Kinase Required for the Biosynthesis of the O-Methyl Phosphoramidate Modifications

Found in the Capsular Polysaccharides of *Campylobacter jejuni*. *J. Am. Chem. Soc*. 139, 9463−9466.

8. Taylor, Z. W., Chamberlain, A. R., and Raushel, F. M. (2018) Substrate Specificity and Chemical Mechanism for the Reaction Catalyzed by Glutamine Kinase. *Biochemistry* 57, 5447−5455.
9. Taylor, Z. W., Brown, H. A., Holden, H. M., and Raushel, F. M. (2017) Biosynthesis of Nucleoside Diphosphoramidates in *Campylobacter jejuni*. *Biochemistry* 56, 6079−6082.
10. Taylor, Z. W., and Raushel, F. M. (2018) Cytidine Diphosphoramidate Kinase: An Enzyme Required for the Biosynthesis of the O-Methyl Phosphoramidate Modification in the Capsular Polysaccharides of *Campylobacter jejuni*. *Biochemistry* 57, 2238− 2244.
11. Cottam, G. L., Kupiecki, F. P., and Coon, M. J. (1968) A Study of the Mechanism of O-Phosphorylhydroxylamine Synthesis Catalyzed by Pyruvate Kinase. *J. Biol. Chem.* 243, 1630−1637.
12. Johnson, K. A. (2010) The Kinetic and Chemical Mechanism of High-Fidelity DNA Polymerases. *Biochim. Biophys. Acta, Proteins Proteomics* 1804, 1041−1048.
13. Tabor, S., and Richardson, C. C. (1989) Effect of Manganese Ions on the Incorporation of Dideoxynucleotides by Bacteriophage T7 DNA Polymerase and *Escherichia coli* DNA Polymerase I. *Proc. Natl. Acad. Sci. U. S. A.* 86, 4076−4080.

14. Fromant, M., Blanquet, S., and Plateau, P. (1995) Direct Random Mutagenesis of Gene-Sized DNA Fragments Using Polymerase Chain Reaction. *Anal. Biochem*. 224, 347−353.
15. Sánchez-Moreno, I., Iturrate, L., Martín-Hoyos, R., Jimeno, M. L., Mena, M., Bastida, A., and García-Junceda, E. (2009) From Kinase to Cyclase: An Unusual Example of Catalytic Promiscuity Modulated by Metal Switching. *ChemBioChem* 10, 225−229.
16. Wehrli, W., Verheyden, D., and Moffatt, J. (1965) Dismutation Reactions of Nucleoside Polyphosphates. II. Specific Chemical Syntheses of α-, β-, and γ-P32-Nucleoside 5′-Triphosphates1. *J. Am. Chem. Soc.* 87, 2265−2277.
17. Watanabe, M., Sato, S., and Wakasugi, K. (1990) The Hydrolytic Property of Imidodiphosphate in Solid and in an Aqueous Medium. *Bull. Chem. Soc. Jpn*. 63, 1243−1245.
18. Ghezal, S., Thomasson, M. S., Lefebvre-Tournier, I., Périgaud, C., Macnaughtan, M. A., and Roy, B. (2014) CDP-Ethanolamine and CDP-Choline: One-pot Synthesis and ^{31}P NMR Study. *Tetrahedron Lett*. 55, 5306−5310.
19. Ghodge, S. V., Cummings, J. A., Williams, H. J., and Raushel, F. M. (2013) Discovery of a Cyclic Phosphodiesterase That Catalyzes the Sequential Hydrolysis of Both Ester Bonds to Phosphorus. *J. Am. Chem. Soc*. 135, 16360−16363.
20. Hove-Jensen, B., McSorley, F. R., and Zechel, D. L. (2011) Physiological Role of phnP-specified Phosphoribosyl Cyclic Phosphodiesterase in Catabolism of

Organophosphonic Acids by the Carbon−Phosphorus Lyase Pathway. *J. Am. Chem. Soc*. 133, 3617− 3624.

21. Vashishtha, A. K., Wang, J., and Konigsberg, W. H. (2016) Different Divalent Cations Alter the Kinetics and Fidelity of DNA Polymerases. *J. Biol. Chem*. 291, 20869−20875.
22. Xia, S., Wang, M., Blaha, G., Konigsberg, W. H., and Wang, J. (2011) Structural Insights into Complete Metal Ion Coordination from Ternary Complexes of B Family RB69 DNA Polymerase. *Biochemistry* 50, 9114−9124.
23. Schertzer, J. W., and Brown, E. D. (2008) Use of CDP-Glycerol as an Alternate Acceptor for the Teichoic Acid Polymerase Reveals that Membrane Association Regulates Polymer Length. *J. Bacteriol*. 190, 6940−6947.
24. Wang, Q., Xu, Y., Perepelov, A. V., Xiong, W., Wei, D., Shashkov, A. S., Knirel, Y. A., Feng, L., and Wang, L. (2010) Characterization of the CDP-2-Glycerol Biosynthetic Pathway in Streptococcus pneumoniae. *J. Bacteriol*. 192, 5506−5514.

7. CONCLUSIONS

7.1. Biosynthesis of 3'-Phosphocytidine-5'-Diphosphoramidate

The first four steps in the biosynthesis of the O-methyl phosphoramidate modification in *Campylobacter jejuni* have been elucidated. The first enzyme, Cj1418, catalyzes the ATP dependent phosphorylation of L-glutamine forming L-glutamine phosphate. This novel reaction represents the first instance of an enzyme catalyzing the phosphorylation of an amide, and is the first enzyme in this family to catalyze the formation of a phosphoramidate bond. The chemical mechanism of Cj1418 was also determined. Cj1418 catalyzes the nucleophilic attack into the β-phosphoryl group of ATP using histidine 737, forming a pyrophosphorylated enzyme intermediate. This pyrophosphorylated enzyme intermediate is then hydrolyzed, resulting in a phosphorylated intermediate. The phosphorylated enzyme intermediate then transfers the β-phosphoryl group from ATP to L-glutamine forming L-glutamine phosphate.

Cj1416, a CTP:phosphoglutamine cytidylyltransferase, catalyzes the formation of CDP-L-glutamine from CTP and L-glutamine phosphate. CDP-L-glutamine is then hydrolyzed by Cj1417, a γ-glutamyl-CDP-amidate hydrolase, forming glutamate and cytidine diphosphoramidate. The fourth enzyme then phosphorylates the 3'-hydrozyl group of cytidine diphosphoramidate, resulting in the 3'-phosphocytidine-5'-diphosphoramidate cofactor. This cofactor shares similarity to 3'-phosphoadenosine-5'-phosphosulfate, a cofactor that is used in the transfer of sulfate.

7.2. Metabolic Fate of 3'-Phosphocytidine-5'-Diphosphoramidate

The metabolic fate of the 3'-phosphocytidine-5'-diphosphoramidate cofactor is currently unknown. The four genes cj1419, cj1420, cj1421, and cj1422 are believed to be responsible for the formation of the O-methyl phosphoramidate modification in the NCTC 11168 strain of *C. jejuni*. Knockout studies on each of these four genes reveals that Cj1421 is responsible for the formation of the phosphoramidate modification found on C3 of the 2-acetamido-2-deoxy-β-D-galactofuranose and Cj1422 is responsible for the modification found on C4 of D-glycero-α-L-*gluco*-heptopyranose (1). Both of these enzymes are annotated transferases and are believed to be responsible for the transfer of the phosphoramidate to the capsule.

Cj1419 and Cj1420 are both annotated SAM dependent methyl transferases. Any strain of *C. jejuni* that contains Cj1418, Cj1417, Cj1416, and Cj1415 always contains a copy of Cj1419 and Cj1420. Both methyltransferases are always present, however they only share a 32% identity to each other; however Cj1419 and Cj1420 across different strains of *C. jejuni* share a >95% identity to their respective counterparts. In the same study that examined the Cj1421 and Cj1422 knockouts, Cj1419 and Cj1420 were analyzed (1). The authors claim that Cj1419 and Cj1420 are not involved in the biosynthesis of the O-methyl phosphoramidate modification, and note that resonances for both phosphoramidate resonances are detected in each Cj1419 and Cj1420 knockouts (1). However, looking at the spectra presented in the paper, both resonances are observed in the Cj1419 knock out, like the authors claim, although the resonance for the phosphoramidate at C3 of the 2-acetamido-2-deoxy-β-D-galactofuranose appears

diminished compared to the wild type control. In the knockout of Cj1420 the resonance for the phosphoramidate on C4 of D-glycero-α-L-*gluco*-heptopyranose is not detected, which clearly implicates Cj1420 in the biosynthesis of the O-methyl phosphoramidate (1).

Two experiments are missing from the study involving the knockouts. Since the authors claim Cj1419 and Cj1420 are not involved in the biosynthesis of the O-methyl phosphoramidate, this should have been supported by a Cj1419 and Cj1420 double mutant. This would have ruled out the possibility that either Cj1419 or Cj1420 contain some degree of promiscuity and can compensate for missing either Cj1419 or Cj1420. The other missing experiment is using ^{31}P NMR to examine the knockout strains of Cj1419 and Cj1420. If this had been done, it is possible that a phosphoramidate resonance could be detected on the capsule, absent the methyl group. This would confirm that the phosphoramidate moiety is transferred to the capsule then methylated. The order of methylation and phosphoramidate transfer is still unknown.

7.3. Future Work

Currently four of the eight enzymes predicted to be responsible for the formation of the O-methyl phosphoramidate modification in the NCTC 11168 strain of *C. jejuni* have been characterized. It is unknown if the phosphoramidate is methylated then transferred to the capsule, or transferred then methylated. The 3'-phosphocytidine-5'-diphoshoramidate cofactor has been assayed for activity with both of the methyl transferases, but no activity was observed. Presumably this means transfer of the

phosphoramidate occurs first however this still needs to be shown. Additionally it is unclear what the actual substrate for Cj1422 and Cj1421 might be. The most likely substrates are either a nucleotide-carbohydrate or the actual capsule. Once the order of methylation and transfer of the phosphoramidate are elucidated, the entire biosynthesis of O-methyl phosphoramidate will be known.

This project has also been conducted in collaboration with the Holden lab at the University of Wisconsin Maddison, who are working on crystalizing these proteins for structural determination. Efforts are currently underway to determine the structures for Cj1418, Cj1416, Cj1417 and Cj1415.

7.4. References

1. McNally, D. J., Lamoureux, M. P., Karlyshev, A. V., Fiori, L. M., Li, J., Thacker, G., Coleman, R. A., Khieu, N. H., Wren, B. W., Brisson, J.-R., Jarrell, H. C., and Szymanski, C. M. (2007) Commonality and Biosynthesis of the O-Methyl Phosphoramidate Capsule Modification in *Campylobacter jejuni*, *J. Biol. Chem. 282*, 28566-28576.